Title: The Physics of Unification

Author: Steven Howard Snyder

Email: steveinternetemail@yahoo.com

Abstract:

To date, a unification is needed with the application of Planck units which unifies not only the force of Newtonian gravity with the electromagnetic force and the strong and weak nuclear forces, but also one which includes quantum field theory and relativity. Herein, a unification as such is accomplished in which the mathematical terms of the conventional fields and the corresponding forces are unified into one general function in Planck units, and the geometry (including internal structure) and functionality of certain aspects of the respective unified field constructed therefrom are described. Accordingly, the geometry and functionality of the unified field are applied for describing certain aspects of electromagnetic, gravitational, and nuclear interaction along with certain aspects of elementary particles (including antiparticles), atoms, molecules, and at the macroscopic scale, astronomical bodies.

GENERAL FUNCTION OF THE UNIFIED FIELD:

A general function of a unified field is formulated herein complemented by a theoretical internal structure which has been constructed for the posited unified field unlike the functions of the conventional forces of Newtonian gravity, the electromagnetic force, the strong and weak nuclear forces, and the functions of conventional spacetime. Wherein, first, equation (1A), which was designed especially for the purposes of the theory herein, is rewritten as a general exponential function which has the form shown in equation (1B):

$$f = z = \pm e^{\frac{1}{N}[n_1 \pm x + n_2 \pm y]} \qquad \text{Eq. (1A)}$$

$$f = z = \pm e^{\left[\frac{1}{N} n_1 \pm x + \frac{1}{N} n_2 \pm y\right]} \qquad \text{Eq. (1B)}$$

In which case, 1/N is a constant such that N=1, 2, 3,…; and n_1 and n_2 are constants such that $1< n_1<2$ and $1>n_2>0$.

Now, substituting $\frac{2\pi(qvr)}{h_q}$ and $\frac{2\pi(mvr)}{h}$ for (x) and (y), respectively, in equation (1B) results in the following more specific function:

$$f = \pm e^{\left[\frac{1}{N} n_1 \frac{\pm 2\pi(qvr)}{h_q} + \frac{1}{N} n_2 \frac{\pm 2\pi(mvr)}{h}\right]}. \qquad \text{Eq. (2)}$$

Here, (q) is charge, (v) is velocity, (r) is radius, (m) is mass, (π) is Pi, and (h) is Planck's constant as applied for the mass aspect of the unified field, and (h_q) is a variation of sorts on Planck's constant which is applied theoretically for the charge aspect of the unified field as will be described more so below.

Equation (2) is expressed as follows when v=c:

$$f = \pm e^{\left[\frac{1}{N} n_1 \frac{\pm 2\pi(qcr)}{h_q} + \frac{1}{N} n_2 \frac{\pm 2\pi(mcr)}{h}\right]}. \qquad \text{Eq. (3A)}$$

The (x) and (y) terms in the exponent (neglecting signs) can each be made approximately equal to a dimensionless value of one when using terms which include Planck units in both variables of the exponent, when h=2πmcr, and when applying the following charge to mass ratio in the (x) variable of the exponent:

$$\frac{\frac{(q_p)}{(m_p)}}{\frac{(q_p)}{(m_p)}} = \frac{\frac{(1.8755x10^{-18}C)}{(2.1765x10^{-8}kg)}}{\frac{(1.8755x10^{-18}C)}{(2.1765x10^{-8}kg)}} = 1$$

Wherein, $\frac{2\pi(qcr)}{h_q} = \frac{2\pi(mcr)}{h}$ as exemplified in figures (1A) and (1B) as follows:

$$x = \frac{2\pi(qcr)}{h_q} = \frac{2\pi(2.1765x10^{-8}kg)\frac{(1.8755x10^{-18}C)}{(2.1765x10^{-8}kg)}\frac{(1.6162x10^{-35}m)}{(5.3911x10^{-44}s)}(1.6162x10^{-35}m)}{\frac{(1.6162x10^{-35}m)^2(2.1765x10^{-8}kg)\frac{(1.8755x10^{-18}C)}{(2.1765x10^{-8}kg)}(5.3911x10^{-44}s)}{(5.3911x10^{-44}s)^2}} \approx 1$$

FIG. 1A

$$y = \frac{2\pi(mcr)}{h} = \frac{2\pi(2.1765x10^{-8}kg)\frac{(1.6162x10^{-35}m)}{(5.3911x10^{-44}s)}(1.6162x10^{-35}m)}{\frac{(1.6162x10^{-35}m)^2(2.1765x10^{-8}kg)(5.3911x10^{-44}s)}{(5.3911x10^{-44}s)^2}} \approx 1$$

FIG. 1B

Here, the (x) variable of the exponent in equation (3A) is made to represent the "charge" aspect of the function with the application of the respective charge to mass ratio, and, as will be shown later, the ratio will be useful for constructing an expression for theoretical and conventional electromagnetic potentials, etc.

Now, equation (3A) is made into unified field function (4A) by first taking equation (3A)

$$f = \pm e^{\left[\frac{1}{N} n_1 \frac{\pm 2\pi(qcr)}{h_q} + \frac{1}{N} n_2 \frac{\pm 2\pi(mcr)}{h}\right]} \qquad \text{Eq. (3A)}$$

and rewriting it as Eq. (3B)

$$f = {}^{\pm}e^{\left[\frac{1}{N} n_1 \frac{\pm 2\pi(qcr)}{h_q}\right]} * {}^{\pm}e^{\left[\frac{1}{N} n_2 \frac{\pm 2\pi(mcr)}{h}\right]}, \qquad \text{Eq. (3B)}$$

and then reflecting the (x) variable (which relates to charge) while treating (c) and 1/N as constants, such that

$$\pm f = {}^{\pm}c \frac{1}{N} * \ln\left[\frac{n_1 * 2\pi(qr)}{h_q}\right] * e^{\left[\frac{1}{N} n_2 * \frac{\pm 2\pi(mcr)}{h}\right]}.$$

Here, the reflection of the function is considered to be a mathematical representation of an important physical aspect of the oscillatory trajectory of the flow of mass-energy in the unified field as will be indicative later.

Then, upon taking one partial derivative by keeping the exponential portion of the function which relates to the (y) variable (mass) constant equation (4A) is produced as follows:

$$\pm f_x(x,y) = {}^{\pm}\frac{1}{N}\frac{h_q c}{n_1 * 2\pi(qr)} * e^{\left[\frac{1}{N}\frac{n_2 *^{\pm} 2\pi(mcr)}{h}\right]}. \qquad \text{Eq. (4A)}$$

In result, equation (4A) is a general unified field function which provides families of functions for the potential of the unified field presented herein, which can be related to the conventional strong, weak, electromagnetic, and gravitational fields.

Equation (4A) can be applied to describe both theoretical and conventional nuclear, electromagnetic, and gravitational potentials. However, the essential difference between the function of equation (4A) and the functions of conventional Newtonian and Coulombic potentials resides in the presence of the exponential term.

In convention, the exponential term is present along with the inverse function in the function which describes nuclear potential (e.g., the Yukawa potential). In which case, the exponential term in the function of conventional nuclear potential is considered to approach a value of one as the mass in the exponent approaches a value of zero. While, the exponential term is absent in the functions which conventionally describe Newtonian gravitational and Coulombic potentials.

However, to the contrary, the exponential term is applied with the inverse function in the unified field function herein, and thus is included in the definition of not only the theoretical nuclear potential, but also included in the definition of the theoretical electromagnetic and gravitational potentials (effectively including modified forms of Newtonian and Coulombic potentials). Wherein, in the present theory, the exponential term only approaches a value of zero in expressions for electromagnetic and gravitational potentials (i.e., the potential is not normalized for the nuclear region as in convention). While, in physical terms, the exponential term plays an important role in the unified field function in allowing for the three dimensional spatial aspect of the function (i.e., the three dimensional aspect of the oscillatory trajectory of the flow of mass-energy in the unified field) as will be indicative more so later.

Next, a theoretical unified field potential equation (4B) representing a portion of the unified field is arrived at by applying the following member functions from the families of functions in equation (4A)

$$f = \frac{1}{N}\frac{h_q c}{n_1 * 2\pi(qr)} * e^{\left[\frac{1}{N}\frac{n_2 * {}^{-}2\pi(mcr)}{h}\right]},$$

and then taking the negative of the functions for convention as shown in equation (4B)

$$f = {}^{-}\frac{1}{N}\frac{h_q c}{n_1 * 2\pi(qr)} * e^{\left[\frac{1}{N}\frac{n_2 * {}^{-}2\pi(mcr)}{h}\right]}. \qquad \text{Eq. (4B)}$$

(Note that the signs used for the families of functions in equation 4A pertain to the signs on the axes which relate to the functions, while the sign of the function in equation 4B relates to the direction of potential in conventional terms.)

Next, the value of the theoretical unified potential function in equation (4B) approximately equals

${}^{-}\frac{1}{2}c^2$ when 1/N is considered equal to one, and $n_1 \approx 2$ and $n_2 \approx 0$,

$$f = \frac{{}^{-}h_q c}{\approx 4\pi(qr)} * e^{\left[\frac{\approx^{-} 0\pi(mcr)}{h}\right]}{}_{\approx}{}^{-}\frac{1}{2}c^2 \qquad \text{Eq. (4C)}$$

or $$f = \frac{{}^{-}h_q c}{\approx 4\pi(qr)} * e^{\left[\frac{\approx^{-} 0*2\pi(mcr)}{h}\right]}{}_{\approx}{}^{-}\frac{1}{2}c^2.$$

Wherein, equation (4C) is considered to represent one half of one portion of the family of unified field potential functions as will be elaborated upon later.

Now, since $\frac{2\pi qcr}{h_q} = \frac{2\pi mcr}{h} \approx 1$, then $\frac{q}{h_q} = \frac{m}{h}$ and $\frac{h_q}{q} = \frac{h}{m}$. Wherein, after taking the gradient of equation (4C), breaking the result down into vector components, and then substituting $\frac{h}{m}$ for $\frac{h_q}{q}$ in one term, equation (4C) can be written as follows in equation (5A) in terms of vector components in the form of electric charge and mass gradients which represent the electromagnetic and gravitational gradient components of the unified field, respectively:

$$\left(\frac{1}{\sqrt{2}}\frac{{}^{-}h_q c}{\approx 4\pi(qr^2)} * e^{\left[\frac{\approx^{-} 0\pi(mcr)}{h}\right]}\right)^2 + \left(\frac{1}{\sqrt{2}}\frac{{}^{-}hc}{\approx 4\pi(mr^2)} * e^{\left[\frac{\approx^{-} 0\pi(mcr)}{h}\right]}\right)^2 = \left(\frac{{}^{-}h_q c}{\approx 4\pi(qr^2)} * e^{\left[\frac{\approx^{-} 0\pi(mcr)}{h}\right]}\right)^2,$$

Eq. (5A)

or one half of the respective unified field gradient portion can be written as

$$\frac{-1}{\approx 2}\nabla\varphi \text{ (unified field gradient portion)} = -\sqrt{\left(\frac{1}{\sqrt{2}}\frac{{}^{-}h_q c}{\approx 4\pi(qr^2)} * e^{\left[\frac{\approx^{-}0\pi(mcr)}{h}\right]}\right)^2 + \left(\frac{1}{\sqrt{2}}\frac{{}^{-}hc}{\approx 4\pi(mr^2)} * e^{\left[\frac{\approx^{-}0\pi(mcr)}{h}\right]}\right)^2} =$$

$$\frac{{}^{-}h_q c}{\approx 4\pi(qr^2)} * e^{\left[\frac{\approx^{-}0\pi(mcr)}{h}\right]}$$

Eq. (5B)

Here (∇) is gradient, and $\varphi = \frac{{}^{-}h_q c}{2\pi(qr)} * e^{\left[\frac{\approx^{-}0\pi(mcr)}{h}\right]} = \frac{{}^{-}K_T q}{r} * e^{\left[\frac{\approx^{-}0\pi(mcr)}{h}\right]}$ wherein K_T is a theoretical precursor to the conventional electrostatic constant K_C as will be described more so later.

The square of one portion of the theoretical gravitational (mass) gradient of the unified field (i.e., a theoretical gravitational field gradient which can be related, for example, to the conventional Newtonian gravitational potential) is represented by the square of one vector component, i.e., the (y) component, in equation (5A). Wherein, in terms of the respective theoretical gravitational potential,

$\frac{{}^{-}hc}{\approx 4\pi(mr)} * e^{\left[\frac{\approx^{-}0\pi(mcr)}{h}\right]} \approx {}^{-}\frac{1}{2}c^2$ when

$h = 2\pi mcr \approx 2\pi(2.1765x10^{-8})\left(\frac{1.6162x10^{-35}}{5.3911x10^{-44}}\right)(1.6162x10^{-35}) = 6.6258x10^{-34}$, such that $e^{\left[\frac{\approx^{-}0\pi(mcr)}{h}\right]} \approx 1$ and the units in $e^{\left[\frac{\approx^{-}0\pi(mcr)}{h}\right]}$ cancel and thus the term can be dropped, and such that $\frac{{}^{-}hc}{\approx 4\pi(mr)} = \frac{{}^{-}2\pi mc^2 r}{\approx 4\pi(mr)} \approx {}^{-}\frac{1}{2}c^2$.

Also, figure (2A) shows the production of approximately one half of the conventional gravitational potential,

i.e., $\approx^{-}\frac{1}{2}G_T * \frac{m}{r}$, after the cancellation of certain units in $\frac{^{-}hc}{\approx 4\pi(mr)}$ (while neglecting the sign).

$$\frac{hc}{\approx 4\pi(mr)} \Rightarrow \frac{(kg*m^2*\cancel{s})}{(s)^2}\frac{(m)}{(\cancel{s})}\frac{(1)}{(kg*m)} \Rightarrow \frac{(m^3)}{(kg*s^2)}\frac{(kg)}{(m)} \Rightarrow \approx \frac{1}{2}G_T\frac{(kg)}{(m)}$$

FIG. 2A

In which case, (G_T) takes on the same numerical value as the conventional gravitational constant, i.e.,

$6.6\,x10^{-11}$, using Planck units as shown below:

$$G_{Planck} = \frac{(m)^3}{(kg)(s)^2} = \frac{(l_p)^3}{(m_P)(t_p)^2} = \frac{(1.6162\,x10^{-35})^3}{(2.1765\,x10^{-8})(5.3911\,x10^{-44})^2} = 6.6738\,x10^{-11}\ .$$

Similarly, the square of one portion of the theoretical electromagnetic (electric charge) gradient of the unified field, (i.e., a theoretical electromagnetic field gradient which can be related to, for example, the conventional Coulombic potential) is represented by the square of the other vector component, i.e., the (x) component, in equation (5A). In which case, an equivalent argument for the terms of the respective theoretical electromagnetic potential can be made in which $\frac{^{-}h_q c}{\approx 4\pi(qr)} * e^{\left[\frac{\approx^{-}0\pi(mcr)}{h}\right]} \approx ^{-}\frac{1}{2}c^2$ when h_q=h=2πmcr, such that

$e^{\left[\frac{\approx^{-} 0\pi(mcr)}{h}\right]} \approx 1$ and thus the term can be dropped, and such that

$\frac{^{-}h_q c}{\approx 4\pi(qr)} = \frac{^{-}hc}{\approx 4\pi(mr)} = \frac{^{-}2\pi mc^2 r}{\approx 4\pi(mr)} \approx {}^{-}\frac{1}{2}c^2$. Wherein, $\frac{^{-}h_q c}{\approx 4\pi(qr)} * e^{\left[\frac{\approx^{-} 0\pi(mcr)}{h}\right]}$ is considered the theoretical electromagnetic potential counterpart to the theoretical gravitational potential shown before.

Moreover, similarly, figure (2B) shows the conversion of the units of theoretical electromagnetic potential $\frac{^{-}h_q c}{\approx 4\pi(qr)}$ into the units of conventional Coulombic potential, including the units of the conventional electrostatic constant, i.e., the units of $\frac{N * m^2}{C^2}$, for the production of a theoretical approximation of one half of the conventional electrostatic potential, i.e., $\approx^{-} \frac{1}{2} K_C * \frac{q}{r}$, after the cancellation of certain units while again applying the following charge to mass ratio $\frac{(q_p)}{(m_p)}$ which has the units $\frac{(C)}{(kg)}$ (also while neglecting the sign):

$$\frac{hc\frac{(q_p)}{(m_p)}}{\approx 4\pi(mr)\frac{(q_p)}{(m_p)}\frac{(q_p)}{(m_p)}} \Rightarrow \frac{h_q c}{\approx 4\pi(qr)\frac{(q_p)}{(m_p)}} \Rightarrow \frac{\cancel{(kg)}\frac{(C)}{\cancel{(kg)}}(m)^2\cancel{(s)}\frac{(m)}{\cancel{(s)}}}{(s)^2\cancel{(kg)}\frac{(C)}{\cancel{(kg)}}\frac{(C)}{(kg)}(m)} \Rightarrow \frac{(N)*(m)^2}{(C)^2}\frac{(C)}{(m)} \Rightarrow \approx \frac{1}{2}K_C\frac{(C)}{(m)}$$

FIG. 2B

Now, substituting $\approx^{-}\frac{1}{2}K_T\frac{q}{r}$ for $\frac{^{-}h_q c}{\approx 4\pi(qr)}$ in equation (4C) provides for a different expression for theoretical unified potential:

$$f = {}^{-}\frac{1}{\approx 2}K_T\frac{q}{r} * e^{\left[\frac{\approx^{-}0\pi(mcr)}{h}\right]} \approx {}^{-}\frac{1}{2}c^2$$

which can be rewritten as Eq. (6)

$$f = {}^{-}\frac{1}{\approx 2}K_T(q) * \frac{e^{\left[\frac{\approx^{-}0\pi(mcr)}{h}\right]}}{r} \approx {}^{-}\frac{1}{2}c^2 .$$ Eq. (6)

Here, equation (6) is considered to be another expression which represents one half of a given portion of the theoretical unified potential. Wherein, a whole portion of theoretical unified potential is arrived at by adding two equivalent portions of the function from equation (6) as shown in equation (7A) as follows:

$$V_{(\text{whole unified field potential portion})} = {}^{-}\frac{1}{\approx 2}K_T(q) * \frac{e^{\left[\frac{\approx^{-}0\pi(mcr)}{h}\right]}}{r} + {}^{-}\frac{1}{\approx 2}K_T(q) * \frac{e^{\left[\frac{\approx^{-}0\pi(mcr)}{h}\right]}}{r} \approx$$

$${}^{-}1K_T(q) * \frac{e^{\left[\frac{^{-}0\pi(mcr)}{h}\right]}}{r} \approx {}^{-}1c^2$$

Eq. (7A)

or

$$V_{(\text{whole unified field potential portion})} \approx {}^{-}K_T\left(\frac{q}{2}+\frac{q}{2}\right) * \frac{e^{\left[\frac{{}^{-}0\pi(mcr)}{h}\right]}}{r} \approx {}^{-}K_T(q) * \frac{e^{\left[\frac{{}^{-}0\pi(mcr)}{h}\right]}}{r} \approx {}^{-}1c^2 .$$

Then, after substituting $\frac{{}^{-}1}{\approx 2} G_T(m) * \frac{e^{\left[\frac{\approx{}^{-}0\pi(mcr)}{h}\right]}}{r}$ for $\frac{{}^{-}1}{\approx 2} K_T(q) * \frac{e^{\left[\frac{\approx{}^{-}0\pi(mcr)}{h}\right]}}{r}$ for one portion (addend) in equation (7A) a different expression for a whole portion of theoretical unified potential is produced in equation (7B) by the addition of theoretical electromagnetic and gravitational potential functions as follows:

$$V_{(\text{whole unified field potential portion})} = \frac{{}^{-}1}{\approx 2} K_T(q) * \frac{e^{\left[\frac{\approx{}^{-}0\pi(mcr)}{h}\right]}}{r} + \frac{{}^{-}1}{\approx 2} G_T(m) * \frac{e^{\left[\frac{\approx{}^{-}0\pi(mcr)}{h}\right]}}{r} \approx$$

$${}^{-}1K_T(q) * \frac{e^{\left[\frac{{}^{-}0\pi(mcr)}{h}\right]}}{r} \approx {}^{-}1c^2$$

Eq. (7B)

when $n_1 \approx 2$ and $n_2 \approx 0$.

While when $n_1 \approx 1$ and $n_2 \approx 1$, then:

$$V_{(\text{whole unified field potential portion})} = {}^{-}\frac{1}{\approx 1} K_T(q) * \frac{e^{\left[\frac{\approx^{-}2\pi(mcr)}{h}\right]}}{r} + {}^{-}\frac{1}{\approx 1} G_T(m) * \frac{e^{\left[\frac{\approx^{-}2\pi(mcr)}{h}\right]}}{r} \approx {}^{-}2K_T(q) * \frac{e^{\left[\frac{^{-}2\pi(mcr)}{h}\right]}}{r} .$$

Eq. (7C)

Note that an equation for a whole portion of unified potential by the addition of electromagnetic and gravitational potential functions for when (n_1) and (n_2) are any of their other complementary values can also be achieved similarly.

Next, returning to gradients, upon substituting $\approx {}^{-}\frac{1}{2} K_T \frac{q}{r^2}$ for $\frac{^{-}h_q c}{\approx 4\pi(qr^2)}$ and $\approx {}^{-}\frac{1}{2} G_T \frac{m}{r^2}$ for $\frac{^{-}hc}{\approx 4\pi(mr^2)}$ in the components in equation (5A), and upon substituting $\approx {}^{-}\frac{1}{2} K_T \frac{q}{r^2}$ for $\frac{^{-}h_q c}{\approx 4\pi(qr^2)}$ in the respective sum in equation (5A), another expression for the addition of the square of theoretical electromagnetic and gravitational gradients is provided in resulting equation (8A):

$$\left({}^{-}\frac{1}{\approx 2\sqrt{2}} K_T(q) * \frac{e^{\left[\frac{\approx^{-}0\pi(mcr)}{h}\right]}}{r^2} \right)^2 + \left({}^{-}\frac{1}{\approx 2\sqrt{2}} G_T(m) * \frac{e^{\left[\frac{\approx^{-}0\pi(mcr)}{h}\right]}}{r^2} \right)^2 \approx \left({}^{-}\frac{1}{2} K_T(q) * \frac{e^{\left[\frac{^{-}0\pi(mcr)}{h}\right]}}{r^2} \right)^2 .$$

Eq. (8A)

Here, equation (8A) is considered to represent another expression for the square of one half of the total unified field gradient of a given portion of the unified field expressed in terms which include electromagnetic and gravitational components. While the square of the whole unified field gradient of a given portion of the unified field in related terms is considered to be arrived at by adding two equivalent gradients in the addend squares of the gradient functions from equation (8A) as follows:

$$\left({}^{-}\frac{1}{\approx 2\sqrt{2}} K_T(q) * \frac{e^{\left[\frac{\approx{}^{-}0\pi(mcr)}{h}\right]}}{r^2} + {}^{-}\frac{1}{\approx 2\sqrt{2}} K_T(q) * \frac{e^{\left[\frac{\approx{}^{-}0\pi(mcr)}{h}\right]}}{r^2} \right)^2 +$$

$$\left({}^{-}\frac{1}{\approx 2\sqrt{2}} G_T(m) * \frac{e^{\left[\frac{\approx{}^{-}0\pi(mcr)}{h}\right]}}{r^2} + {}^{-}\frac{1}{\approx 2\sqrt{2}} G_T(m) * \frac{e^{\left[\frac{\approx{}^{-}0\pi(mcr)}{h}\right]}}{r^2} \right)^2 \approx \left({}^{-}1K_T(q) * \frac{e^{\left[\frac{{}^{-}0\pi(mcr)}{h}\right]}}{r^2} \right)^2$$

such that

$$\left({}^{-}\frac{1}{\approx \sqrt{2}} K_T(q) * \frac{e^{\left[\frac{\approx{}^{-}0\pi(mcr)}{h}\right]}}{r^2} \right)^2 + \left({}^{-}\frac{1}{\approx \sqrt{2}} G_T(m) * \frac{e^{\left[\frac{\approx{}^{-}0\pi(mcr)}{h}\right]}}{r^2} \right)^2 \approx \left({}^{-}1K_T(q) * \frac{e^{\left[\frac{{}^{-}0\pi(mcr)}{h}\right]}}{r^2} \right)^2 .$$

Eq. (8B)

or a whole gradient of a given portion of the unified field can be written as

$$-\sqrt{\left(-\frac{1}{\approx\sqrt{2}}K_T(q)*\frac{e^{\left[\frac{\approx^{-}0\pi(mcr)}{h}\right]}}{r^2}\right)^2+\left(-\frac{1}{\approx\sqrt{2}}G_T(m)*\frac{e^{\left[\frac{\approx^{-}0\pi(mcr)}{h}\right]}}{r^2}\right)^2}\approx^{-}1K_T(q)*\frac{e^{\left[\frac{^{-}0\pi(mcr)}{h}\right]}}{r^2}$$

Eq. (8C)

Here, the addition of two equivalent functions in equation (8B) involves the vector addition of two portions of the unified field which can be more clearly understood by referring to the geometry of the unified field described later as with respect to, in particular, figures 7A, 7B, 7C, and 7D. Note that an equation for the square of the whole gradient of a given portion of the unified field for when (n_1) and (n_2) are any of their other complementary values can also be achieved similarly.

Nevertheless, the theoretical total potential of a static elementary particle can be considered to be arrived at by the following summation shown in equation (9A) (for eight octants):

$$V_{(\text{particle total potential})}=4*\sum V=4*\left[\left(\frac{^{-}h_qc}{n_1*2\pi(qr)}*e^{\left[\frac{n_2*^{-}2\pi(mcr)}{h}\right]}+\frac{^{-}h_qc}{n_1*2\pi(qr)}*e^{\left[\frac{n_2*^{-}2\pi(mcr)}{h}\right]}\right)+\left(\frac{^{-}h_qc}{n_1*2\pi(qr)}*e^{\left[\frac{n_2*^{-}2\pi(mcr)}{h}\right]}+\frac{^{-}h_qc}{n_1*2\pi(qr)}*e^{\left[\frac{n_2*^{-}2\pi(mcr)}{h}\right]}\right)+\ldots\right]\approx 1\frac{^{-}K_T(q)}{r}$$

Eq. (9A)

wherein,

$$4\frac{\approx^{-}K_T(q)}{r}*\frac{1}{e^{\left[\frac{\approx 0\pi(mcr)}{h}\right]}}-8\frac{\approx^{-}K_T(q)}{r}*\frac{1}{e^{\left[\frac{2\pi(mcr)}{h}\right]}}\approx 1\frac{^{-}K_T(q)}{r}.$$

In the summation, (V) is potential, and (n_1) and (n_2) are the same complementary pair for a pair of terms (top and bottom sides) inside parentheses, while (n_1) goes from ≈2 to ≈1 as (n_2) goes from ≈0 to ≈1 sequentially from one parenthetical term to the next in the summation.

While furthermore, the theoretical total potential of a system (e.g., a system of bonded nucleons) can be considered to be arrived at by the following summation shown in equation (9B):

$$V_{\text{(system total potential)}}=\sum 4*V=4*\left[\left(\frac{^{-}h_q c}{n_1*2\pi(qr)}*e^{\left[\frac{n_2*^{-}2\pi(mcr)}{h}\right]}+\frac{^{-}h_q c}{n_1*2\pi(qr)}*e^{\left[\frac{n_2*^{-}2\pi(mcr)}{h}\right]}\right)+\ldots\right]+$$

$$4*\left[\left(\frac{^{-}h_q c}{n_1*2\pi(qr)}*e^{\left[\frac{n_2*^{-}2\pi(mcr)}{h}\right]}+\frac{^{-}h_q c}{n_1*2\pi(qr)}*e^{\left[\frac{n_2*^{-}2\pi(mcr)}{h}\right]}\right)+\ldots\right]+\ldots$$

Eq. (9B)

Wherein, in the summation shown in equation (9B), (n_1) and (n_2) are the same complementary pair for a pair of terms (top and bottom sides) inside parentheses, and (n_1) goes from ≈2 to ≈1 as (n_2) goes from ≈0 to ≈1 sequentially from one parenthetical term to the next in the bracketed terms (particle potentials). In which case, here, the term 1/N is excluded since it is considered to cancel in the summation of whole particles.

Moreover, the resultant gradient extending out from an elementary particle or a system of particles can be written as:

$$\nabla \varphi_{\text{(systeml)}} = \frac{\partial \varphi}{\partial x}\hat{i} + \frac{\partial \varphi}{\partial y}\hat{j} + \frac{\partial \varphi}{\partial z}\hat{k}$$

and the respective Laplacian is:

$$\nabla^2 \varphi = \left(\frac{\partial^2}{\partial x^2} + \frac{\partial^2}{\partial y^2} + \frac{\partial^2}{\partial z^2} \right) \varphi$$

Wherein ∇ is gradient and ∇^2 is the Laplacian such that in both cases $\varphi = 8 * \sum \frac{{}^{-}h_q c}{n_1 * 2\pi(qr)} * e^{\left[\frac{n_2 * {}^{-}2\pi(mcr)}{h}\right]}$;

and $1 < n_1 < 2$ and correspondingly $1 > n_2 > 0$.

Note here how the form of the terms of a time independent particle in quantum mechanics support the form of the potential of the unified field presented herein:

$$\psi(x) = Ae^{-ikx} = {}^{\frac{-i2\pi mcx}{h}} = Ae^{\frac{-i2\pi mcr}{h}}$$ (when k=2πmc/h and x=r)

Wherein, (A) can be a scalar amplitude, such that, for example, $A = 1/2kx^2 \equiv mgh$ which pertains to $\approx {}^{-}G_T m/r$

(when the other mass of potential energy is positioned at infinity) which, herein, is equivalent to $\approx^{-}K_T q/r$; or (A) can be a vector amplitude, e.g., E (electric vector strength), i.e., $^{-}K_C q/r^2$, which is the gradient of the potential $^{-}K_C q/r$ which herein relates to $\approx^{-}K_T q/r$ which again, herein, is equivalent to $\approx^{-}G_T m/r$.

Next, a general theoretical unified force equation (10A) pertaining to a portion of the unified field, which can be related to the conventional strong force (including the conventional residual nuclear force), the conventional weak force, and the conventional electromagnetic and gravitational forces, can be achieved by taking the derivative of the resulting potential of equation (4B) as follows upon substituting $^{-}\frac{1}{N}\frac{1}{n_1}K_T\frac{q}{r}$ for $\frac{1}{N}\frac{^{-}h_q c}{n_1 * 2\pi(qr)}$ (wherein the derivative is denoted here as taking the second regular derivative of a first regular derivative):

$$f' = {}^{-}\frac{1}{N}\frac{1}{n_1}K_T(q)*\frac{e^{\left(\frac{1}{N}\frac{n_2 *^{-} 2\pi(mcr)}{h}\right)}}{r}$$

$$D_u f' = \frac{1}{N}\frac{1}{n_1}K_r * D_u{}^{-}\frac{1}{\left(\frac{1}{q}\frac{(q_p)}{(m_p)} * r * e^{\left[\frac{1}{N}\frac{n_2 * 2\pi(mcr)}{h}\right]}\right)}$$

wherein K_r is the remainder of K_T without the charge to mass ratio $\frac{(q_p)}{(m_p)}$, such that

$$f'' = \frac{1}{N}\frac{1}{n_1}K_r *^{-} \frac{1}{\left(\frac{1}{q}\frac{(q_p)}{(m_p)} * r * e^{\left[\frac{1}{N}\frac{n_2 * 2\pi(mcr)}{h}\right]}\right)^2}.$$

Here, (q) in the numerator is rewritten and placed in the denominator as $\left(\frac{1}{q}\right)$ along with (r), $\frac{(q_p)}{(m_p)}$ (the charge to mass ratio), and $e^{\left[\frac{1}{N}\frac{n_2 * 2\pi(mcr)}{h}\right]}$ such that $\left(\frac{1}{q}\frac{(q_p)}{(m_p)} * r * e^{\left[\frac{1}{N}\frac{n_2 * 2\pi(mcr)}{h}\right]}\right) = u$ in the function

$f = \frac{1}{N}\frac{1}{n_1}K_r \,^{-}\frac{1}{u}$. In which case,

$$D_u \frac{1}{N}\frac{1}{n_1}K_r \,^{-}\frac{1}{u} = \frac{1}{N}\frac{1}{n_1}K_r \frac{1}{u^2} = \frac{1}{N}\frac{1}{n_1}K_r \frac{1}{\left(\frac{1}{q}\frac{(q_p)}{(m_p)} * r * e^{\left[\frac{1}{N}\frac{n_2 * 2\pi(mcr)}{h}\right]}\right)^2}$$

such that:

$$f'' = ^{-}\frac{1}{N}\frac{1}{n_1}K_C \frac{q^2}{r^2} * e^{\left[2 * \left(\frac{1}{N}\frac{n_2 *^{-} 2\pi(mcr)}{h}\right)\right]}$$

or

$$f'' = ^{-}\frac{1}{N}\frac{1}{n_1}K_C (q^2) * \frac{e^{\left[2 * \left(\frac{1}{N}\frac{n_2 *^{-} 2\pi(mcr)}{h}\right)\right]}}{r^2} \qquad \text{Eq. (10A)}$$

Wherein, the negative of the resulting derivative was taken for convention, and the resulting force is in newtons when h=2πmcr, such that the units of $\left[2 * \left(\frac{1}{N} \frac{n_2 * {}^{-}2\pi(mcr)}{h}\right)\right]$ in the exponent cancel.

Then, with respect to the sum in equation (7B), $f'' \approx {}^{-}\frac{1}{N} 1K_C(q^2) * \frac{e^{\left[2 * \left(\frac{1}{N} \frac{{}^{-}0\pi(mcr)}{h}\right)\right]}}{r^2}$ when $n_1 \approx 2$ and $n_2 \approx 0$; and, with respect to the sum in equation (7C), $f'' \approx {}^{-}\frac{1}{N} 2K_C(q^2) * \frac{e^{\left[2 * \left(\frac{1}{N} \frac{{}^{-}2\pi(mcr)}{h}\right)\right]}}{r^2}$ when $n_1 \approx 1$ and $n_2 \approx 1$.

A theoretical electromagnetic force equation (11) for the unified field (i.e., a force equation which can be related, in particular, to the conventional electromagnetic force, e.g., at weak field and low velocity), and a theoretical gravitational force equation (12) for the unified field (i.e., a force equation which can be related, in particular, to the conventional Newtonian gravitational force, e.g., at weak field and low velocity), can be produced from equation (10A), or can be produced by applying a similar second derivative process to each of the two halves of potential which produce the result (sum) of equation (7B) as shown below (while 1/N is considered equal to one):

$$V_{\text{(whole unified field potential portion)}} = {}^{-}\frac{1}{\approx 2} K_T(q) * \frac{e^{\left[\frac{\approx {}^{-}0\pi(mcr)}{h}\right]}}{r} + {}^{-}\frac{1}{\approx 2} G_T(m) * \frac{e^{\left[\frac{\approx {}^{-}0\pi(mcr)}{h}\right]}}{r} \approx {}^{-}1K_T(q) * \frac{e^{\left[\frac{{}^{-}0\pi(mcr)}{h}\right]}}{r} \approx {}^{-}1c^2 .$$

Eq. (7B)

In which case, electromagnetic force equation (11) is arrived at upon taking the second derivative of the charge portion

$$D_u \frac{1}{\approx 2} K_r \, {}^{-}\frac{1}{u} = \frac{1}{\approx 2} K_r \frac{1}{u^2} = \frac{1}{\approx 2} K_r \frac{1}{\left(\frac{1}{q} \frac{(q_p)}{(m_p)} * r * e^{\left[\frac{\approx 0\pi(mcr)}{h} \right]} \right)^2}$$

such that

$$f'' \approx {}^{-}\frac{1}{2} K_C (q^2) * \frac{e^{\left[2 * \left(\frac{{}^{-}0\pi(mcr)}{h} \right) \right]}}{r^2} = em_F \qquad \text{Eq. (11)}$$

and gravitational force equation (12) is arrived at upon taking the second derivative of the mass portion

$$D_u \frac{1}{\approx 2} G_T \, {}^{-}\frac{1}{u} \approx \frac{1}{\approx 2} G_T \frac{1}{u^2} \approx \frac{1}{\approx 2} G_T \frac{1}{\left(\frac{1}{m} * r * e^{\left[\frac{\approx 0\pi(mcr)}{h} \right]} \right)^2}$$

such that

$$f''\approx {}^{-}\frac{1}{2}G_T(m^2)*\frac{e^{\left[2*\left(\frac{^{-}0\pi(mcr)}{h}\right)\right]}}{r^2}=g_F\,. \qquad \text{Eq. (12)}$$

Wherein, $1/n_1$, i.e., ≈½, is treated as a constant in these cases, and, here also, the negatives of the resulting derivatives were taken for convention.

Note that $K_r\dfrac{1}{\left(\dfrac{1}{q}\dfrac{(q_p)}{(m_p)}*r*e^{\left[\frac{\approx 0\pi(mcr)}{h}\right]}\right)^2}=G_T\dfrac{1}{\left(\dfrac{1}{m}*r*e^{\left[\frac{\approx 0\pi(mcr)}{h}\right]}\right)^2}$ in the forgoing derivatives since $\dfrac{1}{q}\dfrac{(q_p)}{(m_p)}=\dfrac{1}{m}$ when $(q)=(q_p)$ and $(m)=(m_p)$. Also, note that the additional charge to mass ratio applied in the denominator in (K_C) in figure (2B) is also derived in the forgoing second derivative which pertains to equation (11) along with the other charge to mass ratio in the numerator, such that only a value of one is effectively applied, which, accordingly, does not affect the respective function (as the first set of charge to mass ratios applied in figure 1A). Furthermore, note that the squaring of the potential functions in the process of taking the second derivatives in order to obtain the electromagnetic and gravitational force functions are considered to pertain to the symmetry of the internal structure, and the self interaction of virtual particles (described later) at Planck scale in the unified field. Moreover, notice that each of two equivalent unified field portions supplies one half of the force needed to create a whole respective force as exemplified in the gravitational lensing effect described later.

Nevertheless, consider the following equivalence of the electromagnetic and gravitational forces from the sum of two half portions of each force at Planck scale from equations (11) and (12) when $n_1 \approx 2$ and $n_2 \approx 0$ wherein the exponential terms for the electromagnetic and gravitational force functions are each approximately one, and thus dropped:

$$\approx^{-} K_C \frac{q^2}{r^2} \approx^{-} 8.98x10^9 * \frac{(1.87x10^{-18})^2}{(1.61x10^{-35})^2} \approx^{-} 1.21x10^{44} \approx F_P$$

$$\approx^{-} G_T \frac{m^2}{r^2} \approx^{-} 6.67x10^{-11} * \frac{(2.17x10^{-8})^2}{(1.61x10^{-35})^2} \approx^{-} 1.21x10^{44} \approx F_P$$

when $(q) = (q_p)$, $(m) = (m_p)$, and $(r) = (l_p)$

Now, consider the relative force strengths shown below with respect to the following approximate equivalences of $^{-}\hbar c$ in Planck units taken from the "fundamental" forces established above:

$$\approx^{-} K_C q^2 \approx^{-} 8.98x10^9 * (1.87x10^{-18})^2 \approx^{-} 3.14x10^{-26} \approx^{-} \hbar c$$

$$\approx^{-} G_T m^2 \approx^{-} 6.67x10^{-11} * (2.17x10^{-8})^2 \approx^{-} 3.14x10^{-26} \approx^{-} \hbar c$$

when $(q) = (q_p)$ and $(m) = (m_p)$

For conventional gravitational force strength:

$$\frac{G_C (\text{proton mass})^2}{\approx K_C (q_P)^2} \approx \frac{^{-}6.67x10^{-11} * (1.67x10^{-27})^2}{^{-}8.98x10^{+9} * (1.87x10^{-18})^2} \approx 5.92x10^{-39}$$

For conventional electromagnetic force strength:

$$\frac{K_C(\text{electron charge})^2}{\approx K_C(q_P)^2} \approx \frac{{}^-8.98x10^{+9} * (1.60x10^{-19})^2}{{}^-8.98x10^{+9} * (1.87x10^{-18})^2} \approx 7.32x10^{-3}$$

For conventional weak force strength:

$$\frac{(\text{electron charge})^2}{\approx K_C(q_P)^2} \approx \frac{{}^-(1.60x10^{-19})^2}{{}^-8.98x10^{+9} * (1.87x10^{-18})^2} \approx 8.15x10^{-13}$$

For conventional strong force strength:

$$\frac{K_C(q_P)^2}{\approx K_C(q_P)^2} \approx \frac{{}^-8.98x10^{+9} * (1.87x10^{-18})^2}{{}^-8.98x10^{+9} * (1.87x10^{-18})^2} \approx 1 .$$

Here, the agreement of these relative force strengths with convention with respect to the terms taken from the fundamental forces at Planck scale established above, which are approximately equal to ${}^-\hbar c$, support the values and forms of the functions of the present theory of unification, and address the problem pertaining to gravitational interactions at the Planck "length scale."

CONSTRUCTION OF THE UNIFIED FIELD:

Now, "virtual particles" (with momentum) are considered to follow the gradient functions previously presented, and are considered to provide substance to the structure and function of the unified field. Accordingly, the unified field theory herein applies a four dimensional gradient vector system which provides for an understanding of the internal structure of the unified field, elementary particles, etc. This greater depth of information proposes to allow for a more detailed understanding of events in physics (e.g., for predictability).

The virtual particles which follow a gradient function in the respective families of functions described previously are considered to transition through values of potential while having complementary values of (n_1) and (n_2), and while having one constant value of 1/N. Wherein, when 1/N is equal to one amongst member functions, the unified field is considered to be in an "elementary" state, while when 1/N is an integer number greater than one amongst member functions, the unified field is considered to experience a macroscopic form of quantization.

The potential of a virtual particle is considered to change as it follows a gradient function due to changes in the values of its parameters as it reflects (screws) in its trajectory during oscillation along its respective virtual particle path (gradient function) as shown in figures (3A) and (3B).

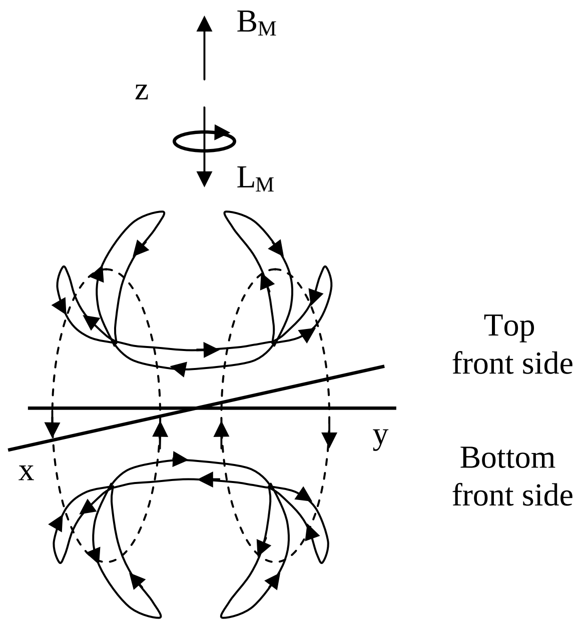

Side view of a
negative unified field

FIG. 3A

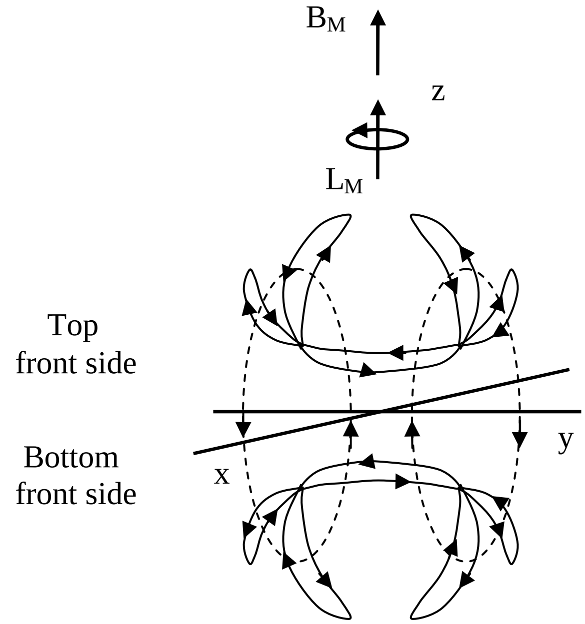

Side view of a
positive unified field

FIG. 3B

Figures (3A) and (3B) show a select few virtual particle paths, which include "more bent" and "less bent" virtual particle paths, in simplified drawings of elementary negative and positive unified fields (conservative vector fields). Wherein, each virtual particle path is comprised in a respective “band” of virtual particle paths, and each band of virtual particle paths comprises a multitude of virtual particle paths which each comprise respective curvature, dimensions, and alignments; complementary values of (n_1) and (n_2); and a constant value of 1/N. (Note that the significance of "more bent" and "less bent" virtual particle paths will be explained more so later as, for example, with respect to in figures 26A and 26B. Also, note that references to the front and back sides in figures 3A and 3B are relative references.)

Virtual particles are considered to account for parameters of a unified field including the respective flow of virtual particle "electric" charge (q) as shown directed along the arrows in figures (3A) and (3B). In which case, the virtual particle paths form currents which produce the unified field of, for example, an elementary electrically charged particle with an intrinsic angular momentum (L_M) (i.e., intrinsic spin), and a "macroscopic" magnetic field (B_M) for the electrically charged particle as a whole along a respective (z) axis (also shown in figures 3A and 3B). While, later it will be understood how the magnetic moment of a static electrically charged particle increases as the bending of its virtual particle paths increase in direct proportion to its respective decrease in mass (wherein this agrees with convention in which the magnetic moment of a static proton is less than the magnetic moment of a static electron of lesser mass). (Note that the opposite electrically charged unified fields are symmetrical reflections, and are considered to comprise the same density so as to represent matter and antimatter unified fields. However, certain portions of the unified field are not “mirror” symmetrical reflections when spin is added to the unified field, e.g., in terms of angular momentum as shown, and, in terms of microscopic spins which are described later.)

The basic "static" geometry of the internal structure of the unified field is considered to be representative of the basic geometry of the internal structure of a static elementary electrically charged particle, and pertinent to the operational terms of black holes (which can not be probed) ranging from a theoretical Planck particle (i.e., a theoretical miniature black hole) to a supermassive black hole. Wherein, the internal structure of the unified field provides parameters for describing certain characteristics of a black hole including the event horizon, accretion disc, jets, etc. (Note that drawings of unified fields such as those shown in figures 3A and 3B, and other drawings which pertain to them, are only intended to be drawn as rough approximations or also exaggerations of what they represent for viewing purposes.)

Nevertheless, each of the virtual particle paths in the top band of virtual particle paths of a negative electrically charged particle are considered to comprise a right hand screw, and each of the virtual particle paths in the bottom band of virtual particle paths of a negative electrically charged particle are considered to comprise a left hand screw. While, each of the virtual particle paths in the top band of virtual particle paths of a positive electrically charged particle are considered to comprise a left hand screw, and each of the virtual particle paths in the bottom band of virtual particle paths of a positive electrically charged particle are considered to comprise a right hand screw.

In more detail, the unified field is considered to be constructed with a simple set of orthogonal vectors which provide for the predicable structure and function of the unified field. Accordingly, each virtual particle path is considered to have orthogonal “microscopic spins" comprising microscopic charge (q), mass (m), and magnetic (B_m) spin vectors.

In terms of static negative and positive electrically charged particles, figures (4A) and (4B) show the left and right hand electric (q), mass (m), and magnetic (B_m) microscopic spin vectors of the example virtual particle paths on the top and bottom sides of the negative and positive unified fields shown in figures (3A) and (3B), respectively. (Note that the length of a vector is not a relevant parameter here and elsewhere throughout the present theory.)

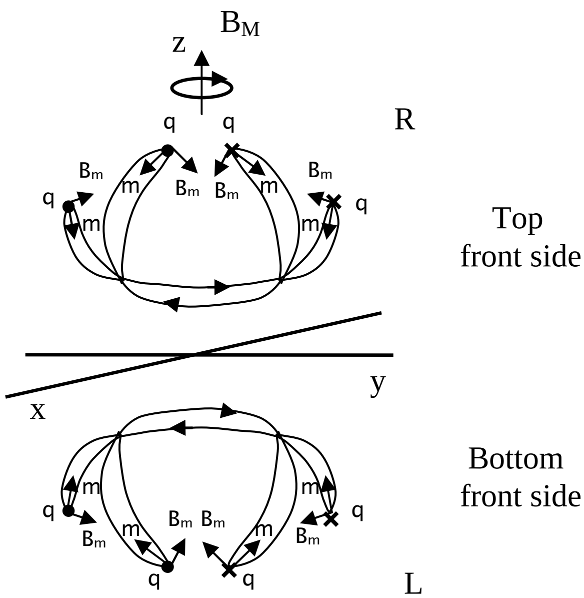

Side view of a negative
electrically charged particle

FIG. 4A

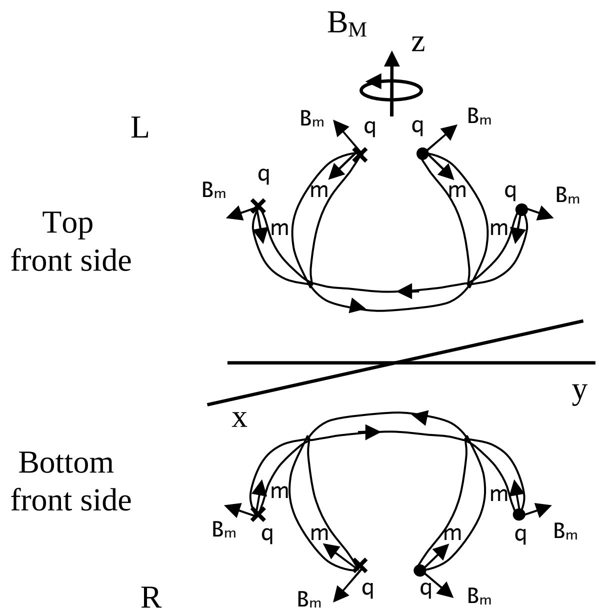

Side view of a positive
electrically charged particle

FIG. 4B

Figures (5A) and (5B) show how the three spin vectors change alignments during portions of oscillation in the nuclear and extranuclear regions in a negative and positive unified field, respectively (wherein, importantly, the microscopic magnetic spin vectors basically have a relatively inverted alignment in the nuclear region compared to the extranuclear region).

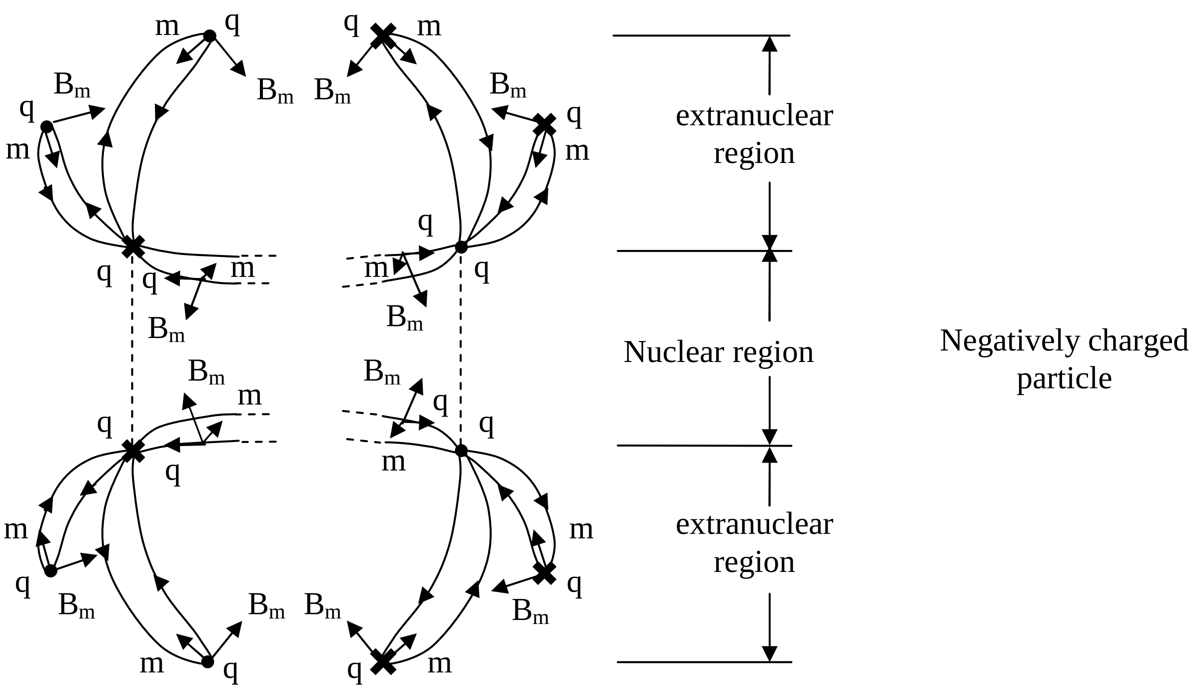
extranuclear region
Nuclear region
extranuclear region
Negatively charged particle

FIG. 5A

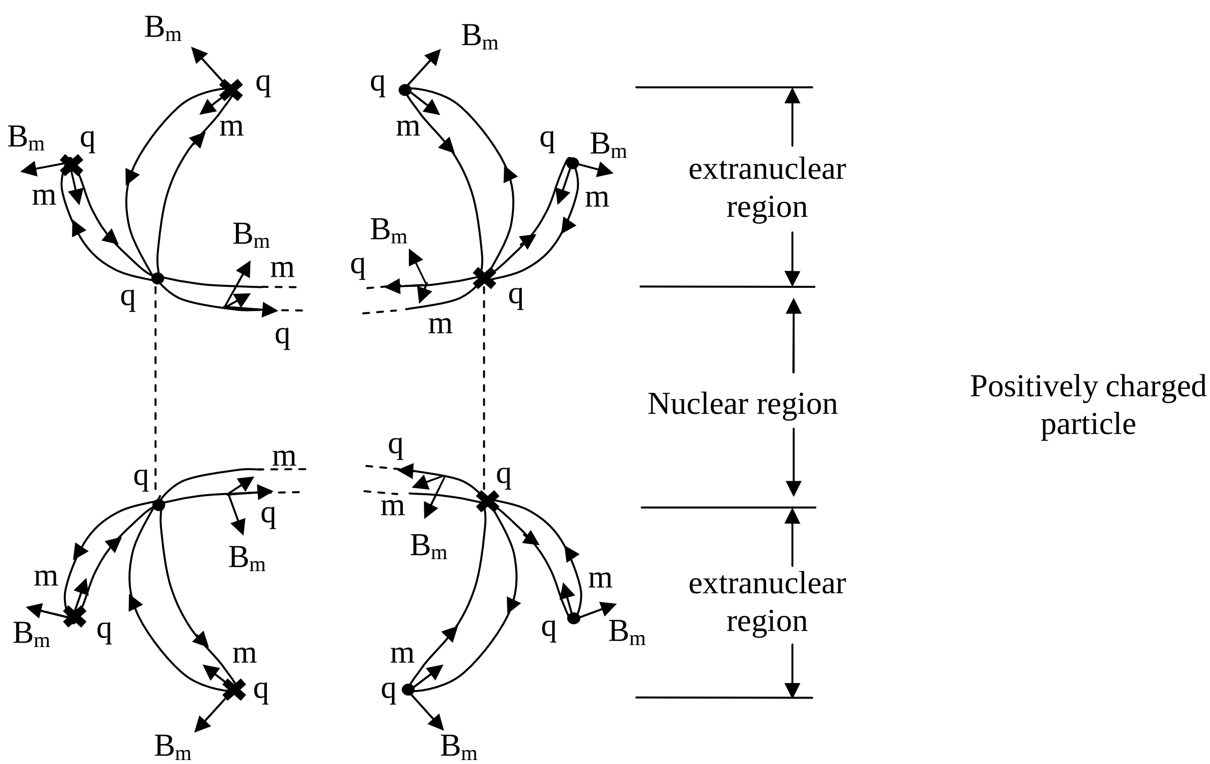
extranuclear region
Nuclear region
extranuclear region
Positively charged particle

FIG. 5B

Note that the nuclear virtual particle paths are shown in figures 3A-5B as merged in the nuclear region such that the theoretical separation of virtual particle paths is not shown. Also, note that virtual particle paths may not be shown with bending hereinafter (for simplification) except, for example, where curvature is emphasized, e.g., in magnetic interactions.

Figure (6A) shows a vector component in the (x-y) plane of a tangent at the leading edge of a select portion of a virtual particle path of a negative electrically charged particle. Wherein, the (x) and (y) axes of the vector component in the (x-y) plane correspond to the constants (n_1) and (n_2) of the components ($^-1/n_1K_Tq/r^2$) and ($1/e^{[n_2(2\pi mcr)/h]}$), respectively, in the gradient function $^-1/n_1K_Tq/r^2 * 1/e^{[n_2(2\pi mcr)/h]}$. In which case, the (x) and (y) axes, and the respective values of (n_1) and ($n_{2,}$) are considered to relate to the energy, geometry, etc., of the given virtual particle path. (Note that the arrow on the virtual particle path corresponds to respective microscopic electric spin vector (q) direction along the gradient function.)

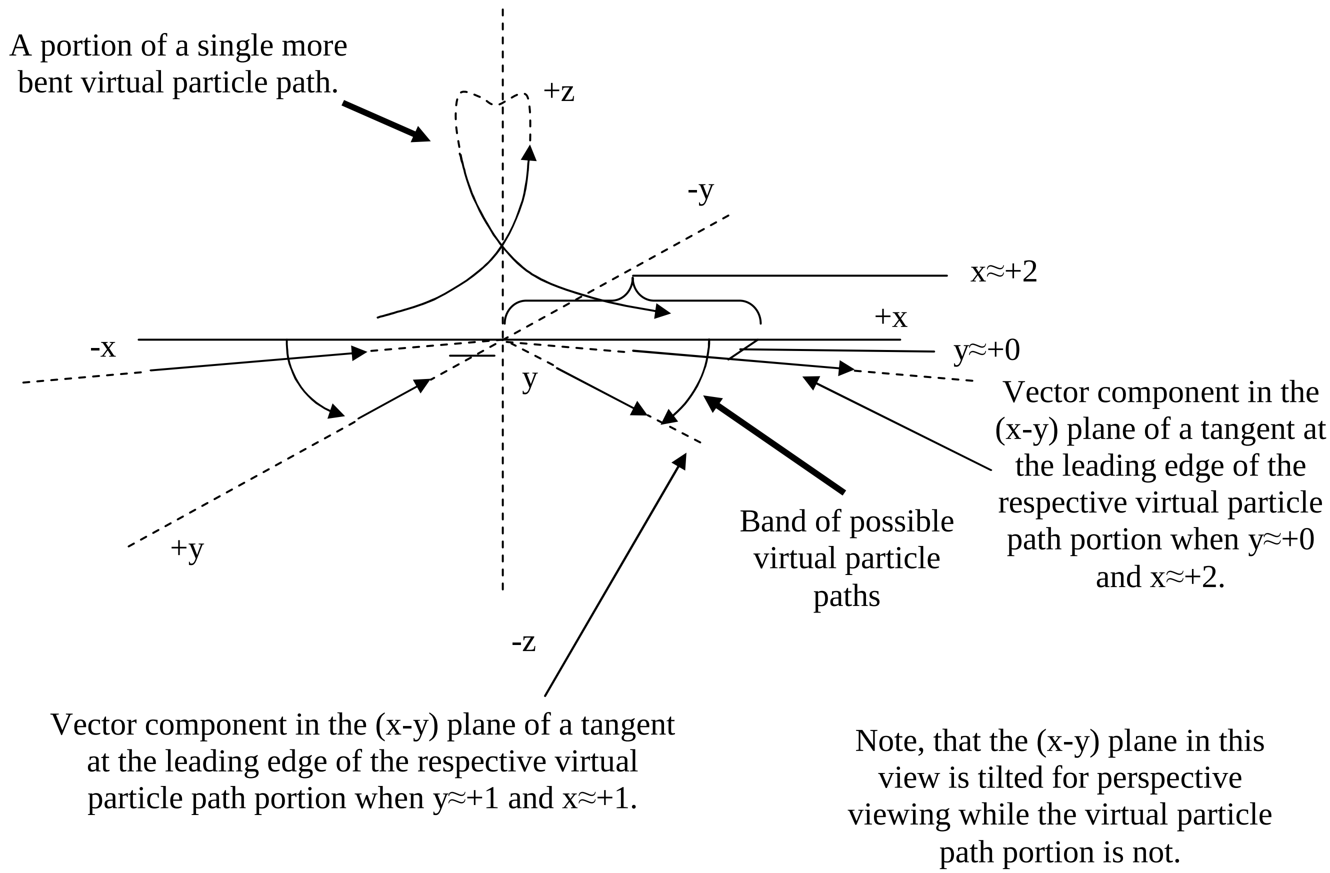

FIG. 6A

Note that when x≈+2 and y≈+0, then the gradient of the virtual particle path is $\approx {}^{-}1/2K_Tq/r^2 * 1/e^{[\approx 0(2\pi mcr)/h]}$ for the given one half portion of the theoretical unified gradient function (top side), and is $\approx {}^{-}1K_Tq/r^2 * 1/e^{[\approx 0(2\pi mcr)/h]}$ for the whole portion (the sum of the top and bottom side portions as described more so later). While, when x≈+1 and y≈+1, then the gradient of the virtual particle path is $\approx {}^{-}1K_Tq/r^2 * 1/e^{[\approx 1(2\pi mcr)/h]}$ for the given one half portion of the theoretical unified gradient function (top side), and is $\approx {}^{-}2K_Tq/r^2 * 1/e^{[\approx 1(2\pi mcr)/h]}$ for the whole portion (the sum of the top and bottom side portions as also described more so later).

Figures (6B) and (6C) describe how certain parameters of the virtual particle paths vary as their angles of trajectory vary. This relates to the (x) and (y) axes of the vector component in the (x-y) plane of the tangent to the given virtual particle path portion, and, correspondingly, (n_1) and (n_2) values of the respective gradient function in figure 6A).

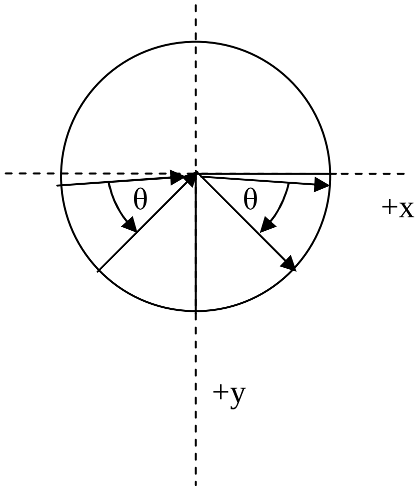

Top view

FIG. 6B

Consider the following conditions to be present for virtual particle paths in a band of virtual particle paths as theta increases for a static particle as shown in figure (6B) (moving from one virtual particle path to another):

1) Spin vector alignments rotate according to the change in potential;
2) Path length and radius decrease for each virtual particle path. In which case, the virtual particles in a virtual particle path propagate with an increased average frequency and a decreased average radius, such that the virtual particle paths can propagate (statically here) in unison as a wave packet;
3) Complementary (n_1) and ($n_{2,}$) values change, and the elliptically helical geometry of the virtual particle paths approach a circularly helical geometry (eccentricity decreases);
4) Densities of the virtual particle paths increase; and,
5) Virtual particles propagate at the same velocity, i.e., virtual particles propagate at the same velocity on all virtual particle paths (refer to the description under the heading "virtual particles, self interaction, and superluminal velocity").

When diagram (6B) is applied to an electron in an atomic orbital the following would occur as theta increases along the direction shown:

1) KE increases;
2) Negative PE increases; and,
3) Positional PE decreases.

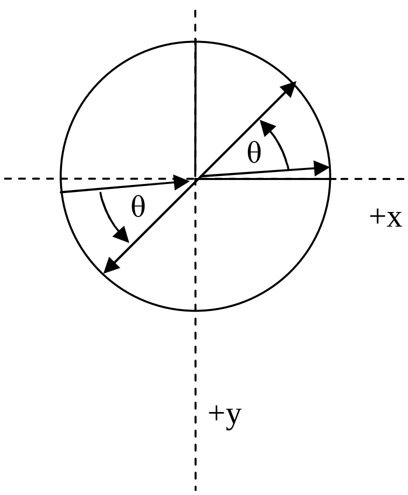

Top view

FIG. 6C

While the conditions of the virtual particle paths for figure (6B) are basically equivalent for the virtual particle paths of a propagating particle as a whole, nevertheless, further consider the following conditions when figure (6B) is modified for forward propagation as in figure (6C), such that theta changes in opposite directions in diagonally positioned quadrants for the leading and trailing edge (for one portion, e.g., the front portion) of a propagating particle as a whole:

1) When this diagram is applied to an accelerated propagating electrically charged particle, “relativistic mass” increases for the particle as a whole (and individual virtual particle paths) as theta increases along the direction shown for the band of virtual particle paths.

2) When this diagram is applied to an electromagnetic field quantum, virtual particle paths on both the top and bottom sides are comprised in a narrow band with constants approximating $n_1 \approx 1$ and $n_2 \approx 1$, wherein the narrow band of virtual particle paths for electromagnetic field quanta of higher energies have virtual particles with higher average frequencies and smaller average radii on virtual particle paths with correspondingly shorter path lengths.

3) When this diagram is applied to special relativity, length contraction and time dilation increase along the (x) axis as theta increases along the direction shown (as explained more so later).

Upon acceleration of an electrically charged particle, the spin vectors of the virtual particles in each of the virtual particle paths are considered to rotate (as relates to in figures 6B-6D, and more specifically depicted later in figures 14A and 14B). Wherein, the rotations of the spin vectors of the virtual particles are considered to affect the parameters of, in particular, a propagating particle including the radius, amplitude, wavelength, frequency, relativistic mass, energy, etc. (in agreement with the self interactions of the respective virtual particles as analogized with the interactions of propagating electrically charged particles described later).

Accordingly, upon rotation of the spin vectors as for the example virtual particle path shown in figure (6D) for forward propagation, theta correspondingly increases, and each virtual particle path changes its trajectory and projects forward. In which case, the eccentricity of each of the virtual particle paths decreases so as to approach a respective circularly helical geometry to a directly proportional extent, and correspondingly, the forward translational velocity of the particle as a whole is considered to increase. (Note that the virtual particle paths propagate in agreement with the "interval" as for the example virtual particle path shown in figure 6D.)

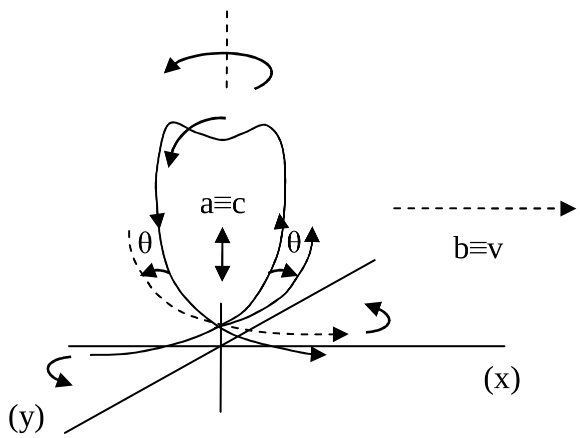

Changes in the trajectory of a virtual particle path in an accelerating propagating particle (excluding size change) as theta increases upon rotations of the virtual particle paths, and corresponding changes in (n_1) and (n_2) values.

FIG. 6D

With respect to relativity, figures (6A-6D), (with particular consideration for figure 6D), and when working with ellipses, assume $\frac{1}{\gamma} \equiv e$, wherein $\left(\frac{1}{\gamma}\right)$ is the reciprocal Lorentz factor and (e) is eccentricity, such that $\frac{1}{\gamma} \equiv e = \sqrt{1-\left(\frac{b}{a}\right)^2}$. In which case, assuming that b≡v and a≡c, then $\frac{1}{\gamma} = \sqrt{1-\left(\frac{v}{c}\right)^2}$. Wherein, for a propagating electrically charged particle as a whole, when v=0, then $\left(\frac{1}{\gamma}\right)$ is equal to one, and each virtual particle path has its respective maximum eccentricity, such that each virtual particle path has a respective minimum Lorentz contraction, minimum time dilation, and minimum relativistic mass. While, when v=c, then

$\left(\frac{1}{\gamma}\right)$ is equal to zero, and each virtual particle path approximates a respective circularly helical geometry, and the virtual particle paths each have a respective maximum Lorentz contraction, maximum time dilation, and maximum relativistic mass.

Changes in (n_2) (mass related changes between $n_2 \approx +0$ and $n_2 \approx +1$) of the exponential component of the potential of a virtual particle path can be interpreted as being especially related to changes in velocity (v) in the conventional Lorentz factor. However, nevertheless, it is considered that each virtual particle path in a band is related to its own Lorentz factor due to their differences in potential, i.e., the basic multiplicative components of a potential are related to, or, (n_1) and (n_2) can be correlated with, their own Lorentz factors, such that corresponding Lorentz factors vary amongst virtual particle paths in a band (affecting scale), and such that such Lorentz factors change in a virtual particle path as the potential changes (e.g., as with respect to changes in the parameters of charge or mass, and radius, or the equivalents) for virtual particles in a virtual particle path as they oscillate, and the virtual particles converge and diverge. Wherein, consequentially, the curvature of a virtual particle path changes as it oscillates due to changes in the directions of the spin vectors, length contractions, etc. as the potential changes.

Thus, consider relativistically, that the function

$$f = \pm e^{\left[\frac{1}{N} n_1 \frac{\pm 2\pi(qcr)}{h_q} + \frac{1}{N} n_2 \frac{\pm 2\pi(mcr)}{h}\right]} \qquad \text{Eq. (3A)}$$

can be reduced to

$f = \pm e^{\left[\frac{1}{\gamma_T^2}^2 * \frac{1}{N} n_1 \frac{\pm 2\pi(qcr)}{h_q} + \frac{1}{\gamma_T^2} * \frac{1}{N} n_2 \frac{\pm 2\pi(mcr)}{h}\right]}$. Then, upon substitution, reflection of the function, and taking the partial derivative the forgoing function becomes:

$$\pm f_x(x,y) = {}^{\pm}\gamma_T{}^2 \frac{1}{N} \frac{h_q c}{n_1 * 2\pi(qr)} * e^{\left[\frac{1}{\gamma_T^2}^2 \frac{1}{N} \frac{n_2 * {}^{\pm} 2\pi(mcr)}{h}\right]} \qquad \text{Eq. (13A)}$$

This is considered a relativistic version of the unified field function shown in equation (4A) such that the square of the Lorentz factor, i.e., $\gamma_T{}^2$, in the unified field function accounts for the two indices of the Lorentz factor in general relativity which conventionally relates to energy and volume (or energy density). (Note, refer to the example below and equation 15 for forms of the theoretical Lorentz factor applicable in the present theory.)

For example, as relates to the figure (6D) and the square of the Lorentz factor for a portion of the charge component of the unified potential (along the x-axis), consider $\gamma_T{}^2 = \frac{1}{\left(\frac{\Delta n_1}{1}\right)^2}$ such that when (Δn_1)=2, then $\gamma_T{}^2$=¼, i.e., $1/(2\text{-}0)^2/(1)$=¼ (expressed in terms of a fraction with respect to the relevant interval);

and, as relates to the figure (6D) and the square of the Lorentz factor for a related portion of the mass component of the unified potential (along the y-axis), consider $\frac{1}{\gamma_T{}^2} = \left(\frac{\Delta n_2}{1}\right)^2$ such that when (Δn_2)=0, then $1/\gamma_T{}^2=0$, i.e., $(1\text{-}1)^2/(1)=0$; wherein,

$$\left(\gamma^2\right) * 4 * 2 * \frac{{}^{-}1}{\approx 2} \frac{K_T(q)}{r} * \frac{1}{e^{\left[\gamma^2 \frac{\approx 0\pi(mcr)}{h}\right]}} \approx \left(\frac{1}{4}\right) * 4 * 2 * \frac{{}^{-}1}{2} \frac{K_T(q)}{r} * \frac{1}{e^{\left[0 * \frac{0\pi(mcr)}{h}\right]}} \approx \frac{{}^{-}K_T(q)}{r}$$

Eq. (13B)

In which case, (13B) is the extreme relativistic unified field potential function of the most eccentric virtual particle path.

Then, for the extreme relativistic unified field potential function of the least eccentric virtual particle path, when $(\Delta n_1)=1$, accordingly, $\gamma_T{}^2=1$, i.e., $1/(2-1)^2/(1)=1$; and when $(\Delta n_2)=1$, accordingly, $1/\gamma_T{}^2=1$, i.e., $(1-0)^2/(1)=1$ such that:

$$\left(\gamma^2\right) * 4 * 2 \frac{\approx {}^{-}K_T(q)}{r} * \frac{1}{e^{\left[\gamma^2 \frac{\approx 2\pi(mcr)}{h}\right]}} \approx (1) * 4 * 2 \frac{{}^{-}K_T(q)}{r} * \frac{1}{e^{\left[1 * \frac{2\pi(mcr)}{h}\right]}} \approx 8 \frac{{}^{-}K_T(q)}{r} * \frac{1}{e^{\left[\frac{2\pi(mcr)}{h}\right]}} .$$

Eq. (13C)

Accordingly, while

$$4 \frac{\approx {}^{-}K_T(q)}{r} * \frac{1}{e^{\left[\frac{\approx 0\pi(mcr)}{h}\right]}} - 8 \frac{\approx {}^{-}K_T(q)}{r} * \frac{1}{e^{\left[\frac{2\pi(mcr)}{h}\right]}} \approx 1 \frac{{}^{-}K_T(q)}{r}$$ (as stated before for an elementary particle for equation 9A), nevertheless, "relativistically,"

$$8 \frac{\approx {}^{-}K_T(q)}{r} * \frac{1}{e^{\left[\frac{2\pi(mcr)}{h}\right]}} - \frac{\approx {}^{-}K_T(q)}{r} \approx 2 \frac{{}^{-}K_T(q)}{r}$$

(In theory, the difference in potentials could be expressed as **≈** $^{-}1K_Tq/r$ + **≈** $^{-}1G_Tm/r$ **≈** $^{-}2K_Tq/r$.

Also, note that a theoretical version of the Schwarzschild radius can be derived from the forgoing difference in potentials such that $r_T \approx 2G_T M/c^2$ when G_T is substituted for $^{-}K_T$.)

Next, the vector sum of the gradient components of the unified field with respect to equations (5A), (5B), (8A), (8B), and (8C) can be related to the geometry of the unified field as depicted in figures (7A), (7B), and (7C). In this case, only the basic multiplicative factor of the vector summation process is shown (note that a positively charged particle can be presented similarly).

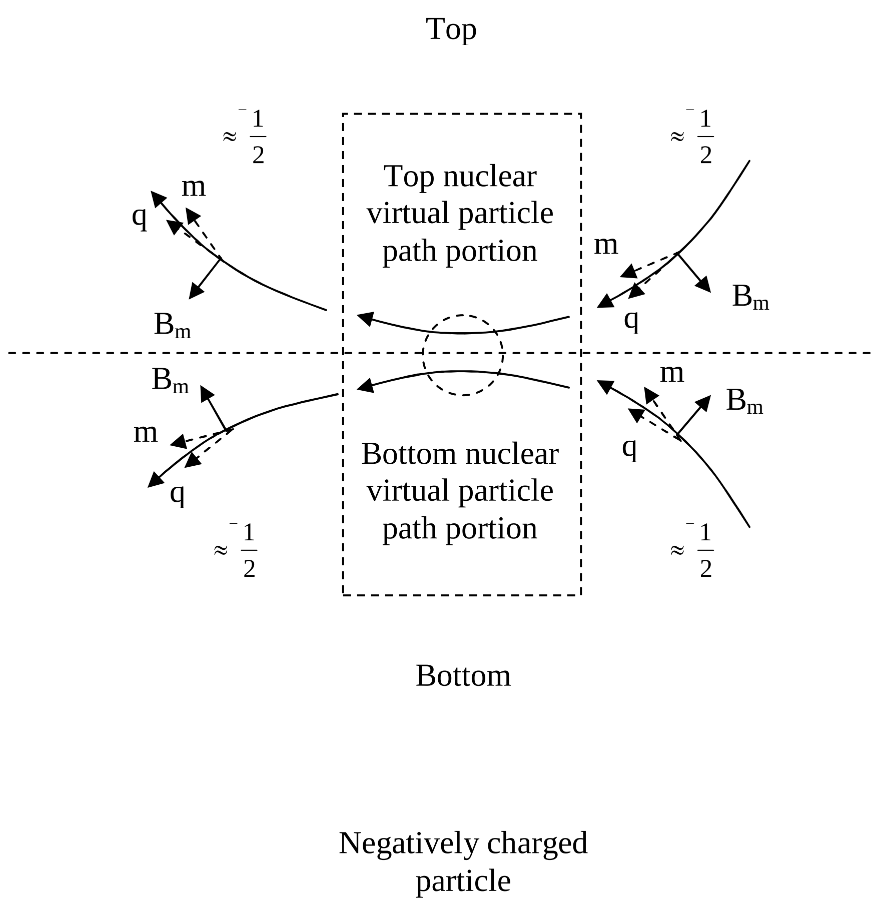

Here, the vector resultant gradients of the top and bottom virtual particle paths when $(n_1) \approx 2$ and $(n_2) \approx 0$ can propagate into the nuclear region and add as $\approx {}^{-}1/2 + \approx {}^{-}1/2 \approx {}^{-}1$. Alternatively, vector components can propagate into the nuclear region and add as follows so to produce the resultant gradient ${}^{-}\sqrt{(\approx {}^{-}1/2\sqrt{2} + \approx {}^{-}1/2\sqrt{2})^2 + (\approx {}^{-}1/2\sqrt{2} + \approx {}^{-}1/2\sqrt{2})^2} \approx {}^{-}1$.

FIG. 7A

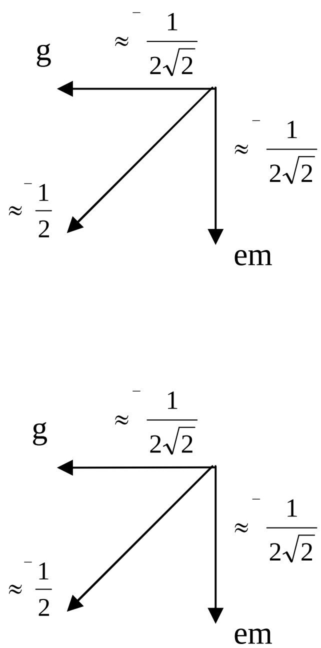

Basic geometry of (em) and (g) gradient vector components of the top and bottom virtual particle paths when $(n_1) \approx 2$ and $(n_2) \approx 0$.

FIG. 7B

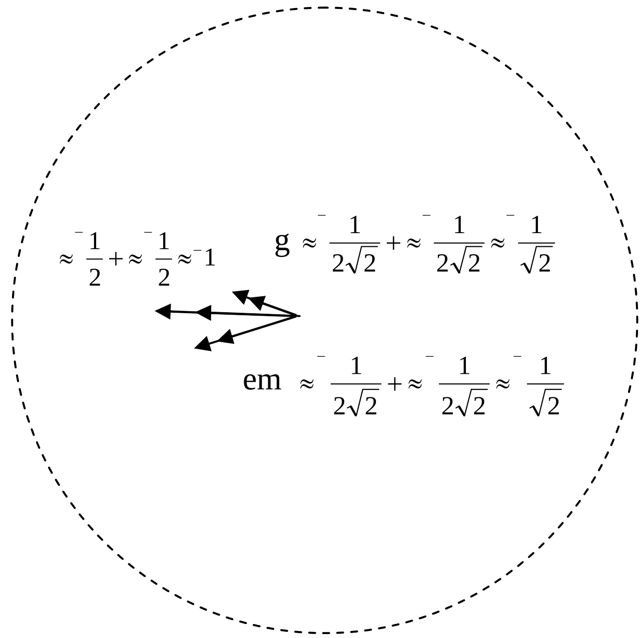

An enlarged perspective view of what is occurring in the dashed circle in figure (7A) which shows the basic geometry of the respective addition of vector components of (em) and (g) of the top and bottom virtual particle paths in the nuclear region when $(n_1) \approx 2$ and $(n_2) \approx 0$.

FIG. 7C

Figure (7D) shows the symmetrical vector components of a portion of one example virtual particle path in terms of electromagnetic and gravitational gradient components.

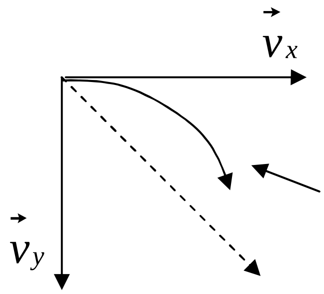

$\frac{\partial}{\partial x} \approx^{-} 1/2\sqrt{2}*K_Tq/r^2*1/e^{[\approx 0(2\pi mcr)/h]}$

A portion of one eccentric virtual particle path in,
for example, the nuclear region on the top side

$1/2\nabla\varphi_R \approx^{-} 1/2*K_Tq/r^2*1/e^{[\approx 0(2\pi mcr)/h]}$ (dashed resultant vector gradient)

$\frac{\partial}{\partial y} \approx^{-} 1/2\sqrt{2}*G_Tm/r^2*1/e^{[\approx 0(2\pi mcr)/h]}$

Top view

Here, the vector components ($\vec{v}_x$ and $\vec{v}_y$) of the electromagnetic and gravitational gradient components along the ($^+$x) and ($^+$y) axes of the theoretical unified gradient resultant $\approx^{-} 1/2K_Tq/r^2 *1/e^{[\approx 0(2\pi mcr)/h]}$ are shown in the nuclear region, such that $^{-}\sqrt{(\approx^{-} 1/2\sqrt{2}K_Tq/r^2*1/e^{[\approx 0(2\pi mcr)/h]})^2 + (\approx^{-} 1/2\sqrt{2}G_Tm/r^2*1/e^{[\approx 0(2\pi mcr)/h]})^2} \approx^{-} 1/2K_Tq/r^2*1/e^{[0(2\pi mcr)/h]}$ (dashed line).

FIG. 7D

CHARGED PARTICLE INTERACTION:

It has been a longstanding contentious issue as to how electrically charged particles interact. Wherein, while Newtonian physics suggests that gravitational interactions are based on instantaneous action-at-a-distance, relativity proposes that gravitational interactions are based on the action of the curvature of spacetime on mass over velocity (c).

Herein, electrically charged particles are considered to interact over relatively long distances ("locally") by the "extranuclear" virtual particle paths of a particle extending outward to, and interacting with, another particle (or other particles) over a superluminal velocity. In which case, long range interaction of one particle with another can cause attractive or repulsive effects which included particle acceleration, the formation of molecules with molecular orbitals, etc. (refer to the description under the heading "virtual particles, self interaction, and superluminal velocity" for the mathematical derivation of superluminal velocity).

For example, figure (8) shows a top view of two possible general directions of the four possible varieties of virtual particle paths of the extended extranuclear field of a given irregular distribution of static positive electrically charged particles which can interact with a negatively charged particle. (Note that the dashed lines in figure 8 represent virtual particle paths hidden from view.)

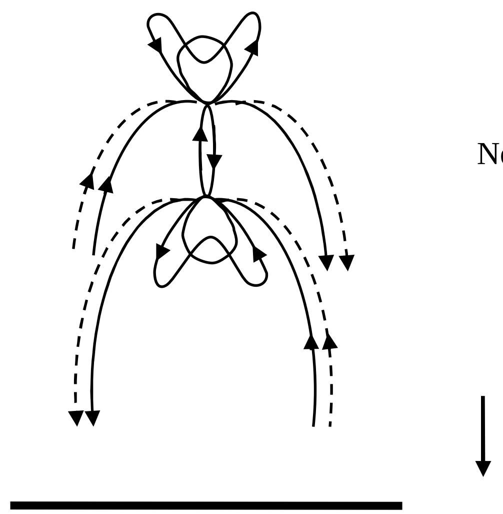

Electromagnetic and gravitational attraction

FIG. 8

In this case, the virtual particle paths of the extended extranuclear fields of the irregular distribution of positively charged particles enter, and subsequently exit, along the portion of the nuclear region on respective sides of the negative particle where the virtual particle paths converge and diverge. (Note that the top side where virtual particle paths enter and exit represents the front side of the negative particle with respect to figure 4A, and the bottom side where virtual particle paths enter and exit represents the back side of the negative particle with respect to figure 4A. Also, note that the constituents of the four possible virtual particle paths of the irregular distribution of positively charged particles can be visualized as comprising an irregular distribution of the two varieties of virtual particle paths which extend out going in opposite directions from the top side of each positive electrically charged particle (with respect to figure 4B); and, in addition, comprising an irregular distribution of the two varieties of virtual particle paths which extend out going in opposite directions from the bottom side of each inverted positive particle (with respect to figure 4B).

Figure (9) shows a perspective view of certain portions of the interacting particles shown in figure (8).

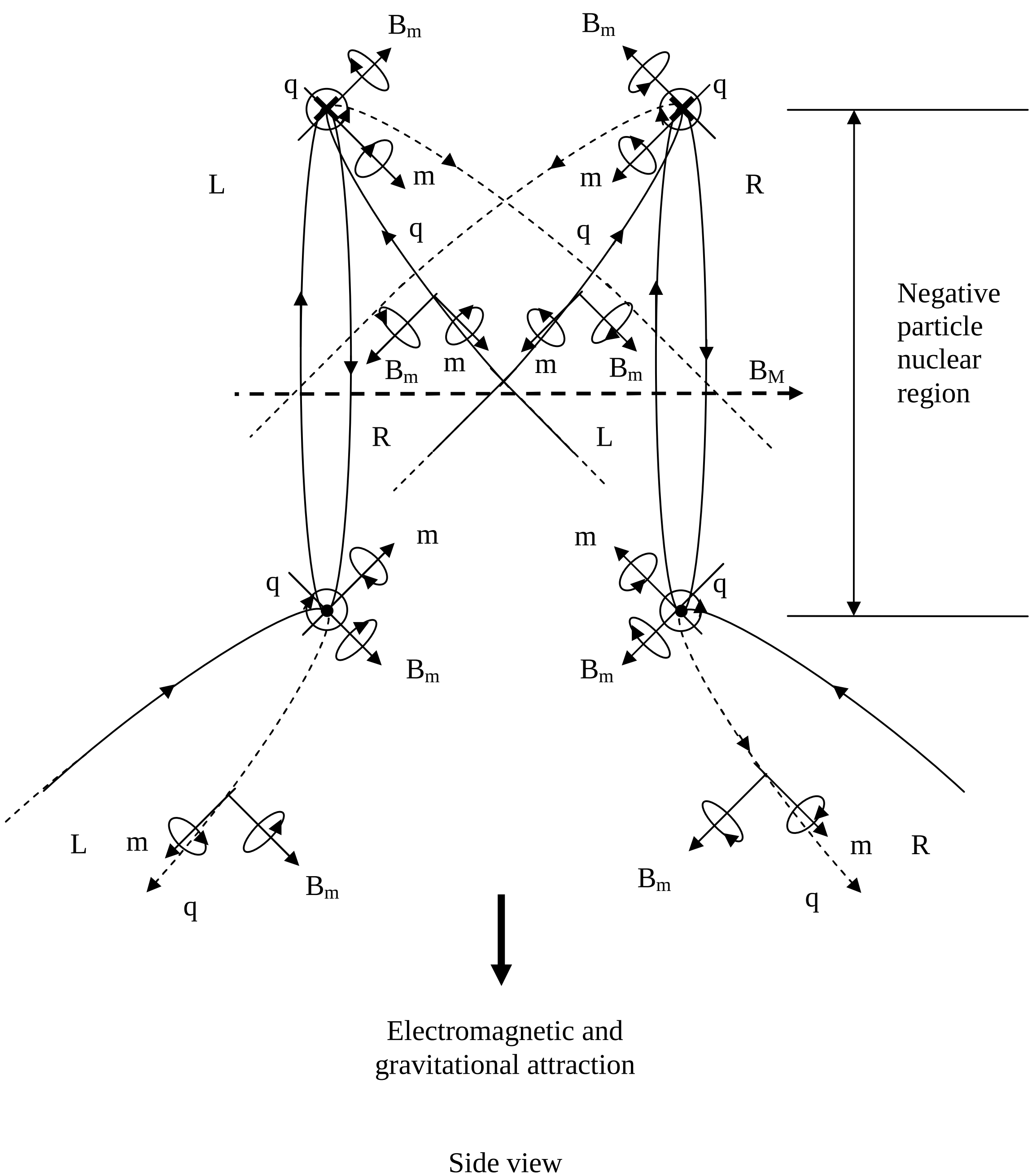

FIG. 9

In figure (9), the four possible effective varieties of virtual particle paths of the extranuclear fields of the irregular distribution of positive particles which can interact with the negative particle are shown along with their respective microscopic spins. Also, figure (9) shows the example virtual particle paths of the nuclear field region of the negative particle which is interacted upon, their respective microscopic spins, and the macroscopic magnetic field alignment of the particle as a whole.

In this case, the effective virtual particle paths from the irregular distribution of positive particles entering the nuclear region on the top section of the negative particle have microscopic charge (q) and mass (m) spins which are parallel with the microscopic charge (q) and mass (m) spins comprised by the virtual particle paths in the nuclear region of the negatively charged particle so as to attract. While, the effective virtual particle paths from the irregular distribution of positive particles entering the nuclear region on the top section of the negative particle also have microscopic magnetic spins (B_m) which are antiparallel with the microscopic magnetic spins (B_m) comprised by the virtual particle paths of the top section of the nuclear region of the negatively charged particle so as to also produce attraction. In effect, the virtual particle paths interacting on the top section of the negative particle are considered to attract, such that the top section of the unified field of the negative particle shown in figure (9) is considered to increase in mass and accelerate to an extent. Note that in figures (9) and (18) the interacting spins are separated for viewing purposes. Thus, one must conceptually reposition each orthogonal set of virtual particle path spins from the irregular distribution of positive particles while keeping them aligned as they are so that the origins of the spins from the irregular distribution of positive particles are almost abutting with the origins of the orthogonal set of nuclear spins of the charged particle interacted upon (here, the negatively charged particle) for proper alignments.

Similarly, in figure (9), the microscopic charge spins (q) of the effective virtual particle paths from the irregular distribution of positive particles which enter the nuclear region on the bottom section of the negative particle are parallel to the microscopic charge spins (q) of the virtual particle paths of the bottom section of the nuclear region of the negative particle so as to attract. Yet, the microscopic magnetic spins (B_m) of the effective virtual particle paths from the irregular distribution of positive particles which enter the nuclear region on the bottom section of the negative particle are parallel to the microscopic magnetic spins (B_m) of the virtual particle paths of the bottom section of the nuclear region of the negative particle so as to repel. While, the microscopic mass spins (m) of the effective virtual particle paths from the irregular distribution of positive particles which enter the nuclear region on the bottom section of the negative particle are antiparallel to the microscopic mass spins (m) of the virtual particle paths of the bottom section of the nuclear region of the negative particle so as to also repel, and in effect produce a form of "mass repulsion."

In this case, the virtual particle paths which are interacting on the bottom section of the negative particle are considered to relatively repel due to the repulsion of respective microscopic magnetic and mass spins. Wherein, the bottom section of the unified field of the negative particle shown in figure (9) is considered to decrease in mass and decelerate to an extent.

Consequently, the top section of the negative particle as shown in figures (9) and (10) (starting in the nuclear region where the virtual particle paths begin to converge on the front side of the negative particle) is considered to project forward and downward, and, in effect, establish the leading edge of the particle as indicated in the perspective view of the nuclear region of the negatively charged particle shown in figure (10).

Edge formation of an accelerated
negative particle

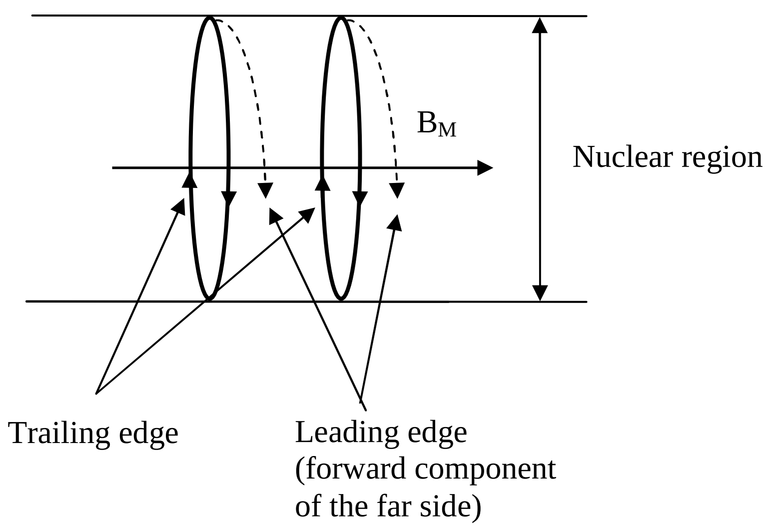

FIG. 10

Correspondingly, the bottom section of the negative particle (in figures 9 and 10) is considered to rotate around with a changed geometrical path (difference not shown) and follow the leading edge, such that, in effect, this portion of the unified field of the particle establishes the trailing edge of the particle.

The attractive, repulsive, or neutral condition of coupling charge and mass spins is considered to occur according to the alignment of the respectively coupled microscopic charge and mass spin vectors (analogous to the manner in which conventional magnetic fields generated by circulating currents of electric charge are considered to interact). Figures (11A) and (11B) show how two right hand and two left hand charge and mass microscopic spin vectors can have totally attractive, totally repulsive, or "neutral" alignment (wherein partial attraction would be situated between neutral and total attraction, and partial repulsion would be situated between neutral and total repulsion). Note that parallel electric spin (q) alignment is a special requirement for "coupling" of (q) spin vectors (or respective components) in certain interactions including those where the entrance of an interacting virtual particle path from one particle into the nuclear region of another particle is pertinent.

Microscopic charge and mass spin vector attraction, repulsion, and neutral alignment

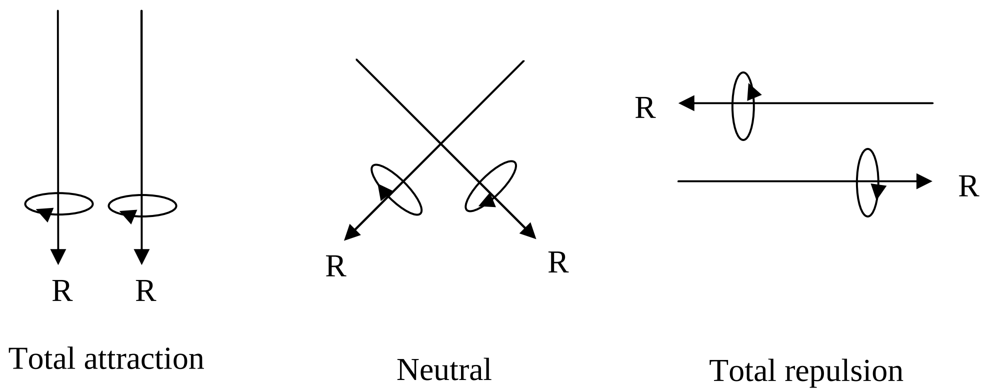

FIG. 11A

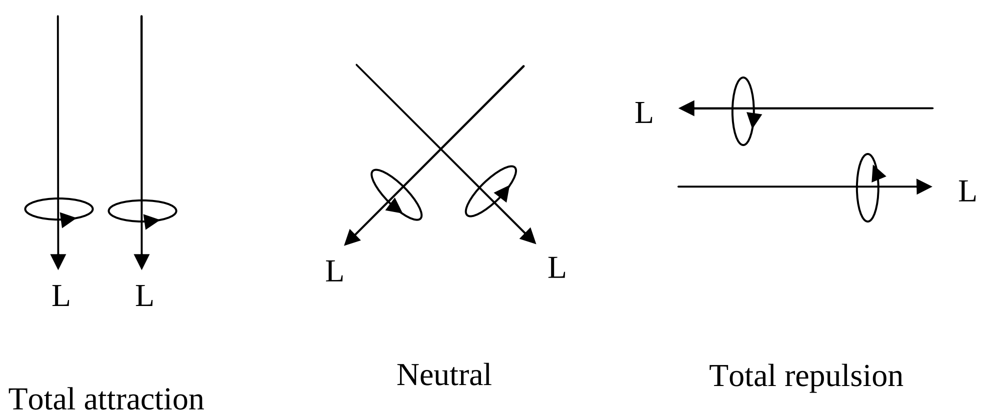

FIG. 11B

However, the attractive, repulsive, or "neutral" condition of coupling microscopic magnetic spins is considered to occur according to the alignment of the respectively coupled microscopic magnetic spin vectors in an effectively different manner. Figures (12A) and (12B) show how two right hand and two left hand microscopic magnetic spin vectors can have totally attractive, totally repulsive, or "neutral" alignment (wherein, similarly, partial attraction would be situated between neutral and total attraction, and partial repulsion would be situated between neutral and total repulsion).

Microscopic magnetic spin vector attraction, repulsion, and neutral alignment

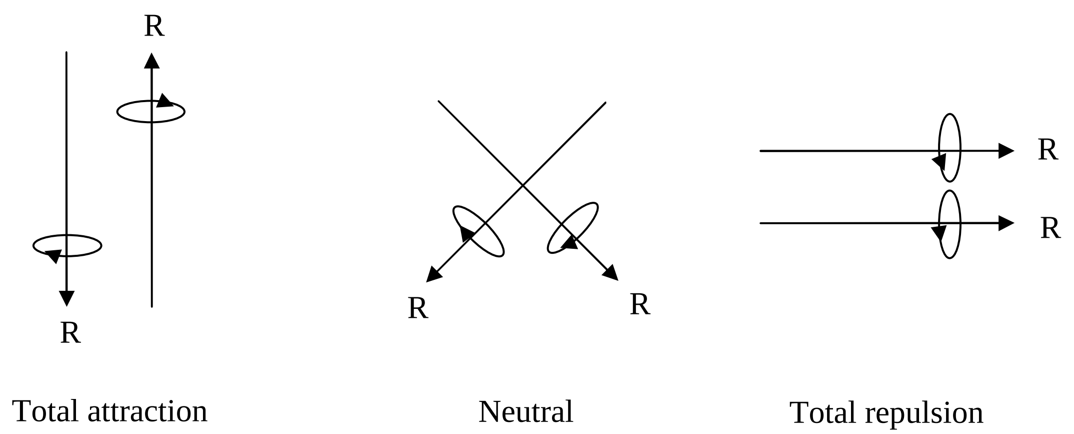

FIG. 12A

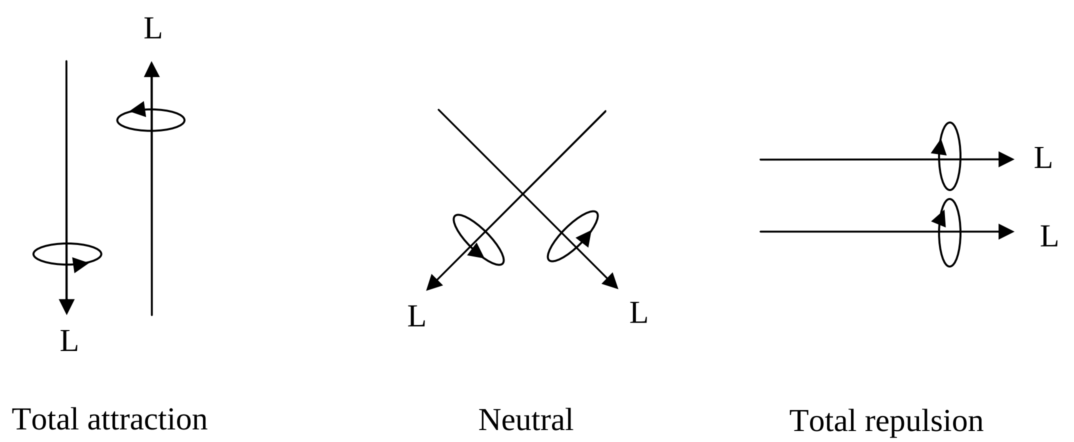

FIG. 12B

Nevertheless, continuing with the interaction of the irregular distribution of positive particles with the negative particle, as the negative particle rotates around and realigns itself in the interacting extranuclear field extended by the irregular distribution of positive particles, the relatively decelerated trailing edge of the negative particle aligns itself with the field like the leading edge, and establishes the accelerated conditions equivalent to those of the leading edge. Wherein, the negative particle propagates towards the irregular distribution of positive particles as the attractive spin vectors of the extranuclear virtual particle paths of the positive particles continue to accelerate the negative particle, such that the electromagnetic and gravitational attraction of the negative particle by the positive particles results.

Then, the extended extranuclear fields of the positive particles continue to interact with the transformed geometry of the unified field of the propagating negative particle, such that the propagating negatively charged particle moves forward towards the irregular distribution of positive particles according to spin vector interactions, and accelerates according to the increase in the angular rotation of the orthogonal spin vectors of the extranuclear virtual particle paths from the positive particles in conjunction with the increase in the density of the extranuclear virtual particle paths from the positive particles as the negative particle approaches the positive particles. While, the virtual particle paths of the top and bottom sides of the accelerated negative particle propagate side-by-side with respective elliptical helicities and relative orientations.

Figures (13A) and (13B) show how the leading edge of example top and bottom virtual particle paths of an accelerated positively and negatively electrically charged particle effectively reflect around certain lines (including lines which are aligned along the vertical dashed lines shown, and the horizontal dashed line which is in the plane of symmetry separating the top and bottom sides), and project forward in order to establish the respectively combined right and left hand elliptically helical virtual particle paths of the top and bottom sides of a propagating electrically charged particle.

Reflections of an accelerated negative particle

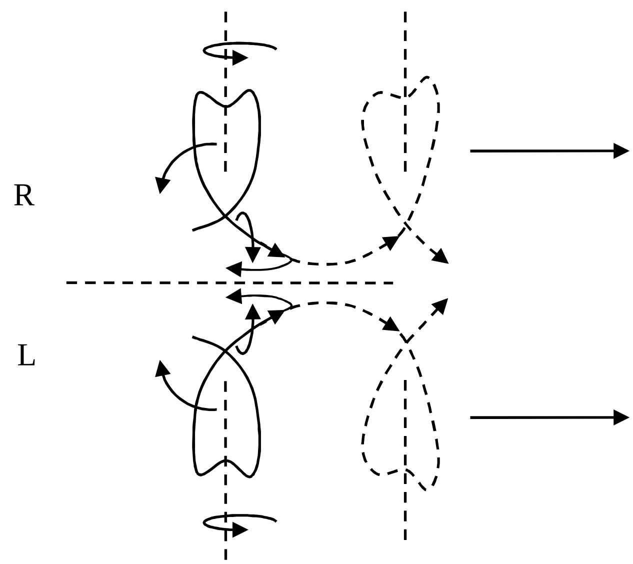

FIG. 13A

Reflections of an accelerated positive
particle

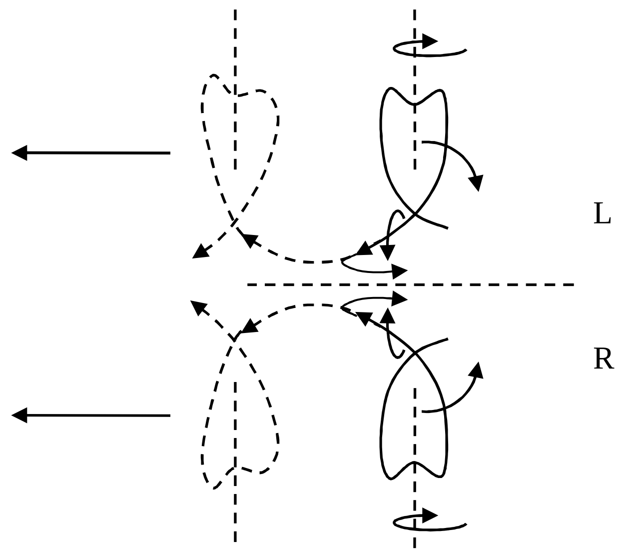

FIG. 13B

Figures (14A) and (14B) show a front view (with respect to the direction of propagation) of the rotations of the microscopic spin vectors (at the leading edge) of some example nuclear virtual particle paths of a negatively charged particle and a positively charged particle which are each accelerated and propagating out of the page. It is considered that the spin vectors rotate around orthogonal rotational axes using the intersecting point of the spin vectors at a tangent point along a respective virtual particle path as a pivot point. (Note that these rotations are considered equivalent to the rotations experienced by virtual particle paths going from the extranuclear region into the nuclear region in electrically charged particles as pertains to figures 5A and 5B; and are considered equivalent to the rotations experienced by the virtual particle paths of accelerated electrically charged particles as pertains to figure 6D, and figures 13A and 13B).

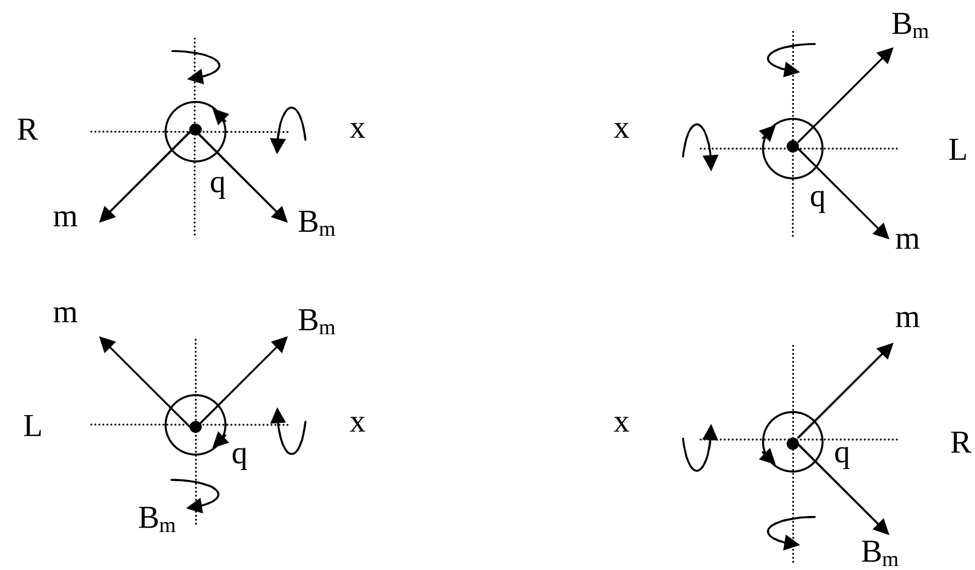

Rotations of nuclear virtual particle paths (at the leading edge) of the front side of a negative particle in the nuclear region due to acceleration.

Rotations of nuclear virtual particle paths (at the leading edge) of the front side of a positive particle in the nuclear region due to acceleration.

Note that the directions of rotation invert as the orthogonal spins invert.

FIG. 14A FIG. 14B

Figures (15A) and (15B) show front views of example top and bottom more bent and less bent virtual particle paths of the front portion of propagating negative and positive electrically charged particles.

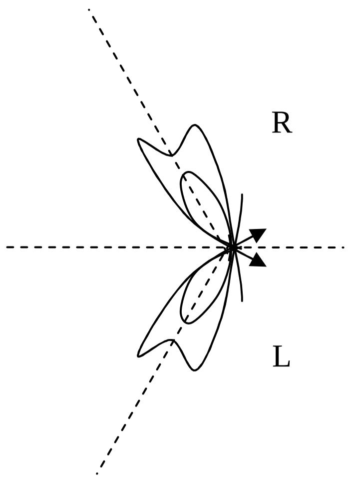

Front view of more and less bent virtual particle paths of a negatively electrically charged particle propagating out of the page

FIG. 15A

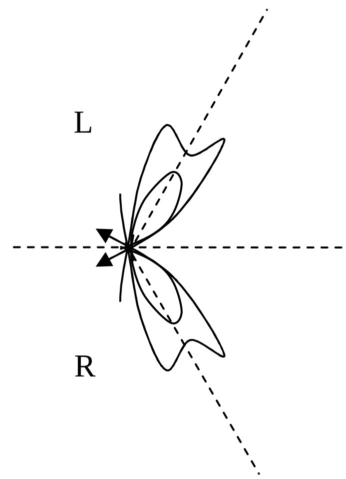

Front view of more and less bent virtual particle paths of a positively electrically charged particle propagating out of the page

FIG. 15B

As shown in figures (15A) and (15B), it is considered that the virtual particle paths of an electrically charged particle only partially reflect around the horizontal dashed line in the plane of symmetry which separates the top and bottom sides while propagating in an elliptically helical manner around respective axes and one common central axis, such that the top and bottom virtual particle paths of an electrically charged particle do not completely come together. Respectively, it is considered that the virtual particle paths in a band of virtual particle paths comprised in an electrically charged particle have relatively different angular alignments (in a graduated way), and are rotated to respectively different extents upon acceleration. Wherein, in effect, each virtual particle path in a particle has a respectively different energy attributable to it before and during propagation. While, as the degree of rotation around the respective rotational axes changes for all of the virtual particle paths in the respective bands of virtual particle paths in an accelerated particle, the energy (including "relativistic mass") for an accelerated particle as a whole changes.

Consider here how the form of the function for a time dependent particle in quantum mechanics corresponds to the unified field presented herein:

$$\psi(x) = Ae^{-ikx-\omega t} = Ae^{\frac{-i2\pi mcr}{h} - (kc)t} = Ae^{\frac{-i2\pi mcr}{h} - \frac{2\pi mc^2 t}{h}} = Ae^{\frac{-i2\pi mcr}{h} - \frac{2\pi mcr}{h}}$$

(when $k=2\pi mc/h$ and $x=r$)

Wherein, quantum mechanically, (A) can be a scalar amplitude, such that, for example, $A=1/2kx^2 \equiv mgh$ which pertains to $\approx {}^{-}G_T m/r$ (when the other mass of potential energy is positioned at infinity) which, herein, is equivalent to $\approx {}^{-}K_T q/r$; or (A) can be a vector amplitude, e.g., E (electric vector strength), i.e., ${}^{-}K_C q/r^2$, which is the gradient of the potential ${}^{-}K_C q/r$ which herein relates to $\approx {}^{-}K_T q/r$ which again, herein, is equivalent to $\approx {}^{-}G_T m/r$.

Inertia has been a curious issue over the centuries particularly since Galileo. Respectively, the virtual particle paths in a band of virtual particle paths in an electrically charged particle are considered to interact (in self interaction) and resist acceleration while having "inertia" (i.e., requiring potential or force to change their respective alignments), and, additionally, virtual particle paths from an electrically charged particle are considered to interact with the virtual particle paths of an interacting particle during electromagnetic and gravitational interactions, thus accounting for the source of the equivalence of inertial and gravitational mass. However, the bands of virtual particle paths in the electromagnetic field quantum (which is described more so later) are considered to be relatively converged due to the absence of a significant extent of their eccentricities, such that the each band of virtual particle paths in the electromagnetic field quantum collectively occupies a relatively narrow band compared to a band of virtual particle paths in a propagating electrically charged particle. In which case, the virtual particles on the top side and the virtual particles on the bottom side of the quantum propagate in a more aligned manner while also having inertia (i.e., also requiring force to change their respective alignments), but while having only an infinitesimal small amount of gravitational mass.

Conventionally, an electron has arguably been considered to be a point particle with no internal structure. However, the structure and function of the present unified field has shown how the virtual particle paths of an electrically charged particle can statically oscillate, and then open upon acceleration such that the internal structure of the static unified field transmutes into the propagating unified field of an electrically charged particle such as a propagating electron or proton. While, the resulting propagating particle comprises top and bottom bands of virtual particle paths which can be considered to comprise a wave packet, which, in furtherance of the equations provided, can be described in terms of families of complex exponential functions representing helically propagating virtual particle paths.

Continuing with the interaction described with respect to figures (8), (9), and (10), wherein, figure (16) shows a side view of the two possible varieties of effective virtual particle paths of the irregular distribution positively charged particles which interact with the virtual particle paths of the propagating negatively charged particle as it propagates down the page. In which case, it is consider that interaction occurs as if a "dense nuclear region" of sorts has been preserved on the top and bottom sides of the propagating electrically charged particle. Accordingly, as shown in figure (16), the respective spin vectors (B_m) and (m) are aligned such that the propagating negatively charged particle is accelerated downward towards the positively charged particles.

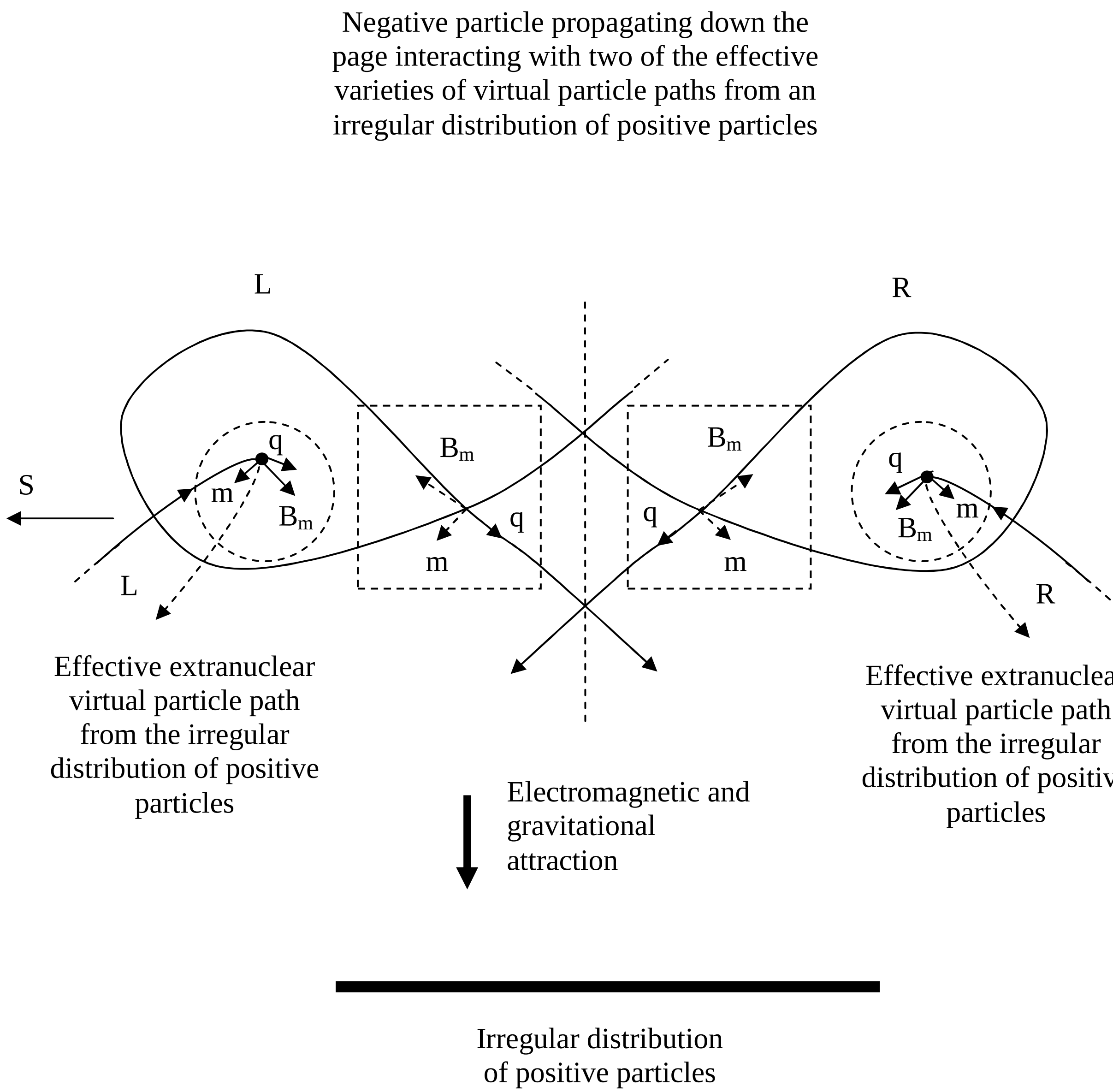

Effective extranuclear virtual particle paths (with spins in dashed circles) extend out from the irregular distribution of positively charged particles (thick solid line) and interact with the "nuclear region" of the propagating negative particle (with spins in dashed squares), such that the charge (q) and mass (m) spins of respectively interacting right and left hand screw sides are parallel and respectively attract, and such that the magnetic spins (B_m) of respectively interacting right and left hand screw sides are antiparallel and respectively attract. (Note that the top and bottom sides of the propagating negative particle tilt out of the page.)

FIG. 16

Note that only the front portion of the negatively charged particle is shown. Furthermore, note that the spin vectors in the dashed squares are aligned in a somewhat tilted manner in and out of the page. Moreover, note that in figure (16) (and in similar drawings) the interacting spins are separated for viewing purposes. Thus, one must conceptually reposition each orthogonal set of extranuclear spins shown in a dashed circle while keeping them aligned as they are so that the origins of the orthogonal set of extranuclear spins are almost abutting with the origins of the orthogonal set of nuclear spins shown in a corresponding dashed square for proper alignments.

Similarly, consider that the positive particles can be accelerated towards the negative particle due to an equivalent process when their fields are aligned accordingly, and also consider that the positive particles can be accelerated towards the negative particle due to the changes in the potentials of their interacting virtual particle paths upon passing through the nuclear region of the negative particle, and then returning to their respective positive particles.

Now, if the irregular distribution of particles creating the extended extranuclear fields and the static particle located a distance away have the same charge, then electromagnetic repulsion will be produced along with the respective gravitational attraction as shown in figures (17), (18), and (19) for an irregular distribution of positively charged particles interacting with a positively charged particle (wherein, in this case, electromagnetic repulsion would dominate over gravitational attraction).

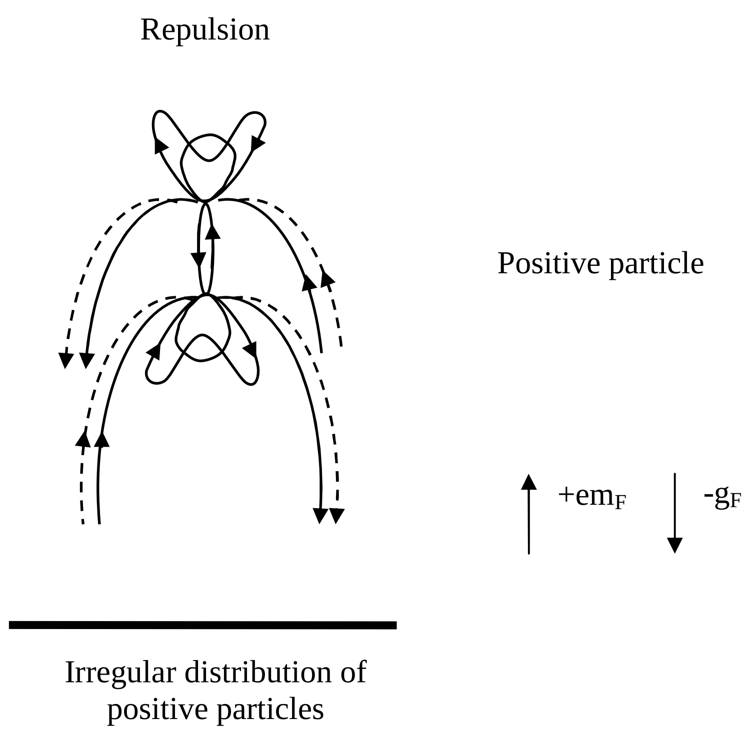
Repulsion
Positive particle
$+em_F$
$-g_F$
Irregular distribution of
positive particles

FIG. 17

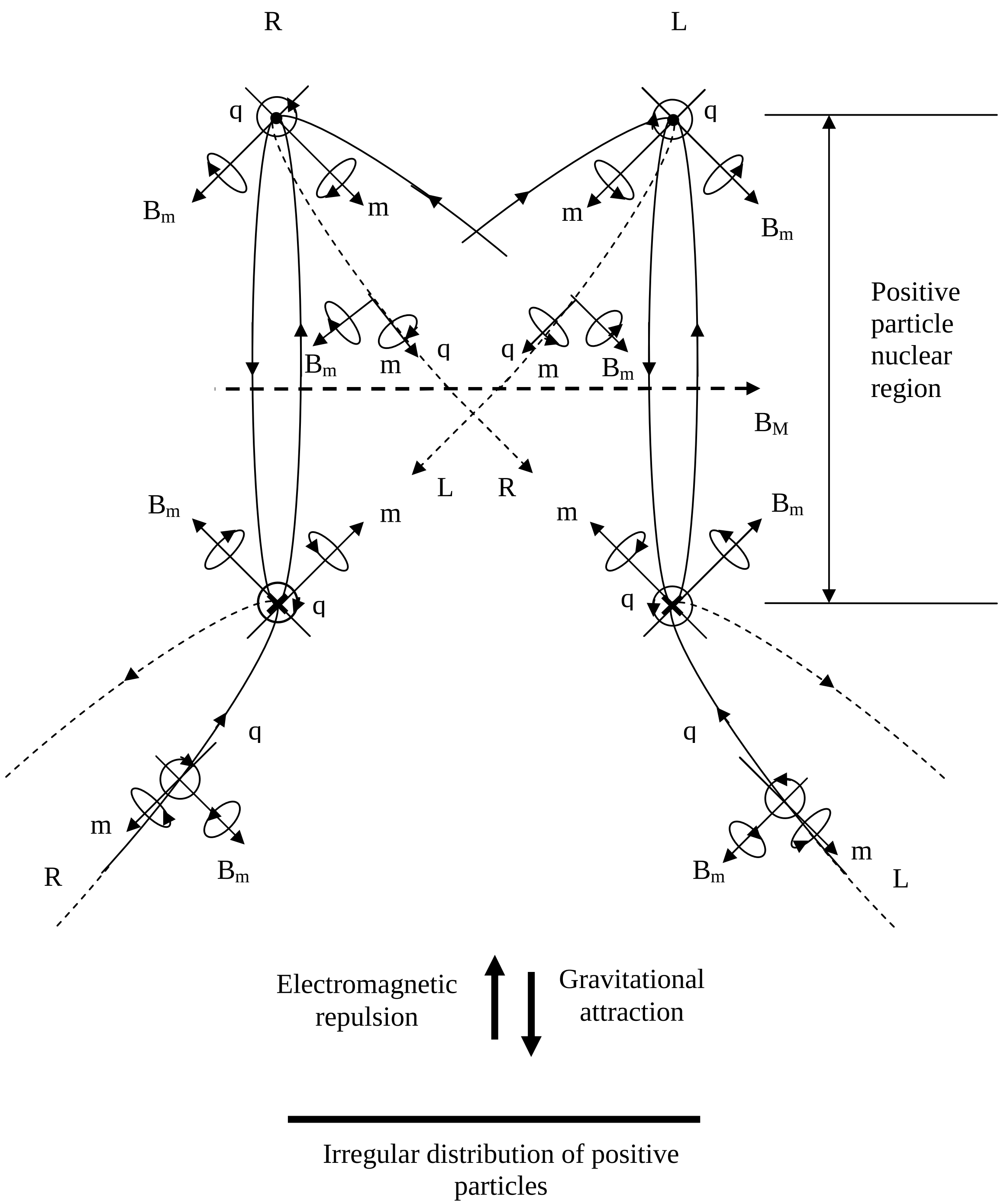
R
L
q
q
Bm
m
m
Bm
Positive
particle
nuclear
region
Bm
m
q
q
m
Bm
BM
L
R
Bm
m
m
Bm
q
q
q
q
m
R
Bm
Bm
m
L
Electromagnetic
repulsion
Gravitational
attraction
Irregular distribution of positive
particles

FIG. 18

Edge formation of an accelerated
positive particle

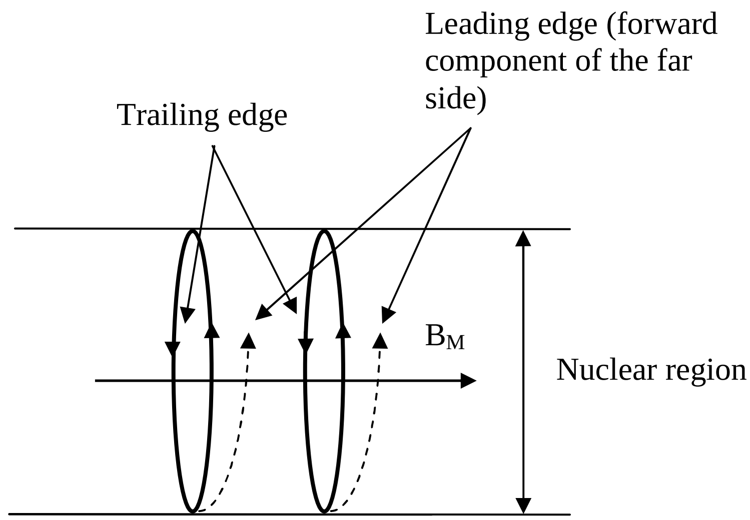

FIG. 19

Figure (20) shows the two possible effective varieties of virtual particle paths of the irregular distribution of positively charged particles which would interact with the virtual particle paths of a positively charged particle if it were initially propagating down the page, such that the positively charged particle is decelerated as it approaches the positively charged particles.

Positive particle propagating down the page interacting with two varieties of effective virtual particle paths from an irregular distribution of positive particles

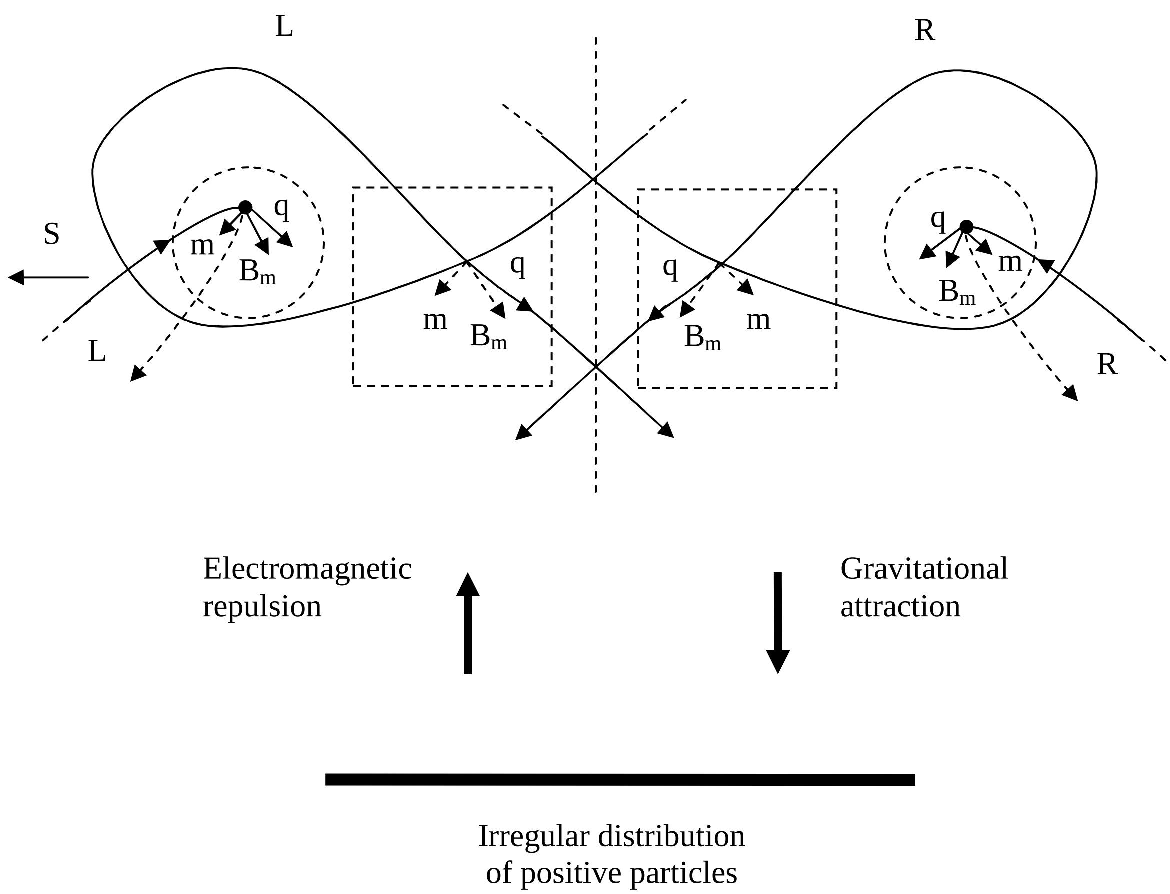

Effective extranuclear virtual particle paths (with spins in dashed circles) extend out from the positively charged particles (thick solid line) and interact with the "nuclear region" of the propagating positive particle (with spins in dashed squares), such that the charge (q) and mass (m) spins of respectively interacting right and left hand screw sides are parallel and respectively attract, and such that the magnetic spins (B_m) of respectively interacting right and left hand screw sides are parallel and repel. (Note that the top and bottom sides of the propagating positive particle tilt out of the page.)

FIG. 20

Here, the virtual particle paths of the irregular distribution of positively charged particles would, in effect, electromagnetically repel the virtual particle paths of the positive particle, and cause the virtual particle paths of the propagating positive particle to change geometry such that the positive particle would decelerate and turn away from the positively charged particles. In this case, the positive particle would turn away from the irregular distribution of positively charged particles against the affect of the gravitational attraction of the virtual particle paths of the same irregular distribution of positively charged particles. Wherein, the gravitational attraction would cancel an extent of the electromagnetic repulsion while attempting to cause (to a respective extent) the opposite turning effect on the positive particle in order that the positive particle "accelerate" toward the positively charged particles (or "decelerate" in terms of its propagation away from the positively charged particles). In effect, the positive particle would be accelerated in the opposite direction away from the irregular distribution of positive particles by electromagnetic repulsion, which in this example, as said, would dominate over gravitational attraction.

Figure (21) shows the two possible varieties of effective virtual particle paths of the irregular distribution of positively charged particles which interact with the virtual particle paths of the propagating positively charged particle which is turned around and accelerated up the page away from the same irregular distribution of positively charged particles. It is particularly worth noting here that the mass spins (m) of respectively interacting right and left hand screw sides are antiparallel and repel in attempt to turn the positive particle around, such that, in effect, the mass spin vectors are producing gravitational attraction as the positive particle is repelled away from the irregular distribution of positive particles.

Positive particle propagating up the page
interacting with two varieties of effective
virtual particle paths from an irregular
distribution of positive particles

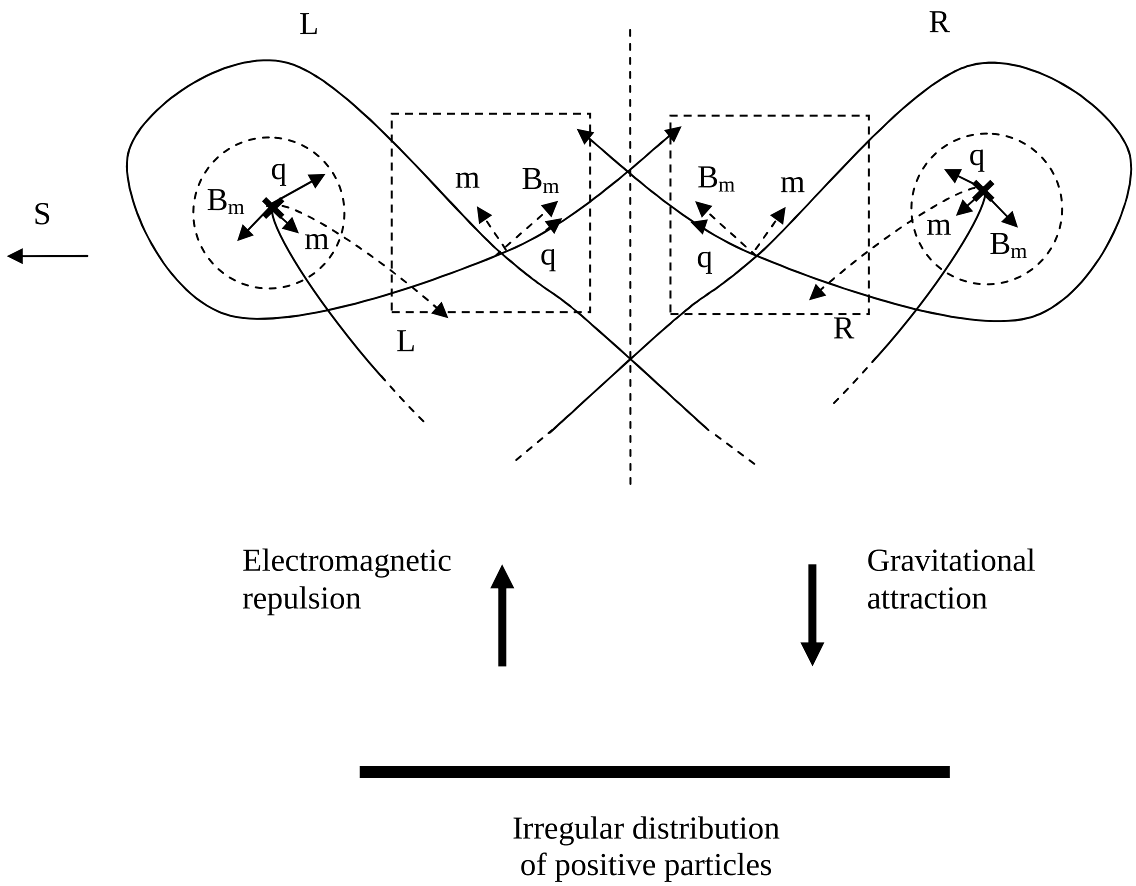

Effective extranuclear virtual particle paths (with spins in dashed circles) extend out from the positively charged particles (thick solid line) and interact with the "nuclear region" of the propagating positive particle (with spins in dashed squares), such that the charge (q) spins of respectively interacting right and left hand screw sides are parallel and respectively attract, and such that the mass spins (m) of respectively interacting right and left hand screw sides are antiparallel and repel (attempting to turn the positive particle around), and furthermore such that the magnetic spins (B_m) of respectively interacting right and left hand screw sides are antiparallel and attract (thus repelling the positive particle away from the irregular distribution of positive particles). (Note that the top and bottom sides of the propagating positive particle now tilt into the page.)

FIG. 21

It is considered that the virtual particle paths of oppositely electrically charged particles can produce electrically neutral effects. Wherein, if a uniform irregular distribution of both positive and negative electrically charged particles (with respective mass) interact with an electrically charged particle, then the microscopic magnetic spins of the four effective varieties of extranuclear virtual particle paths (from eight possible virtual particle paths altogether) from the given positive and negative electrically charged particles would "symmetrically" neutralize so as to neutralize the electromagnetic effects, while the same mass spins would continue to be affective and maintain gravitational attraction. (Note that gravitational attraction occurs with both electromagnetic attraction and electromagnetic repulsion, and thus gravity is perceived as only causing acceleration towards a massive particle.)

As further examples of the symmetrically neutral affects of the virtual particle paths of one or more electrically charged particles, it is considered that a neutron comprises the virtual particle paths of a positive electrically charged proton and a negative electrically charged electron (as elaborated upon later) which can effectively interact together in a symmetrical manner so as to produce an electrically neutral effect. While, an electromagnetic field quantum is considered to comprise top and bottom sides which propagate side-by-side, and interact electromagnetically in an electrically neutral manner upon being "symmetrically" absorbed into a particle (such as an electron) along the nuclear region. While, outside if this sort of interaction, it is considered that an electromagnetic field quantum can not be significantly electrically interacted upon by electrically charged particles due to the particular alignment of the microscopic spin vectors of the virtual particle paths on the top and bottom sides in its internal structure.

Figure (22A) shows a rotated view of the top and bottom virtual particle paths of a quantum with respect to an interacting irregular distribution of positive and negative electrically charged particles (e.g., a star of significant mass).

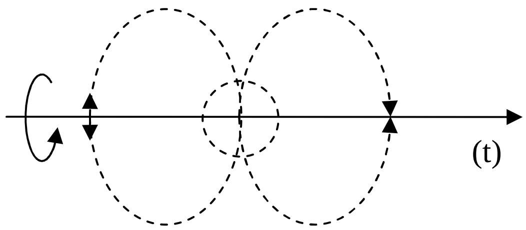

Bottom view

Arrangement of a propagating matter quantum with respect to an interacting irregular distribution of positive and negative electrically charged particles (solid line). Here, the top and bottom virtual particle paths of the quantum are rotated 90 degrees around the (t) axis in order to show the bottom view of the quantum.

FIG. 22A

Figure (22B) is an enlarged view of what is occurring on the bottom portion of the quantum in the dashed sphere in figure (22A) with the spin vectors rotated back 90 degrees around the (t) axis (back to their assumed alignment), and then viewed as would be seen from the front (also 90 degrees rotated).

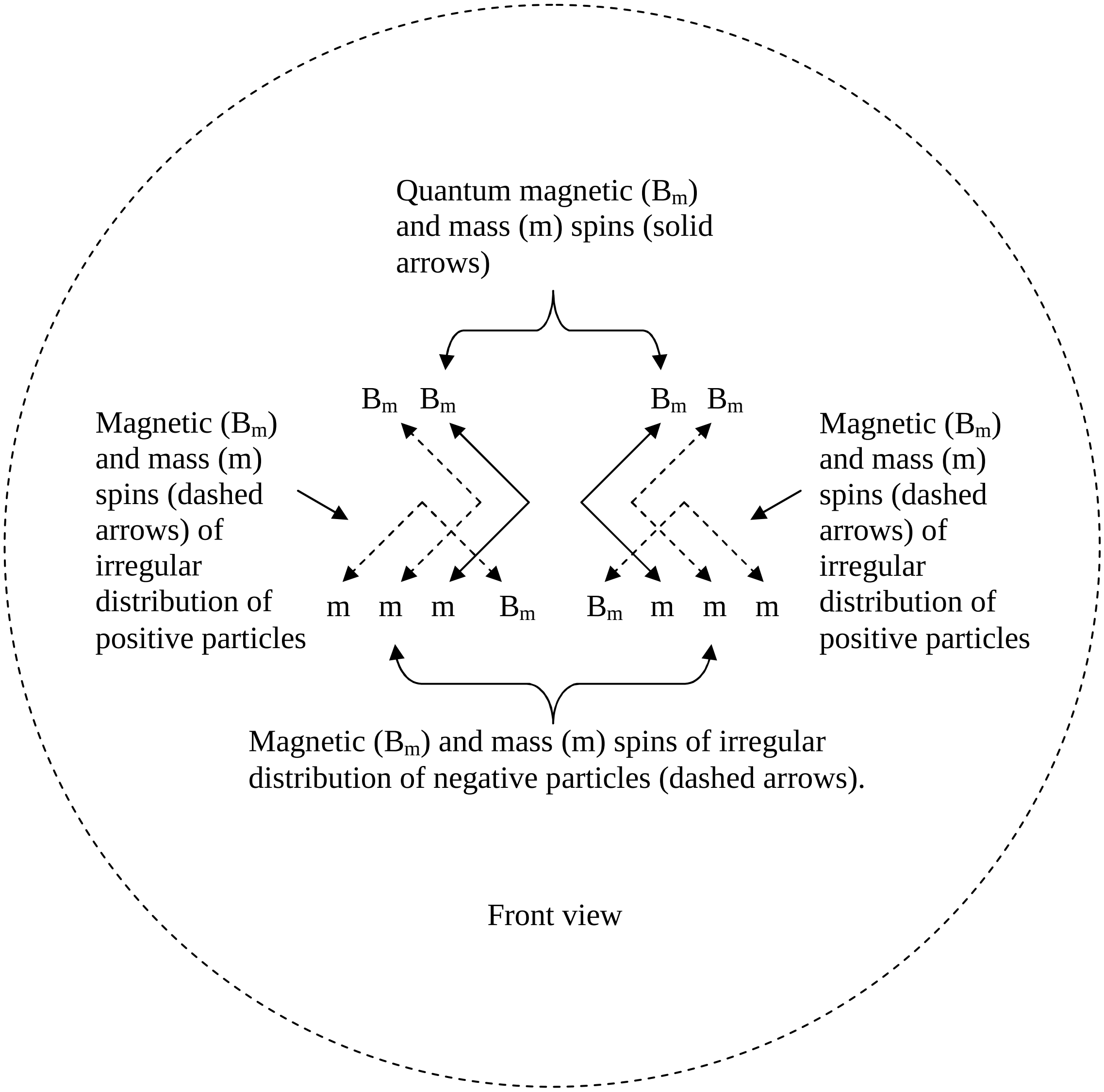

Here, figure (22B) is an enlarged view of what is occurring on the bottom portion of the quantum in the dashed sphere in figure (22A) with the spin vectors rotated 90 degrees around the (t) axis, and as would be seen from the front view (also rotated 90 degrees). Wherein, in figure (22B), the mass spins (m) from the irregular distribution of positive and negative particles are aligned parallel with the matter quantum mass spins (m), and thus all attract so as to produce gravitational attraction. While, the magnetic spins (B_m) of the irregular distribution positive particles are all aligned antiparallel and thus attract, and the magnetic spins (B_m) of the irregular distribution of negative particles are all aligned parallel and thus repel, such that antiparallel and parallel magnetic spins cancel and produce charge neutralization. Note that the quantum top and bottom (B_m) and (m) spin vectors are rotated into the plane of the page, but actually are approximately in the portions of the dashed planes aligned perpendicularly shown in figure (22C).

FIG. 22B

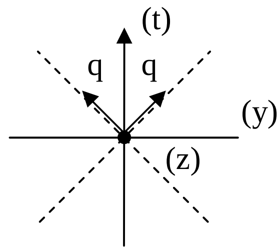

When figure (22B) is viewed from the bottom, the quantum top and bottom (B_m) and (m) microscopic spin vectors are aligned approximately in the dashed planes aligned perpendicularly. While, the (q) spin vectors are aligned perpendicular to their respective (B_m) and (m) spin vectors, and the quantum as a whole would be propagating along the (t) axis.

FIG. 22C

Note that gravitational "attraction" is represented by the attempt to turn the virtual particles around on the top side of the quantum where the mass spins of the quantum invert alignment and are antiparallel with the mass spins of the extranuclear virtual particle paths of the larger mass (as in electromagnetic interaction when the repelled real particle is propagating away from the repulsive source.

Equation (14) shows the theoretical reasoning for the apparent doubling of the gravitational potential in the gravitational lensing effect for a massive irregular distribution of positively and negatively charged particles interacting with a quantum at weak field (the result of which is similar to that of general relativity):

$$V_{\text{(large mass total potential)}} = 4*2*1*\sum V_g =$$

$$4*2*1*\left[\left({}^{-}\frac{1}{\approx 4}G_T\frac{m}{r}*e^{[1*\approx^{-}0\pi(mcr)/h]} + {}^{-}\frac{1}{\approx 4}G_T\frac{m}{r}*e^{[1*\approx^{-}0\pi(mcr)/h]}\right)+\ldots\right]=$$

$$4*2*1*\left[\left({}^{-}\frac{1}{\approx 2}G_T\frac{m}{r}*e^{[1*\approx^{-}0\pi(mcr)/h]}\right)+\ldots\right]=4*\left[\left(\approx{}^{-}1G_T\frac{m}{r}*e^{[\approx^{-}0\pi(mcr)/h]}\right)+\ldots\right]\approx$$

$${}^{-}4G_T\frac{M}{r}*e^{[{}^{-}0\pi(mcr)/h]}\approx{}^{-}4G_T\frac{M}{r}$$

Eq. (14)

Here, photon mass is considered equal to zero, and $e^{[\approx -0\pi(mcr)/h]}$ is considered equal to one. While, all the potentials of the photon have a value of $1/n_1 \approx 1/1$ which is twice the value of the corresponding constant of all the interacting potentials of the constituent electrically charged particles of the larger mass which each have a value of $1/n_1 \approx 1/2$.

Wherein, with respect to equation (14), the net charge of the interacting large mass is equal to zero, and photon mass is considered equal to zero so that only the interacting virtual particle path potential portions which are associated with the masses of the constituent particles of the larger mass are considered. In which case, more specifically, the mass associated interacting potentials of the constituent particles (i.e., $\approx {}^{-}1/4G_Tm/r*1/e^{[\approx 0(2\pi mcr)/h]}$ each) from the larger mass enter the "nuclear region" of the photon by way of their respective gradient virtual particle paths, and interact so as to summate with the mass associated potentials of the photon. While, the mass associated potentials of the constituent particles from the larger mass are doubled upon being multiplied by a factor of two (as shown in equation 14) which is transferred from the doubling of the constant $1/n_1 \approx 1/2$ of each of the electrically charged particles to $1/n_1 \approx 1/1$ (as for the photon).

While, for example, if a relativistically accelerated electrically charged particle is applied instead of a quantum, the internal spin vectors of the electron are rotated (and the constants move along their respective intervals) so that the potential of the larger mass is multiplied times a factor of (½) which corresponds to the square of the Lorentz factor, i.e., $(\Delta n_1)=\sqrt{2}$ such that $1/(\sqrt{2})^2/1=½$, wherein the effective potential is $\approx {}^-4G_Tm/r*1/e^{[.172*\approx 0(2\pi mcr)/h]}*½ \approx {}^-2G_Tm/r*1/e^{[0(2\pi mcr)/h]}$. (Here, for example, consider the partial reflections of the top and bottoms sides of an electrically charged particle relative to the almost total reflections of the top and bottom sides of a quantum described before as relates to figures 13A and 13B, and figures 15A and 15B, while, also, refer to figures 27A and 27B hereinafter as they pertain to the cancellation of one aspect of the rotation of the virtual particle paths during the acceleration of an electrically charged particle.)

Still, if a static electrically charged particle is applied, then the larger mass is multiplied times yet another factor of (½) according to the square of the Lorentz factor, i.e., $(\Delta n_1)=2$ such that $1/(2)^2/1=¼$, wherein, the gravitational potential of the larger mass is then $\approx {}^-4G_Tm/r * 1/e^{[0*\approx 0(2\pi mcr)/h]} * ¼ \approx {}^-1G_Tm/r$. (Nevertheless, note that according to the present unified field theory, and contrary to convention, it is considered that a quantum can be electrically interacted upon by an electrically charged particle to an infinitesimally small extent, i.e., in particular, a large collection of electrically charged particles comprising the same electrical charge could electrically interact in a observable way with a quantum according to the spins of the charged particles and the spins of the quantum.)

Now, it is considered that the virtual particle paths which extend out from a particle interact by summating (i.e., adding and subtracting) with the potentials of the virtual particle paths of another particle in agreement with their respective spins, so as to effectively attract or repel, and consequently cause a respective extent of electromagnetic attraction or repulsion and gravitational attraction. Wherein, in order to unify "spacetime" (as considered with respect to the unified field herein) with the mass-energy of the unified field, the Lorentz factor is related to the geometry of the propagation of the mass-energy of the unified field (or of a particle) (as with respect to figure 6D and the reasoning which follows immediately thereafter), and the reciprocal Lorentz factor is redefined according to a change in potential as shown in equation (15) below:

$$\frac{1}{\gamma_T} \equiv \sqrt{1-\frac{v^2}{c^2}} = \sqrt{\frac{c^2}{c^2}-\frac{v^2}{c^2}} = \sqrt{\frac{c^2-v^2}{c^2}} \equiv$$

$$\sqrt{\frac{8*\sum\frac{1}{n_1}K_T(q)*\frac{e^{\left[\frac{n_2^{-}2\pi(mcr)}{h}\right]}}{r} - 8*\sum\frac{1}{n_1}K_T(q)*\frac{e^{\left[\frac{n_2^{-}2\pi(mcr)}{h}\right]}}{r}}{8*\sum\frac{1}{n_1}K_T(q)*\frac{e^{\left[\frac{n_2^{-}2\pi(mcr)}{h}\right]}}{r}}} =$$

$$\sqrt{\frac{\Delta 8*\sum\frac{1}{n_1}K_T(q)*\frac{e^{\left[\frac{n_2^{-}2\pi(mcr)}{h}\right]}}{r}}{8*\sum\frac{1}{n_1}K_T(q)*\frac{e^{\left[\frac{n_2^{-}2\pi(mcr)}{h}\right]}}{r}}}$$

such that $\frac{1}{\gamma_T} = \sqrt{\frac{\Delta V}{V}}$ and

$$\frac{1}{\gamma^2{}_T} = \frac{\Delta V}{V} \qquad \text{Eq. (15)}$$

Accordingly, it is considered that the Lorentz factor is "carried" by the virtual particle paths (mass-energy) and the respective volume subtended by the virtual particles (virtual particle paths) of the unified field, such that the parameters of Lorentz transformations are inherent in the unified field (providing background independence). Thus, the gradient of a single virtual particle path (or a four dimensional array of virtual particle paths) provides the gravitational (and electromagnetic) energy of interaction, and effectively supplies the Lorentz factor. While, the path along which a respective body interacted upon travels is effectively produced by the respectively interacting virtual particle path (or paths) and the body interacted upon according to such terms which include the potentials and corresponding alignments of the virtual particle paths of the interacting fields before, and as a consequence of, interaction.

In result, the mass-energy and the "spacetime" of "gravity" are both comprised by the virtual particle paths of the unified field, and are applied together in a more direct manner then in general relativity. Yet, the unified field described herein unifies "spacetime" with not only mass, but also electric charge. Wherein, for example, a virtual particle path of the unified field (which, again, carries the Lorentz factor of "spacetime,") comprises both a gravitational component which accounts for conventional gravitational interaction, and an electromagnetic component which accounts for conventional electromagnetic interaction, while both account for "nuclear interaction." In which case, for example, in proton-proton nuclear interaction, the electromagnetic component includes attractive spins, while the gravitational component includes repulsive spins as will be described later (wherein gravity is considered negligible in conventional terms in this latter case).

In view of what has been presented thus far, the theory herein does not support the existence of gravitons, and therefore neither supports gravitons as mediators of the gravitational interaction nor gravitational waves as existing independent of electromagnetic waves. Similarly, the theory herein does not support photons as the gauge boson mediators of the electromagnetic interaction. Wherein, overall, the present unified field theory neither supports "gauge bosons" as the force carriers of interactions nor the standard model for the most part. In response, the unification herein proposes that the gravitational and electromagnetic components of the unified field together mediate gravitational and electromagnetic interactions (etc.) in a unified manner by way of virtual particles as described before, and, more so later.

CHARGED PARTICLE PROPAGATION AND INTERACTION:

Now, consider that a propagating electrically charged particle has an intrinsic spin (S) which is aligned through the elliptical virtual particle paths which only partially reflect around the axis in the plane of symmetry which separates the top and bottom sides as shown for a propagating negatively charged particle in figures (23A), (23B), and (23C), and for a positively charged propagating particle in figures (24A), (24B) and (24C). (Note that only the front portion of each propagating particle is shown.)

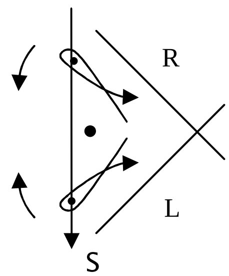

Front view

FIG. 23A

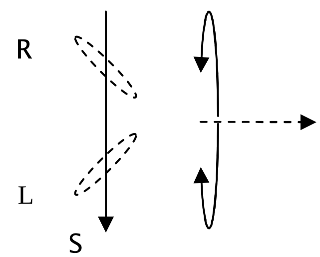

Side view

FIG. 23B

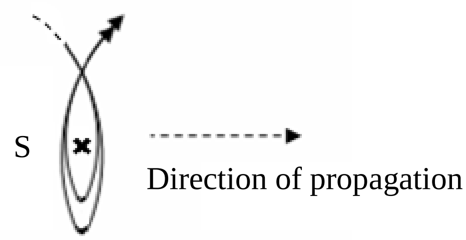

Top view

Intrinsic spin for a propagating negatively charged particle. Note that (S) is into the page using the right hand rule.

FIG. 23C

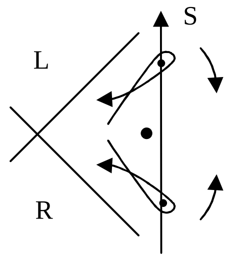

Front view

FIG. 24A

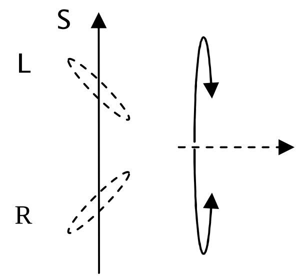

Side view

FIG. 24B

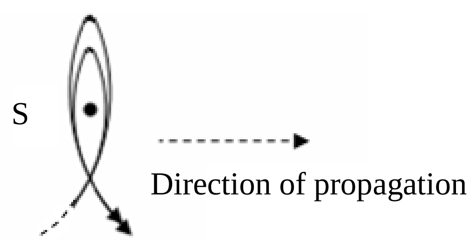

Top view

Intrinsic spin for a propagating positively charged particle. Note that (S) is out of the page using the right hand rule.

FIG. 24C

Next, it is considered that propagating negatively charged particles prefer to be relatively upright during interaction while propagating in parallel or antiparallel, and similarly for propagating positively charged particles as shown in figure (25A) for juxtaposed parallel propagating negatively and positively charged particles. While, similar alignment is shown in figure (25C) for vertically aligned parallel propagating negatively and positively charged particles. On the other hand, it is considered that propagating positively and negatively charged particles prefer to be relatively inverted during interaction while propagating in parallel or antiparallel as shown in figure (25B) for juxtaposed parallel propagating positively and negatively charged particles, and as shown in figure (25D) for vertically aligned parallel propagating positively and negatively charged particles. Wherein, in each case, the intrinsic spins are aligned parallel.

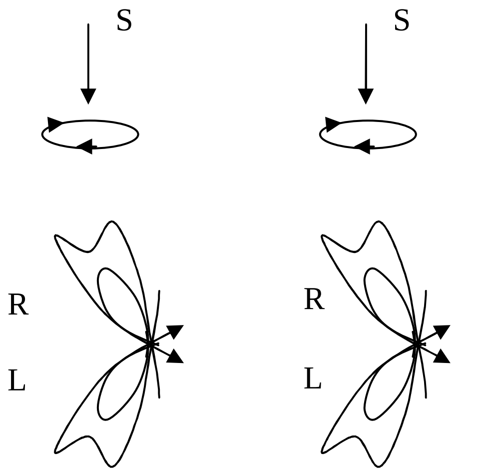

Upright juxtaposed negatively charged
particles propagating
in parallel out of the page

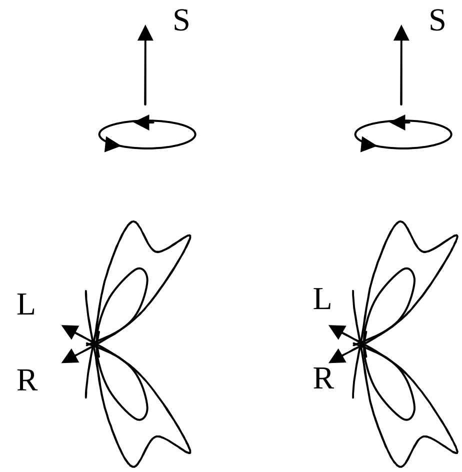

Upright juxtaposed positively charged
particles propagating
in parallel out of the page

FIG. 25A

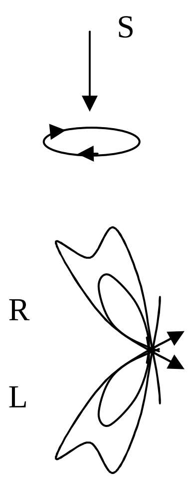

Inverted positively
charged particle

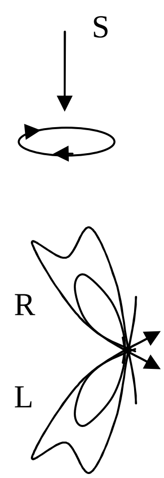

Upright negatively
charged particle

Juxtaposed positively and negatively charged particles
propagating in parallel out of the page

FIG. 25B

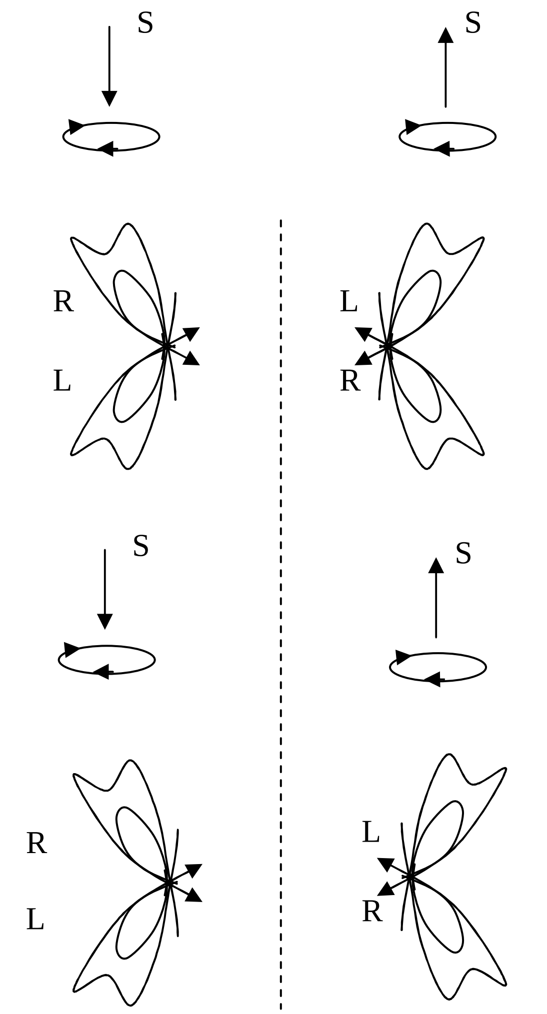

Upright vertically aligned negatively charged particles propagating in parallel out of the page

Upright vertically aligned positively charged particles propagating in parallel out of the page

FIG. 25C

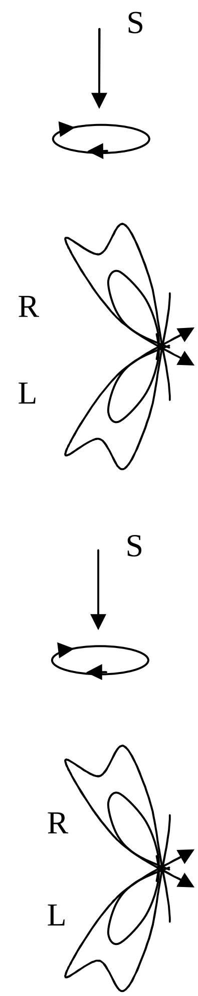

Inverted positively charged particle (top) propagating out of the page and vertically aligned with an upright negatively charged particle (bottom) propagating in parallel out of the page

FIG. 25D

Consider especially important for certain interactions (e.g., for interactions of electrically charged particles which are in a orderly aligned distribution as in the case of the interaction of spin aligned propagating electrically charged particles, the self interaction of virtual particles paths, the interaction of magnets, and molecular interactions), that the microscopic spin vectors of extended more bent virtual particle paths are relatively inverted due to "bending” compared to less bent virtual particle paths, such that, for example, the microscopic electric spin vector (q) rotation around the respective (z) axis is reversed, and, importantly, the magnetic (B_m) and mass (m) spin vectors are inverted as shown in figures (26A) and (26B), for example, for the extranuclear field region on the front top right hand screw side of a negatively charged particle. Wherein, this inversion characteristic, or the lack thereof, affects the alignment and rotational directions of the spin vectors of interacting virtual particle paths, and thus affects the respective attraction or repulsion of spin vectors during certain interactions.

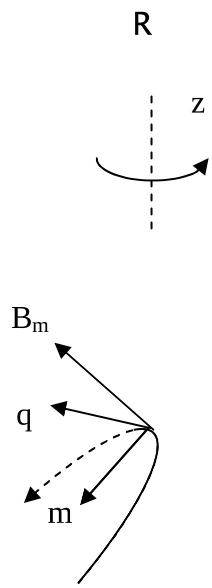

FIG. 26A

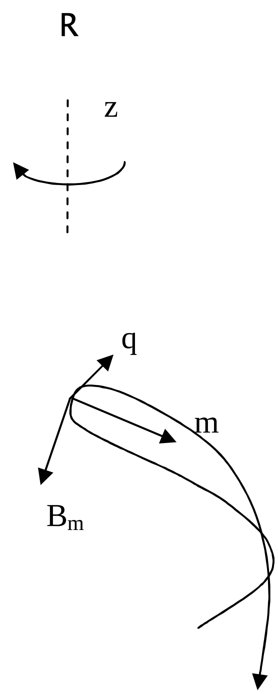

FIG. 26B

Spin rotation reversal around the (z) axis depicted for electric spin vector (q) such that the direction of the rotation is relatively inverted in the less bent virtual particle path shown in figure (26A) compared to the electric spin vector (q) in the more bent virtual particle path shown in figure (26B) in the extranuclear field region on the front top right hand screw side of a negatively charged particle. While, importantly, the microscopic magnetic and mass spin vectors are also inverted along respective axes accordingly.

Also, consider important for interaction during propagation, that the acceleration of the unified field causes relatively different rotations in different portions of a virtual particle path. Wherein, the rotations shown by the dashed curved arrows in figure (27A) for an increase in mass for the microscopic mass spin vectors (m) are in relatively different directions for different portions of a virtual particle path. Then, when considered together as shown by the dashed curved arrows in figure (27B), the bent condition of a more bent virtual particle path is maintained as the different portions of the virtual particle path rotate in opposite directions, and as the relativistic mass of the electrically charged particle as a whole increases.

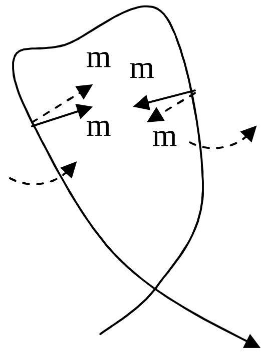

FIG. 27A

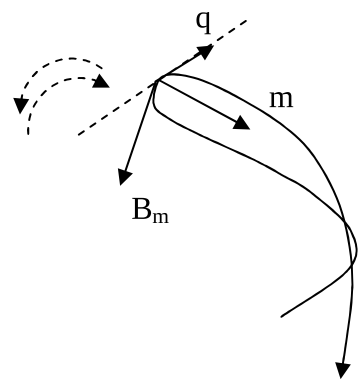

FIG. 27B

Here, as different portions of the example virtual particle path rotate in opposite directions as shown in figure (27A), nevertheless, the bent condition of a more bent virtual particle path is maintained where such rotations cancel each other out as shown by the curved arrows in figure (27B).

Now, figure (28) shows how the microscopic magnetic spin vector component (B_{mc}) of a more bent virtual particle path (dashed oval) of the right hand screw side of the upright negatively charged particle propagating on the bottom is aligned antiparallel (in a horizontal plane) to the microscopic magnetic spin vector component (B_{mc}) of the coupling virtual particle path of the right hand screw side in the "nuclear region" (dashed rectangle) of the upright negatively charged particle propagating in parallel on the top, thus causing magnetic attraction.

Note that the particles in figures 28-31 are shown separated. Thus, one must conceptually reposition each orthogonal set of extranuclear spins shown in a dashed oval while keeping them aligned as they are so that the origins of the spin vectors in an oval are almost abutting with the origins of the orthogonal set of nuclear spins shown in the dashed rectangle of the other relevant charged particle for proper alignments. Also, note that the vertical component of (q) is effective in both parallel and antiparallel propagating cases. Furthermore, note that the following examples of propagating electrically charged particle interaction also include attraction or repulsion according to the microscopic charge, mass, and magnetic spin vectors of the respectively less bent virtual particle paths of the extranuclear field of a propagating electrically charged particle with the nuclear region of the opposing propagating charged particle, i.e., in particular, during juxtaposed propagating charged particle interaction, so as to account for electric and respective gravitational interaction accordingly. Wherein, in figures 28-31, the less bent virtual particle paths are shown separated from, and adjacent to, their respective more bent virtual particle paths. Moreover, note that two equivalently arranged positively charged propagating particles are considered to interact similarly.

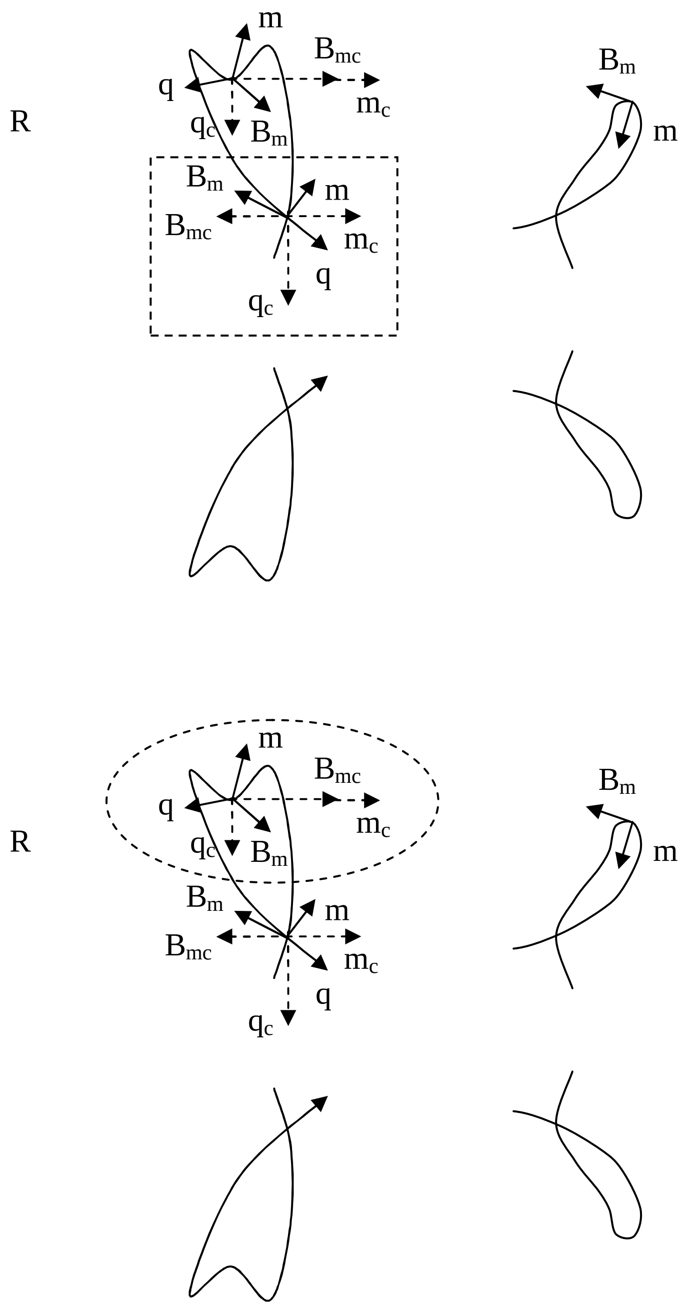

Here, the microscopic magnetic spin vector component (B_{mc}) of the more bent virtual particle path (dashed oval) of an upright negative particle propagating out of the page on the bottom is aligned antiparallel in the horizontal plane to the microscopic magnetic spin vector component (B_{mc}) of the "nuclear region" (dashed rectangle) of an upright negative particle propagating in parallel out of the page on the top, thus causing magnetic attraction.

FIG. 28

Figure (29) shows how the microscopic magnetic spin vector component (B_{mc}) of a more bent virtual particle path (dashed oval) of the right hand screw side of the upright negatively charged particle propagating on the bottom is aligned parallel to the microscopic magnetic spin vector component (B_{mc}) of the coupling virtual particle path of the right hand screw side in the “nuclear region” (dashed rectangle) of the upright negatively charged particle propagating antiparallel on the top, thus causing magnetic repulsion. (Note that the spins of the propagating charged particles shown in figures (29) and (31), which include antiparallel mass components which attempt to turn the particles around, are considered to especially disclose the role they could play in a two-body problem.)

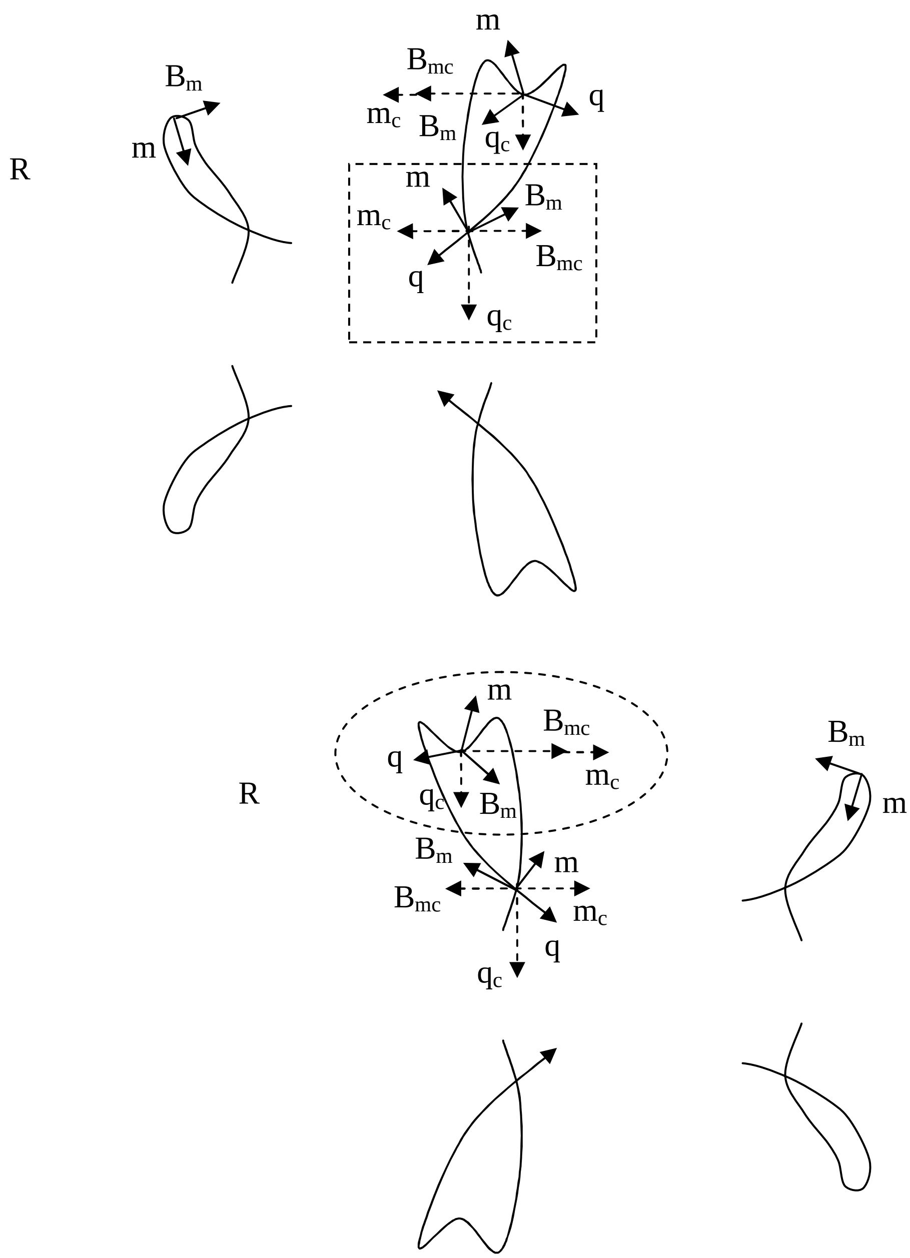

Here, the microscopic magnetic spin vector component (B_{mc}) of the more bent virtual particle path (dashed oval) of an upright negative particle propagating out of the page on the bottom is aligned parallel in the horizontal plane to the microscopic magnetic spin vector component (B_{mc}) of the "nuclear region" (dashed rectangle) of an upright negative particle propagating antiparallel into the page on the top, thus causing magnetic repulsion.

FIG. 29

Figures (30) and (31) show the arrangement for the interaction of negative and positive propagating particles. Wherein, in figure (30), the microscopic magnetic spin vector component (B_{mc}) of the more bent virtual particle path (dashed oval) of the right hand screw side of the negatively charged particle propagating on the bottom is aligned parallel to the microscopic magnetic spin vector component (B_{mc}) of the coupling virtual particle path of the right hand screw side in the "nuclear region" (dashed rectangle) of the inverted positively electrically charged particle which is propagating in parallel on the top, thus causing magnetic repulsion.

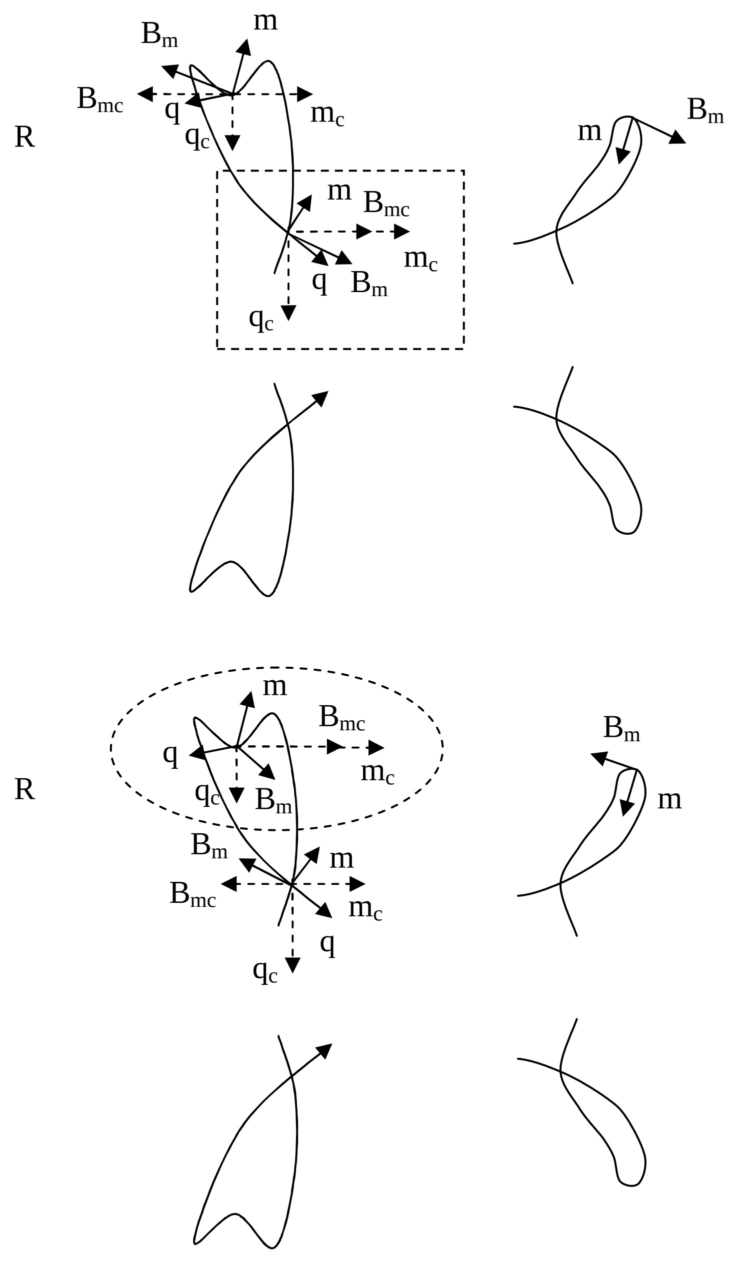

Here, the microscopic magnetic spin vector component (B_{mc}) of the more bent virtual particle path (dashed oval) of an upright negative particle propagating out of the page on the bottom is aligned parallel in the horizontal plane to the microscopic magnetic spin vector component (B_{mc}) of the "nuclear region" (dashed rectangle) of an inverted positive particle propagating in parallel out of the page on the top, thus causing magnetic repulsion.

FIG. 30

While, figure (31) shows how the microscopic magnetic spin vector component (B_{mc}) of the more bent virtual particle path (dashed oval) of the right hand screw side of the negatively charged particle propagating on the bottom is aligned antiparallel to the microscopic magnetic spin vector component (B_{mc}) of the coupling virtual particle path of the right hand screw side in the “nuclear region” (dashed rectangle) of the inverted positively electrically charged particle which is propagating antiparallel on the top, thus causing magnetic attraction.

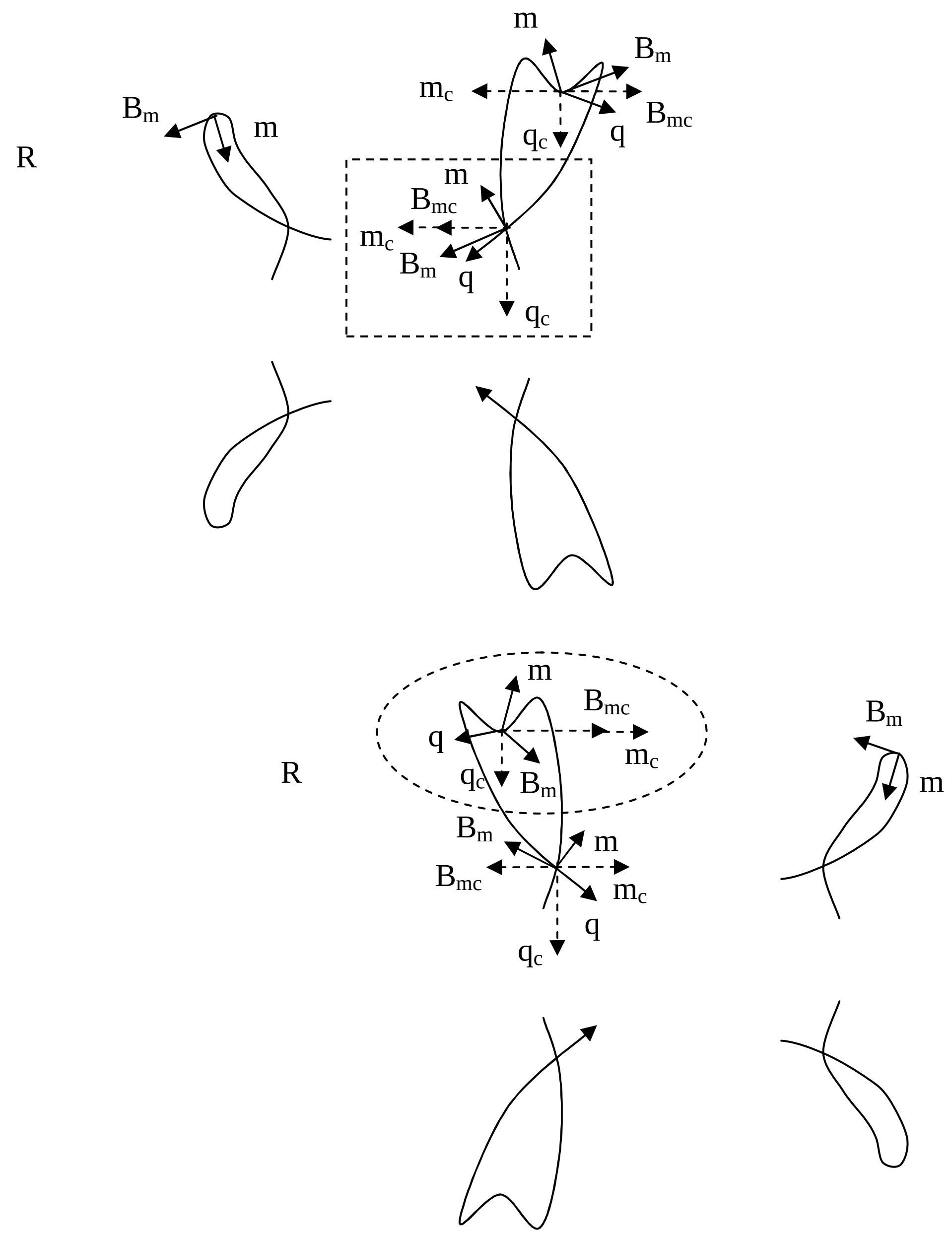

Here, the microscopic magnetic spin vector component (B_{mc}) of the more bent virtual particle path (dashed oval) of an upright negative particle propagating out of the page on the bottom is aligned antiparallel in the horizontal plane to the microscopic magnetic spin vector component (B_{mc}) of the “nuclear region” (dashed rectangle) of an inverted positive particle propagating antiparallel into the page on the top, thus causing magnetic attraction.

FIG. 31

VIRTUAL PARTICLES, SELF INTERACTION, AND SUPERLUMINAL VELOCITY:

Conventionally it has been difficult to detect and measure the parameters of particles thought to govern the internal structure of matter, e.g., due to the confinement of "quarks (the existence of which the present theory does not support)," etc. Herein, the theory of unification reuses the same parameters for "everything" for structure, function, and simplicity, such that virtual particles constitute the internal structure of mass-energy, and have an internal structure and function which is analogous to propagating electrically charged particles (wherein virtual particles comprise "virtual-virtual particles," etc.).

Accordingly, "self interacting" virtual particle paths (which account for internal bonding) align in agreement with their respectively interacting spin vectors so as to effectively produce the shape of the virtual particle paths, and consequentially the shape of a static or propagating particle as a whole. In which case, virtual particles on the top and bottom sides of negatively and positively charged particles are considered to self interact with virtual particles on the same side by way of the respective right-right and left-left hand spin vector interactions, such that parallel microscopic charge and mass spin vector interactions are attractive, and antiparallel microscopic magnetic spin vector interactions are attractive, etc. This is because virtual particles are also considered, in their own way, to comprise top and bottom sides which are either right or left hand screw. Similarly, it is considered that virtual particles on the top and bottom sides interact with virtual particles on their opposing sides in self interaction by way of respective right-right and left-left hand spin vector interactions. Figure (32A) shows the virtual particles posited for the front side of example virtual particle paths on the top and bottom sides in the nuclear region of negative and positive electrically charged particles.

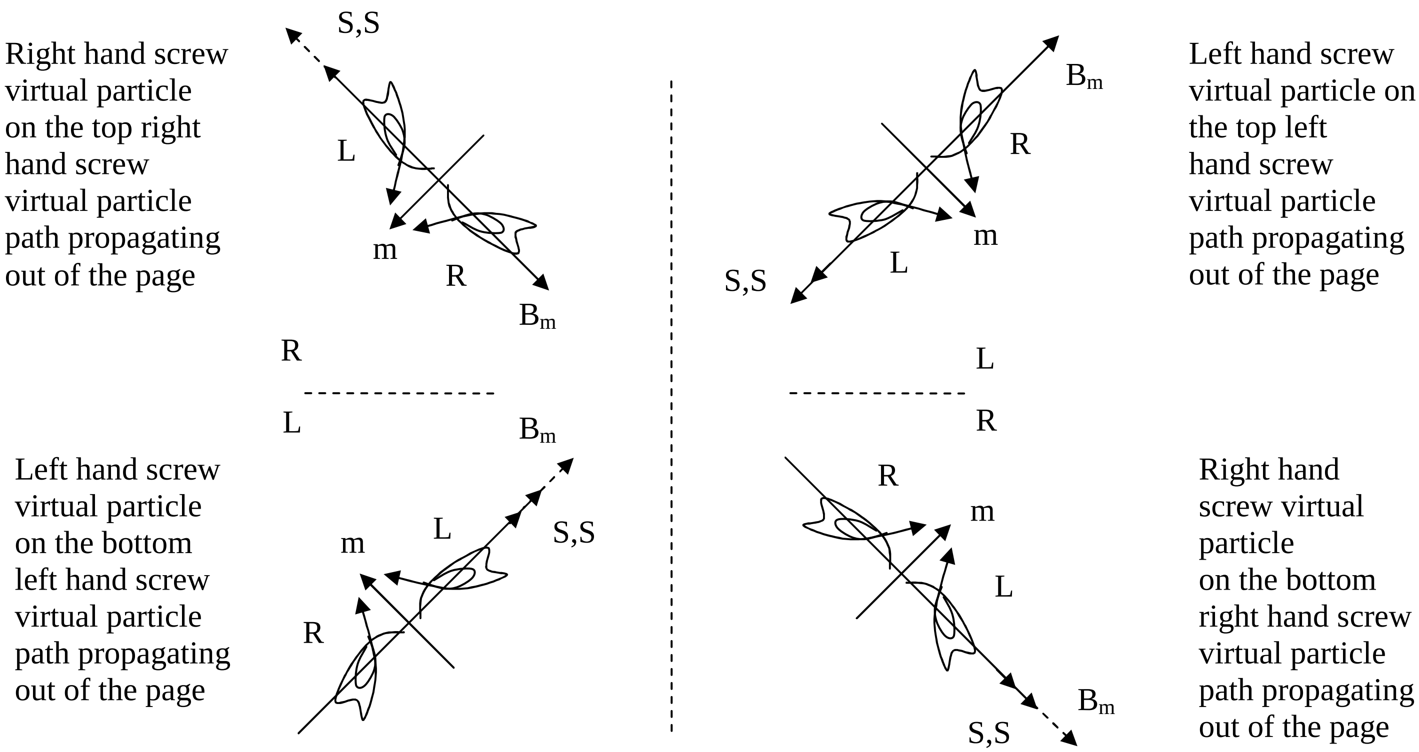

Virtual particles of top and bottom example virtual particle paths on the front side in the nuclear region of a negative particle

Virtual particles of top and bottom example virtual particle paths on the front side in the nuclear region of a positive particle

FIG. 32A

However, as shown in figure (32A), virtual particles have microscopic magnetic spin vectors (B_m) which are aligned according to the screw (charge) of the particle in which they are comprised by switching hand rules (as with magnetic moments). Wherein, a right hand screw virtual particle in a negatively charged particle and a right hand screw virtual particle in a positively charged particle have oppositely aligned microscopic magnetic spin vectors (B_m) when their intrinsic spins are aligned parallel, and similarly for the left hand screw virtual particles.

For example, as described for propagating charged particle interaction before, "real" propagating electrically charged particles of, for example, opposite electric charge which are propagating in parallel with parallel intrinsic spins would have electric attraction based on virtual particles on less bent virtual particle paths which are propagating with "antiparallel" microscopic magnetic spins. Yet, conversely, the virtual particles would also magnetically repel because of the more bent virtual particle paths on which the virtual particles are propagating in the extranuclear region of one of the real propagating particles relative to the virtual particle paths in the nuclear region of the other real propagating particle during interaction. Wherein, a more bent virtual particle path relatively inverts the interacting virtual particles, and causes repelling parallel microscopic magnetic spins which would otherwise be antiparallel and cause magnetic attraction. In which case, the differences in the microscopic magnetic spins of the virtual particles of the same spin in opposite screw particles (i.e., here, in oppositely electrically charged propagating particles) are accounted for accordingly.

Still, virtual particles from charged particles which mediate electromagnetic and gravitational interaction (as described before) are considered to attract or repel analogous to the way propagating electrically charged particles attract or repel during interaction. While, virtual particles bonded in a band in a particle, e.g., bonded in a band of virtual particles in a system of opposing sides as in the nuclear region of a static electrically charged particle, are also considered to interact analogous to the way propagating electrically charged particles interact, but in a way in which they change in spacing (increasing vertically and horizontally in an outward manner from the center) and rotate (increasing in the less massive, or more decelerated, rotational direction in an outward manner from the center) as shown in figure (32B). Wherein, such bonding occurs in order to maximize attraction and minimize repulsion in conjunction with the bends in their "virtual-virtual" particle paths (which function analogous to the more and less bent virtual particle paths of interacting propagating electrically charged particles described before), thus effectively contributing to the shape of the unified field.

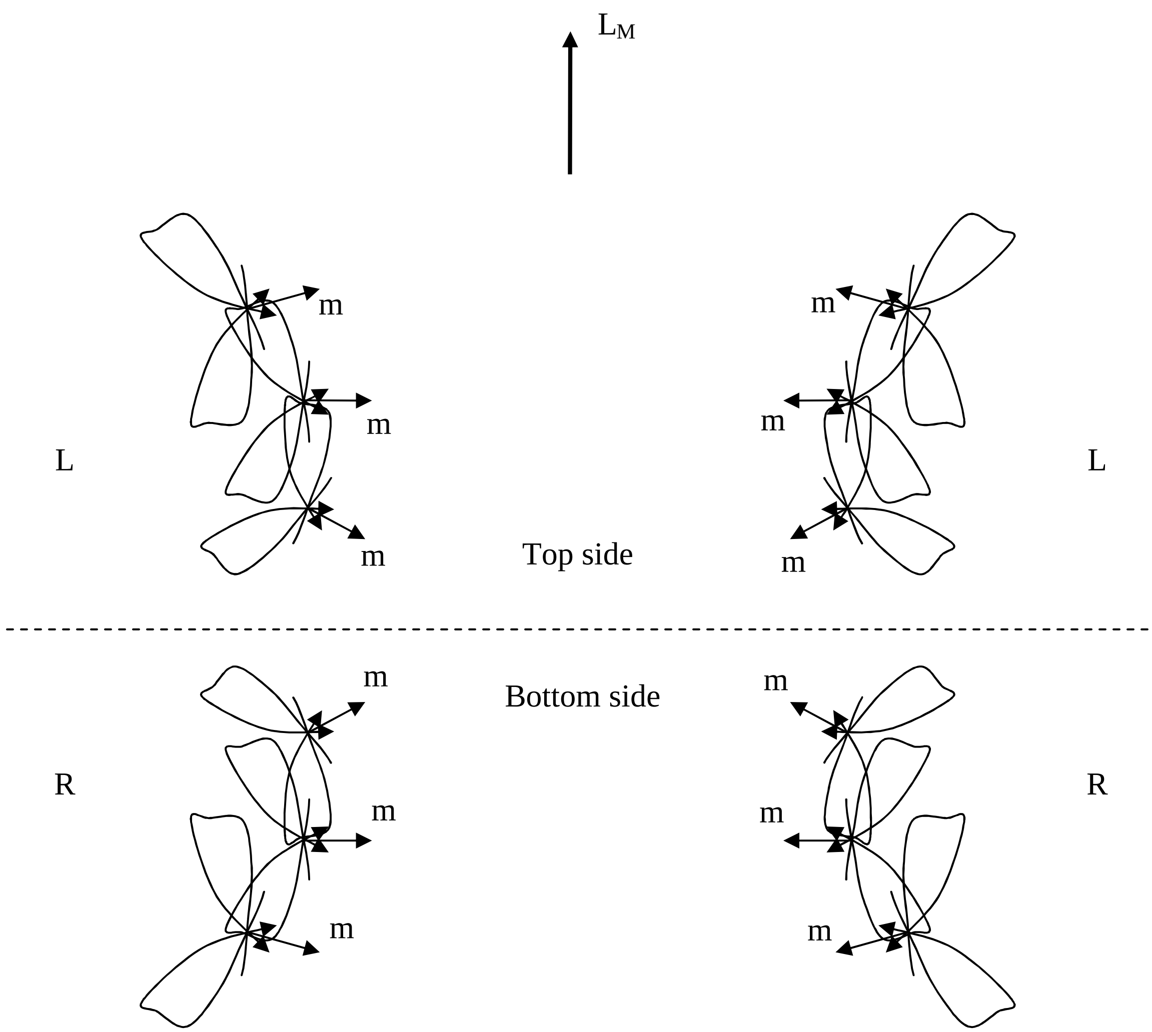

Example virtual particles in virtual particle paths propagating out of the page (left portion) and propagating into the page (right portion) on the top and bottom front and back sides of the nuclear region of a static proton.

FIG. 32B

Now, as pertains to the geometry of virtual particle paths and velocity, it is considered in the present theory that $h = 2\pi mcr \approx 2\pi(2.1765x10^{-8})\left(\frac{1.6162x10^{-35}}{5.3911x10^{-44}}\right)(1.6162x10^{-35}) = 6.6258x10^{-34}$. Wherein, 2πmcr/2π=h/2π is reduced Planck constant (h-bar); and Planck length (1.6162x10^{-35})/Planck time (5.3911x10^{-44}) = speed (c), which, given direction, represents a translational velocity. In which case, (h), i.e., unreduced Planck constant (2πmcr), is applied herein in a context in which it relates to the geometry of the virtual particle paths of the unified field, such that 2π*1.6162x10^{-35} (i.e., 2π r) is "unreduced" Planck length when r=1.6162x10^{-35}, and is applied such that 2π*1.6162x10^{-35} (unreduced Planck length)/5.3911x10^{-44} (Planck time)=1.8835x10^{+9} m/s, which, herein, is the superluminal velocity of virtual particles propagating over virtual particle paths.

ELECTROMAGNETIC FIELD QUANTUM ("MASSLESS" PARTICLES):

Consider that an "electromagnetic field quantum" produces a conventional alternating electromagnetic field comprising an alternating electric field (E_A) aligned along the (y) axis which is perpendicular to the axis around which the top and bottom sides reflect in the plane of symmetry which separates the top and bottom sides, and perpendicular to the direction of propagation as shown in the perspective views in figures (33A) and (33B). Furthermore, consider that an electromagnetic field quantum also produces a conventional alternating magnetic field (B_A), perpendicularly, which is generated as the virtual particle paths helically propagate left and right, and which is also aligned along the (z) axis perpendicular to the axis around which the top and bottom sides reflect in the plane of symmetry which separates the top and bottom sides, and perpendicular to the direction of propagation as also shown in figures (33A) and (33B).

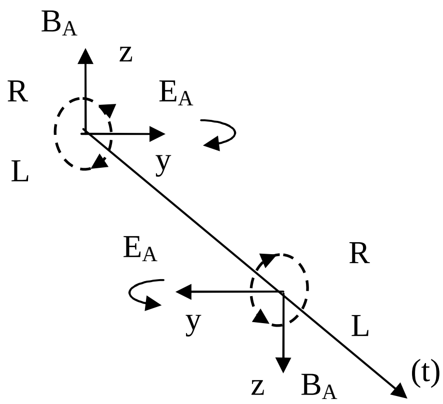

Matter
electromagnetic field
quantum

FIG. 33A

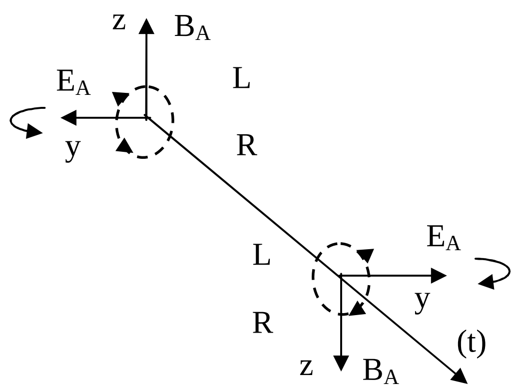

Antimatter
electromagnetic field
quantum

FIG. 33B

The electric field (E_A) and magnetic field (B_A) axes are considered to be aligned as shown in the front views for matter and antimatter electromagnetic field quanta in figures (34A) and (34B), and as also shown in perspective views in figures (35A) and (35B) (as they would also be aligned in an analogous manner, and for similar reasons, for a negatively and positively electrically charged particle, respectively). Note that the top and bottom sides shown in figures (34A) and (34B) are propagating around a common central axis, such that the infinitesimally small separation of the top and bottom sides is not shown. In this regard, the spin of an electromagnetic field quantum is almost entirely eliminated when considered in the same context as that of the spin of an electrically charged particle in the theory herein. Also, note that the helical geometry of the virtual particle paths of the electromagnetic field quantum in the present theory is supported by conventional theory in which a photon is considered to comprise right and left helical components. Furthermore, note that conventionally polarized electromagnetic fields could be achieved by rotating the spins of the virtual particle paths of the quantum (or equivalently an electrically charged particle) so that they follow an elliptical trajectory.

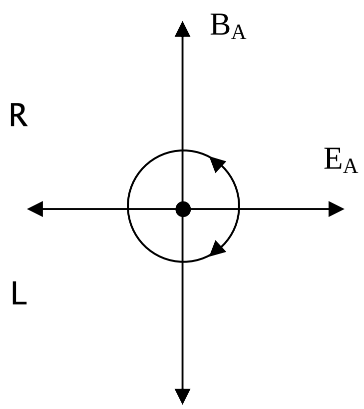

Matter quantum

FIG. 34A

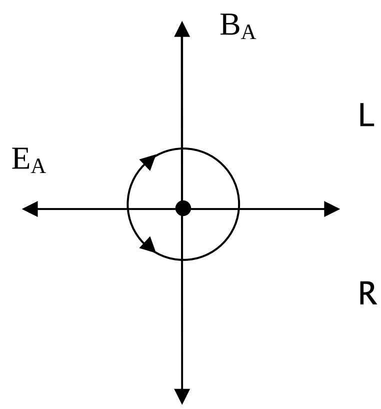

Antimatter quantum

FIG. 34B

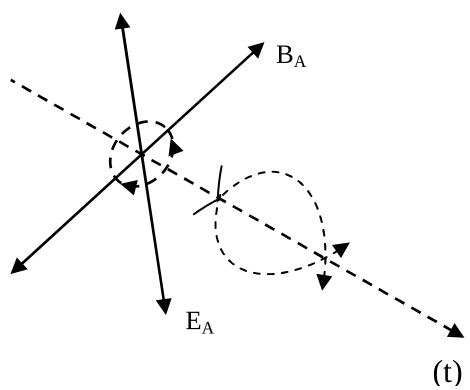

Matter quantum

FIG. 35A

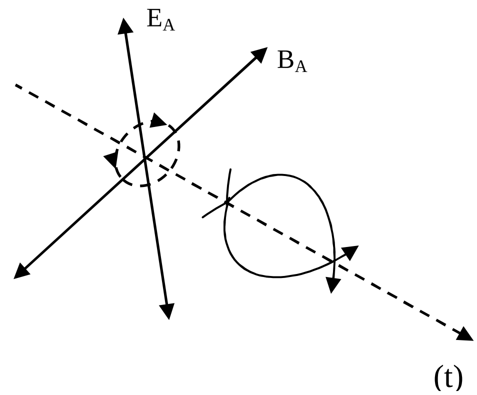

Antimatter quantum

FIG. 35B

It is also worth noting here that a matter quantum is considered to be emitted, for example, by an electron, and an antimatter quantum is considered to be emitted, for example, by a positron, and it will be shown later how an antimatter quantum can interact in a manner which is equivalent to a matter quantum, and vice versa.

The electric and magnetic fields of an electromagnetic field quantum (or an electrically charged particle) are considered to be detected during measurement as a consequence of the affect that the virtual particle paths of the propagating electromagnetic field quantum (or an electrically charged particle) have on another particle upon interaction. In figure (36), for example, consider that the right and left hand screw virtual particle paths of the matter quantum would align, and be respectively absorbed by, the top and bottom sides of the electron shown, such that the virtual particle paths of the quantum interact with the virtual particle paths of the electron, and thus cause the nuclear virtual particle paths of the electron to accelerate and project forward so as to establish the combined right and left elliptically helical top and bottom sides of a propagating electron along the direction of the propagating quantum (which is propagating into the page). Here, consider that the quantum is absorbed due to a lack of repulsion because of its field geometry (comprising a lack of eccentricity) thus allowing the quantum's field to merge with the electron's field, and then become eccentric with the eccentric geometry of the electron's field upon deceleration (refer to the description later herein regarding the quantum's unified field spin vector geometry with respect to annihilation and pair production under the heading "particle transmutation and generation").

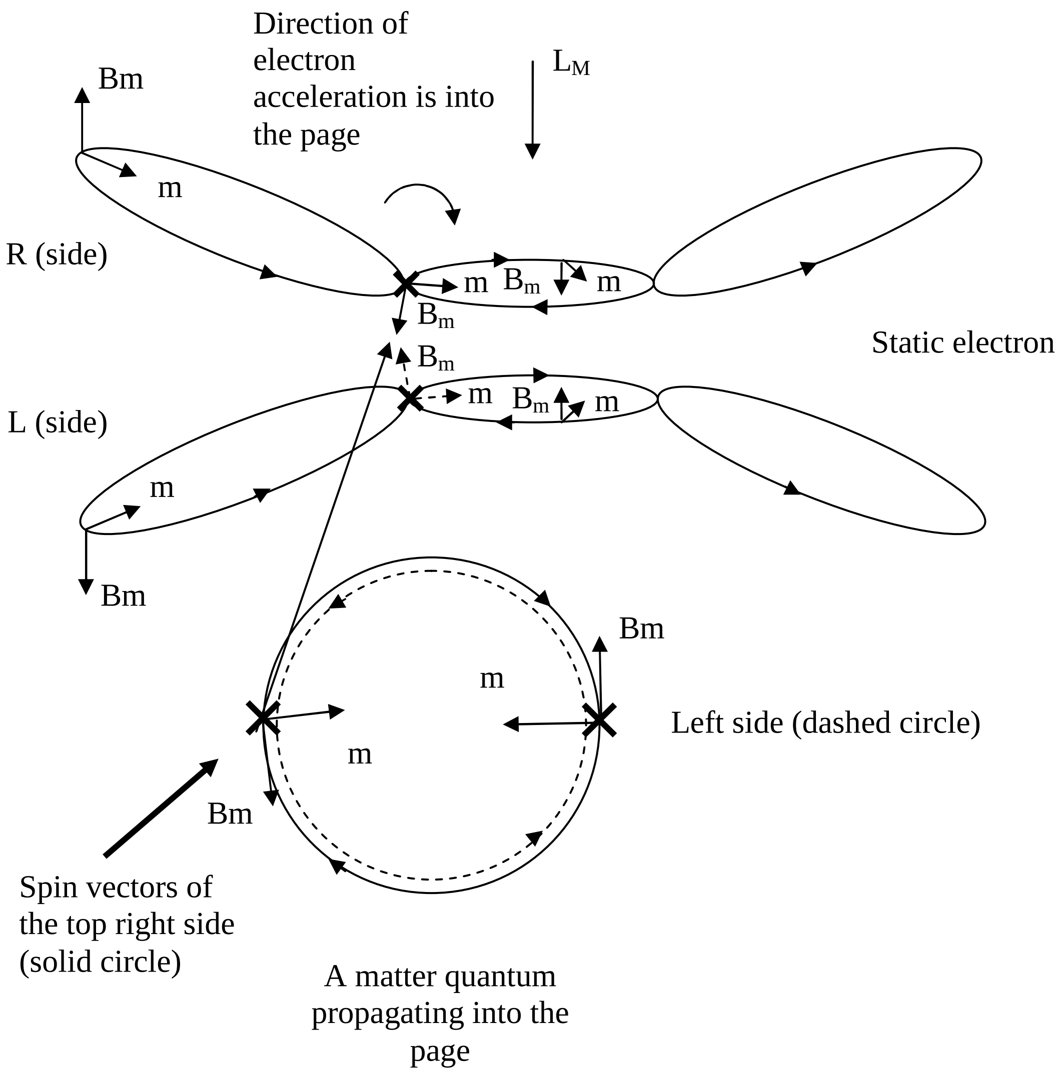

Static electron acceleration during absorption of the energy of an electromagnetic field matter quantum (only certain details of the absorption of top right side are shown)

FIG. 36

MAGNETIC INTERACTION:

Now, certain longstanding questions about magnetic fields can be addressed by examining the internal structure of the unified fields of static electrically charged particles as presented herein, e.g., the conclusion that the existence of magnetic monopoles is not supported by the present theory can be made. Wherein, in a description of a magnetic field produced by magnets herein, consider that the more bent virtual particle paths from the top side of each of a number of electrons propagating in the north pole of one magnet, and the more bent virtual particle paths from the bottom side of each of a number of electrons propagating in the south pole of an opposing magnet, respectively extend out to produce the virtual particle paths of the static magnetic field between the north and south poles of two magnets. In which case, the more bent virtual particle paths of electrons which are propagating in parallel with parallel intrinsic spins in orbitals magnetically interact attractively with electrons which are propagating in parallel with parallel intrinsic spins in orbitals in the opposing magnet as shown for the interaction of north pole electrons with south pole electrons in figure (37). Consequentially, in two such magnets, electrons in orbitals of protons in one magnet would be magnetically accelerated in an attractive manner towards parallel propagating electrons in orbitals of protons in the opposing magnet, such that the atoms in the opposing magnetic materials would accelerate towards each other.

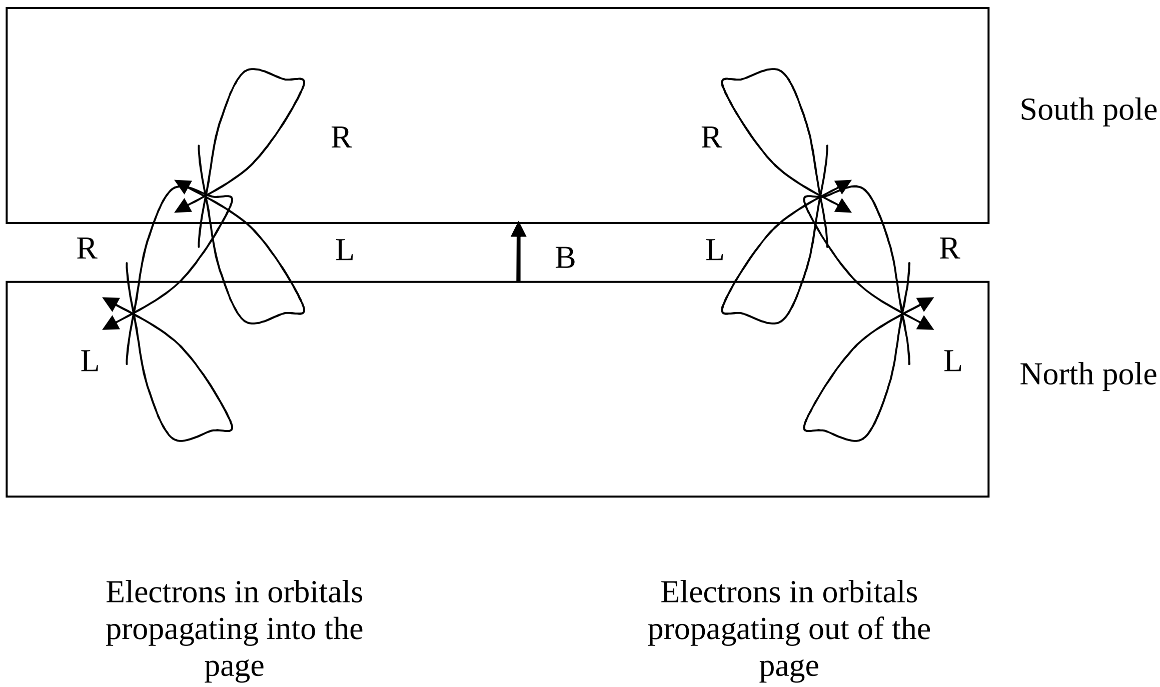

Here, example virtual particle paths extend out from parallel propagating electrons in one magnetic (e.g., the north pole here) into the opposing magnetic, and interact in a magnetically attractive manner with the nuclear regions of parallel propagating electrons in the opposing magnet (as for the interaction of propagating electrically charged particle interaction described previously).

FIG. 37

Figure (38A) shows the magnetic field produced between two magnets by the right and left hand screw sides of certain more bent virtual particle paths extending out from electrons comprised in the opposing magnets. While, figure (38A) also shows how the virtual particle paths of the magnetic field would interact with the top and bottom sides of negatively and positively charged particles which are propagating out of the page while propagating in, and perpendicular to, the magnetic field such that the top and bottom sides are accelerated in a respectively curved path. Wherein, the negatively and positively charged particles turn to the right and left (as shown looking into the page at figure 38A) for a negatively and positively charged propagating particle, respectively, due to the repulsion and attraction, respectively, of, in particular, the microscopic magnetic spin vector components (B_{mc}) of the curved portions of the more bent extranuclear virtual particle paths of the opposing magnets on the nuclear microscopic magnetic spin vector components (B_{mc}) of the negatively and positively charged propagating particles (i.e., the propagating negatively and positively electrically charged particles are accelerated in a direction which is perpendicular to the direction of the magnetic field (B) according to conventional left and right hand rules, respectively).

Magnetic field between magnetic poles generated by certain more bent virtual particle paths extending out from oscillating electrons in opposing magnets

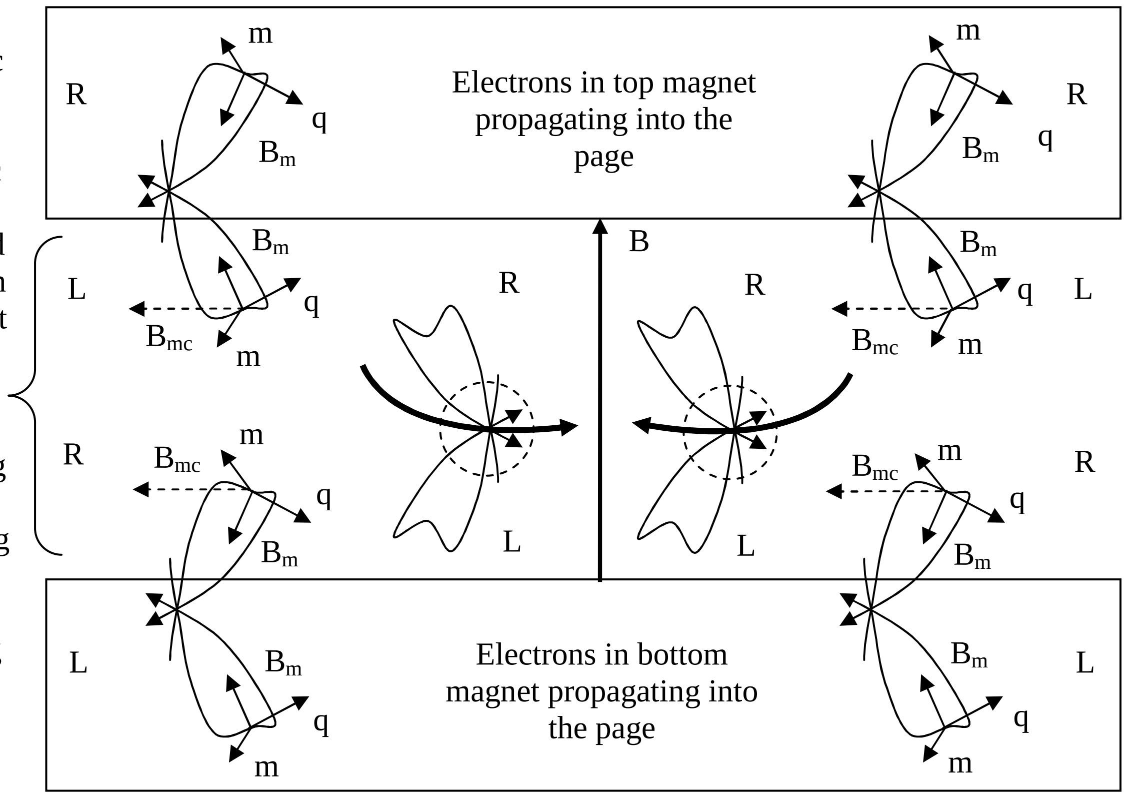

Nuclear microscopic spin vectors of the upright negative particle propagating out of the page

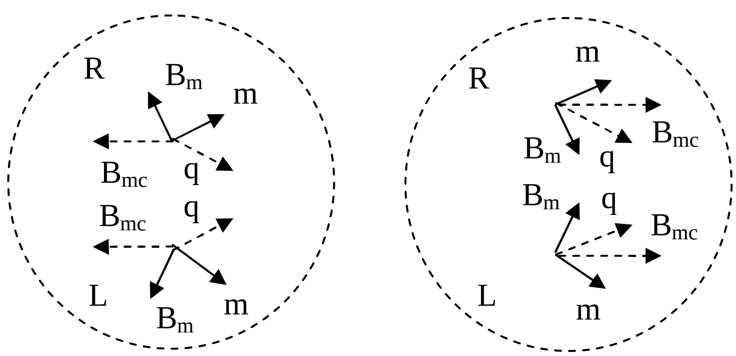

Nuclear microscopic spin vectors of the inverted positive particle propagating out of the page

The upright negative particle propagates in a curved path to the right (front view) due to parallel repulsion of the microscopic magnetic spin vector components (B_{mc}) produced by the interacting curved more bent virtual particle paths of the magnetic field.

The inverted positive particle propagates in a curved path to the left (front view) due to antiparallel attraction of the microscopic magnetic spin vector components (B_{mc}) produced by the interacting curved more bent virtual particle paths of the magnetic field.

FIG. 38A

Figure (38B) shows the microscopic charge spin vector (q) and vertical component (q_c) of a right hand screw more bent virtual particle path of a portion of the magnetic field depicted in figure (38A) aligned with the charge spin vector (q) and vertical component (q_c) in the nuclear region of the right hand screw side of an upright negatively charged particle propagating in, and perpendicular to, a portion of the magnetic field.

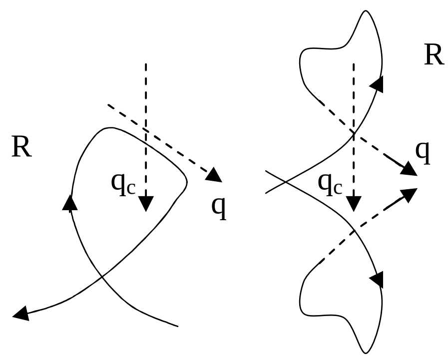

The microscopic charge spin vector (q) and vertical component (q_c) of a portion of the magnetic field shown in figure (38A) aligned with the charge spin vector (q) and vertical component (q_c) in the nuclear region of an upright negatively charged particle propagating to the right in, and perpendicular to, the given portion of the magnetic field.

FIG. 38B

In application, for example, the spiral courses of negative and positive electrically charged propagating particles (and the undeflected course of neutral propagating particles) in, for example, a bubble chamber can be more clearly understood.

NUCLEAR INTERACTION:

Figure (39) shows some orthogonal charge, mass, and magnetic microscopic spin vectors of example virtual particle paths in the nuclear region of a static positively electrically charged particle, i.e., here, a static proton. (Note that the distances which separate the virtual particle paths with respect to the origins of the spins shown in figures 39-42B are arbitrarily drawn, and thus are not relevant in those cases.)

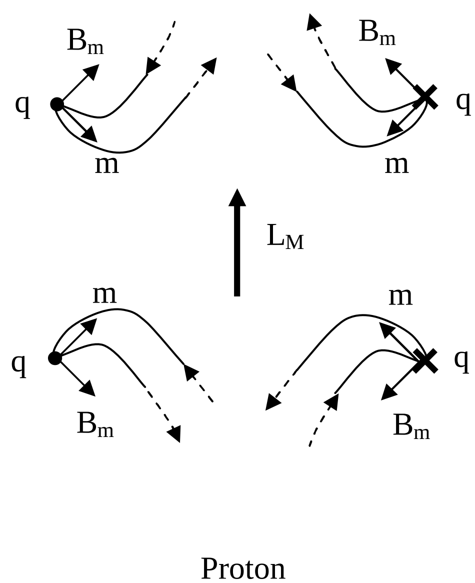

FIG. 39

Figure (40) shows some orthogonal charge, mass, and magnetic microscopic spin vectors of example virtual particle paths in the nuclear region of a static negatively electrically charged particle, i.e., here, a static electron.

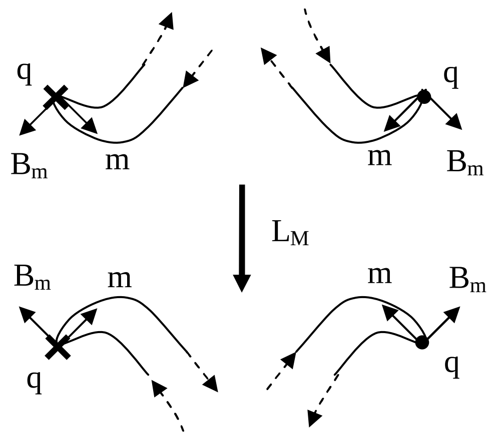

Electron

FIG. 40

Again, consider that the virtual particles in the virtual particle paths on the top, bottom, and top and bottom sides self interact as propagating electrically charged particles interact by way of the respective right-right and left-left hand (q), (m), and (B_m) spin vector interactions, and consequentially experience respective attractive, repulsive, or neutral alignment (internal bonding).

It is considered that a proton can bond with an electron to form a neutron as has been long argued by some in conventional physics. Figure (41A) shows the spin vectors which could exist for certain virtual particle paths of one side of an entirely isolated proton and electron before a possible "nuclear" interaction, and figure (41B) shows the alignment of the spin vectors of the virtual particle paths of one side of the proton and electron which could exist after forming a "nuclear bond" in the formation of a neutron. Wherein, the microscopic spin vectors of respective virtual particle paths are considered to rotate around respective orthogonal rotational axes upon interaction for a proton-electron bond in the formation of a neutron as shown by the curved arrows in figure (41A), for example, for the microscopic magnetic and mass spin vectors rotating around the microscopic electric spin vector axes for the given example virtual particle paths. Accordingly, note how the accelerated condition of an electron in electron capture can facilitate the formation of a neutron.

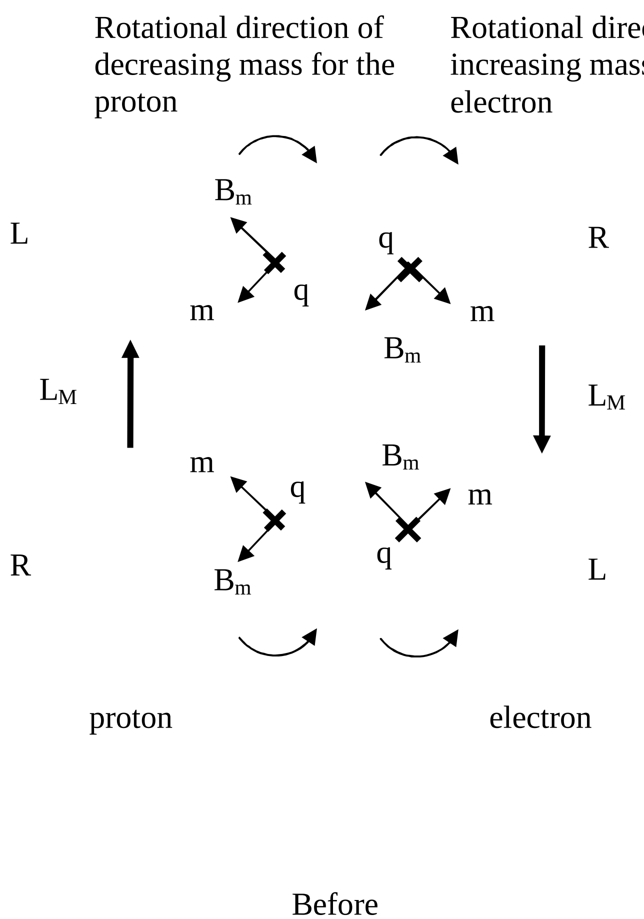

FIG. 41A

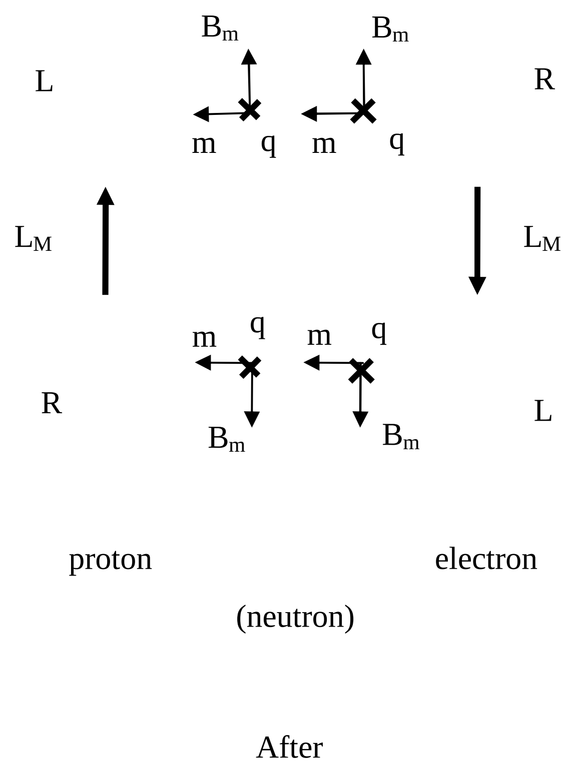

FIG. 41B

In the case of the proton-electron bond, the spin vectors are considered to rotate such that, in effect, there is a net increase in their total mass (an increase in mass for the electron and a lesser decrease in mass for the proton). In which case, for respectively interacting virtual particle paths positioned diagonally (right-right and left-left hand sides), the microscopic electric (q) and mass (m) spin vectors are respectively aligned parallel and attract, while the microscopic magnetic spin vectors (B_m) are aligned antiparallel and attract.

However, microscopic spin vectors of the virtual particle paths of a proton are considered to rotate around the orthogonal rotational axes upon interaction in the formation a proton-neutron bond as shown by the curved arrows in figure (42A), for example, for the microscopic magnetic and mass spin vectors rotating around the microscopic electric spin vector axes for the given example virtual particle paths.

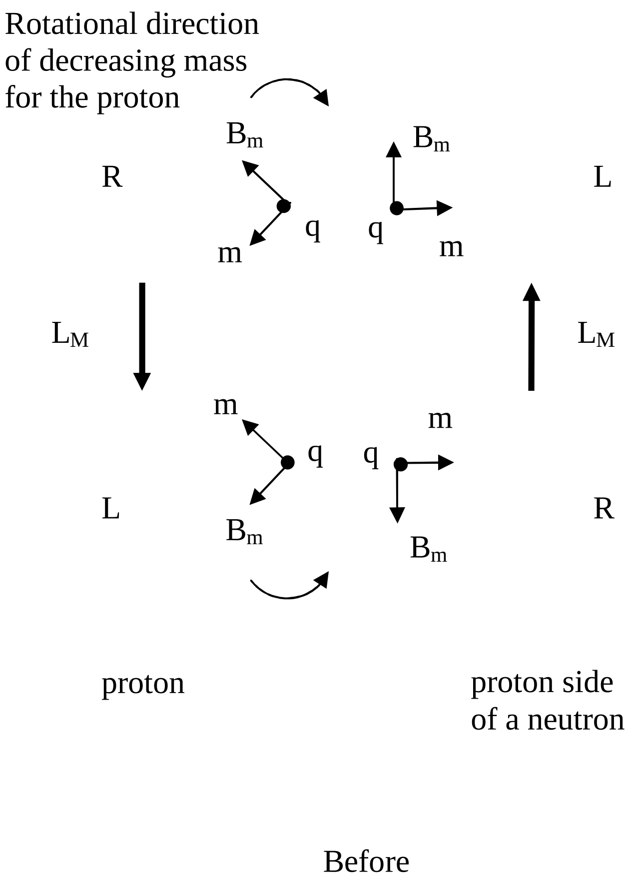

FIG. 42A

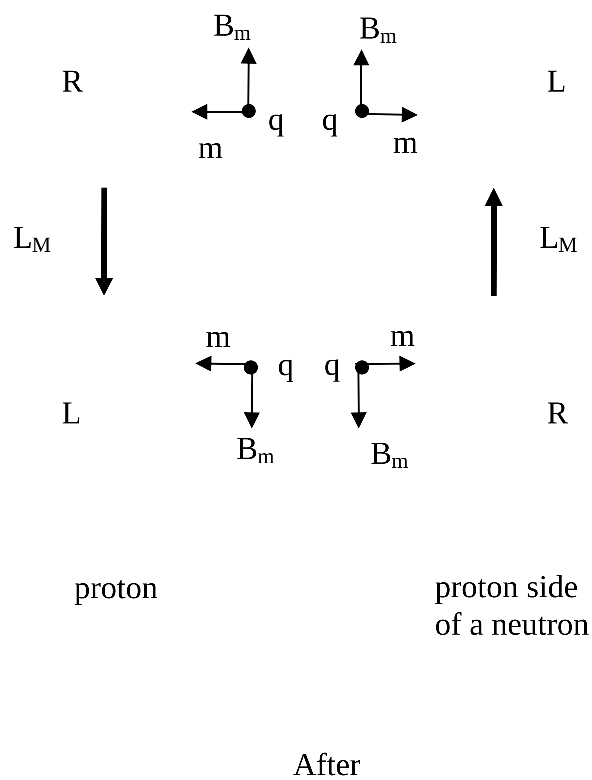

FIG. 42B

In the case of the proton-neutron bond, the spin vectors of the newly bonded proton are considered to rotate to a less massive alignment such that, in effect, the total mass of the nuclearly bonded proton and neutron decreases so as to produce a mass defect. Wherein, in respectively interacting virtual particle paths positioned diagonally, the microscopic electric spin vectors (q) align parallel and thus attract, the mass spin vectors (m) align antiparallel and thus repel, and the microscopic magnetic spin vector (B_m) align antiparallel and thus attract.

Thus, the unified theory herein depicts the physical meaning of mass defect and binding energy.

Note that for the proton-neutron bond, microscopic spin vector alignments are equivalent to the alignments of the microscopic spin vectors in extranuclear interaction for electromagnetic repulsion and gravitational "attraction" (which, in the latter case, attempts to turn the particle around) for particles of the same electric charge when the repelled particle is propagating away from the repulsive source as described for figure (21). This is considered the preferred alignment of such particles in both cases, such that in the case of nuclear bonding, this alignment of the microscopic spin vectors represents the electromagnetic attraction and the gravitational "repulsion" of nucleons, i.e., in the latter case, a form of mass repulsion or "antigravity" which, along with the other cases of mass repulsion described herein, addresses the essence of the longstanding issue in physics questioning the existence of the property of antigravity.

In this train of thought, the properties of the unified field, which include both attractive and repulsive aspects, need to be considered (in accordance with the behavior of the functions of the unified field potentials) when accounting for dark energy and dark matter. Accordingly, consider a supermassive black hole in which a significant amount of less bent virtual particle paths of the top and bottom sides from a supermassive black hole are concentrated along the event horizon, accretion disc, and beyond. Wherein, the attractive and repulsive aspects of the black hole, and their net outcome, can change as the spin vectors rotate with changes in the bends of the respective virtual particle paths of the black hole. (Note here how the consumption of mass-energy by, and the expulsion of mass-energy from, a black hole can change the geometry, e.g., the more and less bent geometry, of a black hole, and therefore change the behavior of a black hole accordingly.)

In effect, the electromagnetic and gravitational components of the virtual particle paths of the top and bottom sides of the black hole would present forces on ordinary matter (comprising positively and negatively charged ordinary matter) including an electromagnetic force by virtue of the electromagnetic component of the unified field, and also a gravitational force by virtue of the gravitational component, thus enabling a supermassive black hole to, for example, maintain a galaxy. While still, however, it is considered that a black hole can have both gravitational and electromagnetic attraction and repulsion on another black hole depending upon the spin vectors of their respective virtual particle paths. In which case, the repulsive interaction between black holes as such needs to be considered when accounting for the expansion of the universe, etc.

Nevertheless, continuing with the principles of nuclear bonding from before, the proton and electron in the neutron attract, and the sum of their masses is more than their resulting mass due to the respective rotations and realignments of their spin vectors. In which case, the electron is considered to “accelerate” (increase in mass) to a greater extent than the proton is considered to "decelerate" (decrease in mass) due to the disproportionate affect of the proton on the electron. While, the nuclearly bonded proton and neutron each attract, and yet, nevertheless, the sum of their masses is less than their resulting mass according to the rotations and realignments of the spin vectors of the decelerated proton.

As the spin vectors in a particle change alignment upon bonding, the virtual particle paths are redistributed in a denser manner for acceleration (resulting in an increase in mass), and are distributed in a less dense manner for deceleration (resulting in a decrease in mass). In which case, for example, the extranuclear virtual particle paths in a nuclearly bonded proton in an atom comprising two or more nucleons have a certain amount of sideways bend due to the changes in their trajectories, and, in result, produce the proper alignment for a respective orbital portion (as described more so later).

Now, the energy of an electron antineutrino which is associated with the formation of a neutron can be related to the acceleration ("compression") of the unified field of the bonded electron, and to the overall more massive condition which is created due to changes in its spin vector alignments and the redistribution of its respective virtual particle paths to an overall more dense condition. Wherein, when a neutron decays in the process of beta decay, the proton and electron separate, and the compressed unified field of the electron recovers to a respectively less compressed condition. In which case, it is considered that the energy of the electron antineutrino which is associated with beta decay corresponds to the release of the energy stored in the compressed unified field of the electron upon separation of the electron from the proton. Then, the antineutrino is produced from the resulting "accelerated" beta particle due to such changes (refer to the description of particle generation by acceleration later herein under the heading "particle transmutation and generation").

ATOMS AND MOLECULES

In conventional physics, the Pauli exclusion principle is considered to play a significant role in the structure and function of matter (or mass-energy) (e.g., in the stability of atoms). The present unified field theory shows how this is the case.

First, consider that the neutron assists in the bonding of protons according to the Pauli exclusion principle which includes assisting in the manner of nuclear bonding described hereinbefore. In the example shown in figure (43), three protons can be bonded by the placement of an electron between the two protons which have the same alignments of angular momenta. Wherein, one proton and a respectively bonded electron act as a neutron. (Note that the relative sizes of a proton and an electron relate to mass not radius, and are for pictorial purposes.)

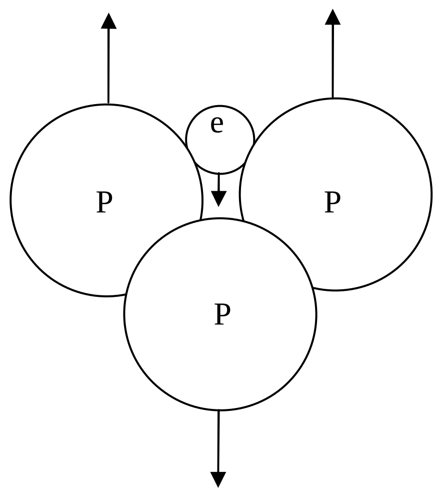

Bonding of protons with an electron according to the Pauli exclusion principle (showing respective angular momenta).

FIG. (43)

Figures (44A) and (44B) show the nucleonic bonding in the (x-y) plane of a few nuclei in agreement with the Pauli exclusion principle. In particular, in figure (44B), notice how, according to up and down alignments, there is no net intrinsic spin in terms of protons or electrons, and there is no net magnetic moment in terms of protons or electrons, and also notice the respective quadrupole configuration of the protons.

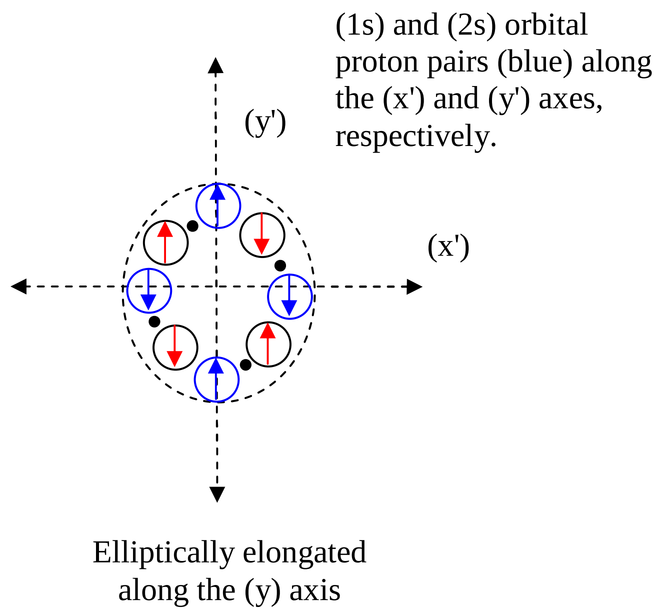

FIG. 44B

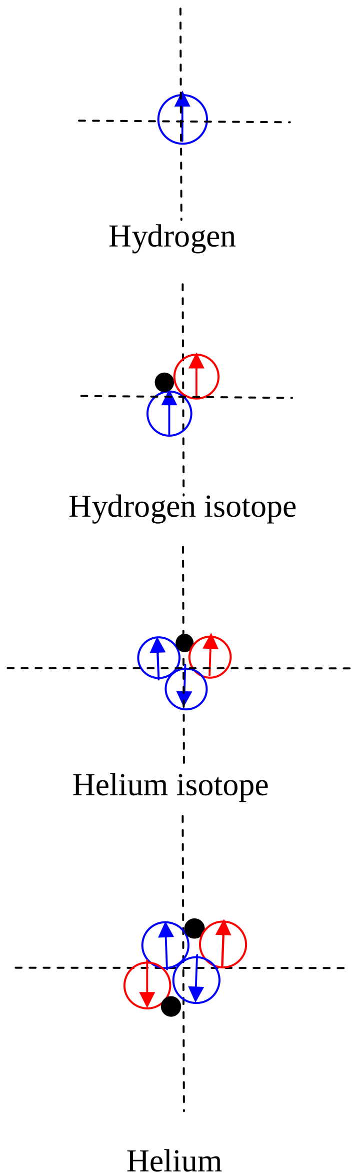

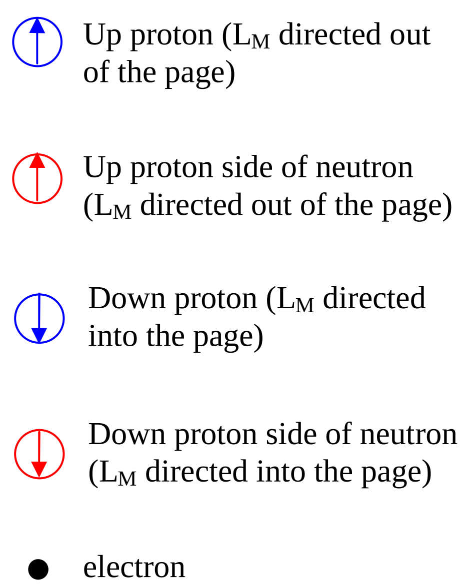

FIG. 44A

Orbital proton and neutron positions are considered not only to be influenced by bond alignments, but are also considered to be influenced by nucleon proximity, in which case the repulsion by a proton or protons, and the neutral presence of a neutron (or neutrons) are considered to affect proton positioning in the nucleus, and thus affect respective orbital positional potential energy. For example, in figure (44B) it is considered that the (1s) orbital is formed first with the (1s) protons along the (x') axis, and, subsequently, repulsion by the (1s) protons affect the potential (and respective spin vector angles) of the protons which attempt to form the (2s) orbital. In which case, repulsion rotates the spin vectors of the approaching protons, and they bond with neutrons at a slightly greater distance from the center than the (1s) protons (here, recall that microscopic spin vector alignments of a nuclearly bonded proton and neutron can be equivalent to the microscopic spin vector alignments, and the rotational directions thereof, of electromagnetic repulsion as described for figure 21, such that, here, electromagnetic repulsion and nuclear bonding can work together). Consequentially, an elliptically shaped octet of nucleons is formed. In result, the (2s) protons along the (y') axis have slightly greater positional potential energy than the (1s) orbital protons (as relates to their spin vector angles, virtual particle path distributions, position relative to the center of the nucleus, etc.), and thus fill after the (1s) orbital protons. Then, certain (p) orbital protons and neutrons form the next octet in the (x-y) plane, etc.

Now, orbital portions are considered to be affected asymmetrically by the repulsion of a proton (or protons) as shown in figure (45).

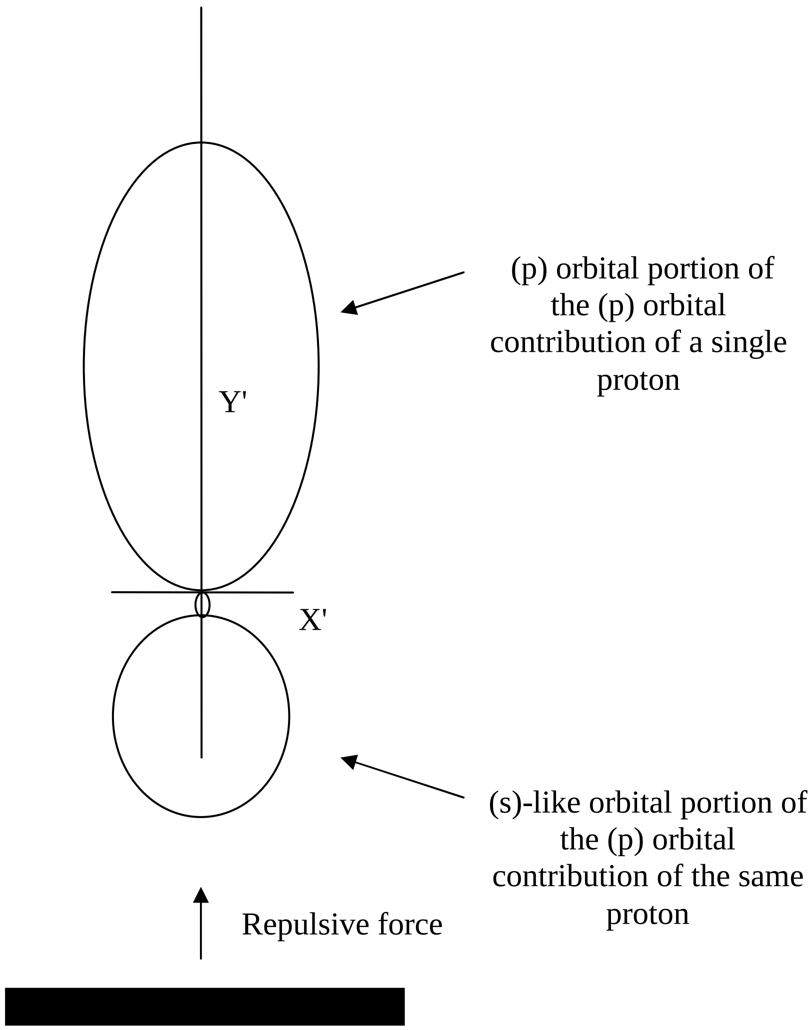

FIG. 45

With respect to figure (45), recall, still again, that the microscopic spin vector alignments of a nuclearly bonded proton and neutron can be equivalent to the microscopic spin vector alignments (and rotational directions thereof) of electromagnetic repulsion as described for figure (21). In this case, initially present protons (solid black rectangle) repel new protons, and thus a new proton bonds in an asymmetrically elliptical configuration, such that the virtual particle paths of each of the newly bonded protons experiences acceleration and deceleration rotations on opposite sides due to repulsion which corresponds to a decrease in mass on one side (i.e., the top side in figure 45), and an increase in mass on the other (i.e., the bottom side in figure 45) as exemplified by the more eccentric (p) orbital virtual particle paths on one side (less massive side) of the proton in contrast to those of the less eccentric (s-like) orbital virtual particle paths on the other side (more massive side) of the proton, respectively. This process is equivalent to the process of acceleration and deceleration on opposite sides of the nuclear region of a positively charged particle due to electromagnetic repulsion by an irregular distribution of positively charged particles as described with respect to figure (18).

Figure (46) shows (z) axis nucleon positioning.

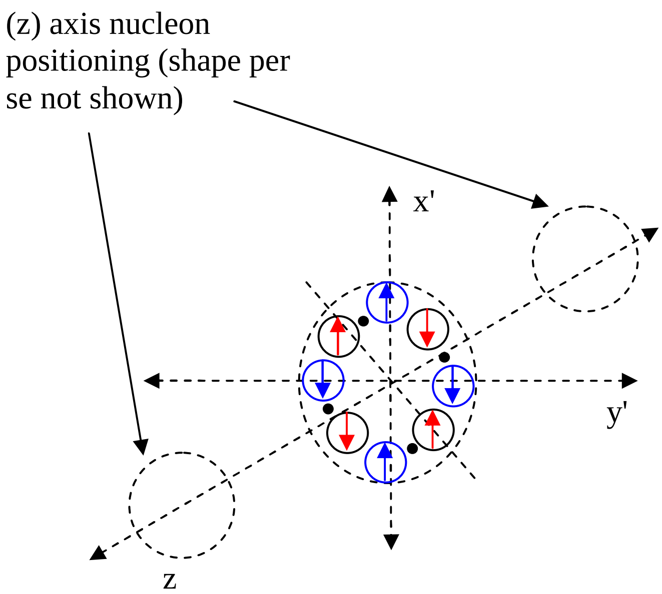

It is considered that in atoms with (z) axis nucleons, that nucleons along the (z) axis establish certain terms which affect nucleon positioning in the nucleus, such that, for example, certain (d) orbital bonding in the (x-y) plane occurs along certain axes due to proton repulsion and neutral neutron positioning of (d) orbital nucleons along the (z) axis.

FIG. 46

Figure (47), shows the (z) axis nucleon bonding of (p), (d), and (f) orbital nucleons on one side of the (x-y) plane, while the configuration of the (z) axis orbital protons on the two sides of the (x-y) plane are considered to symmetrically complement each other upon completion of a sub-shell. Wherein, as (s) and (p) orbital portions are constructed from the virtual particle paths of two protons in the (x-y) plane, certain (d), (f), etc. orbital portions are constructed from tilted versions of virtual particle paths of the same configuration (with respect to the z-axis). In which case, the nucleonic bonding of (z) axis nucleons also occurs in agreement with the Pauli exclusion principle. (Note that the “nesting” of orbital portions is considered to pertain to the ability of an electron to propagate in any orbital portion by switching virtual particle paths where virtual particle paths "combine.")

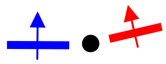

(z) axis (p) orbital proton
on one side of
the (x-y) plane
with a neutron on
one side of the (y-z)
plane

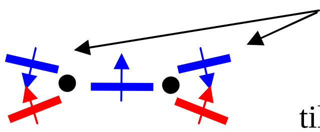

(z) axis (d) orbital
protons
which correspond to
tilted (z) axis (d) orbital
portions

(z) axis (d) orbital
protons and neutrons on
one side of
the (x-y) plane

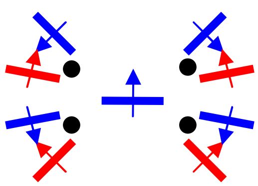

(z) axis (f) orbital
protons and neutrons on
one side
of the (x-y) plane

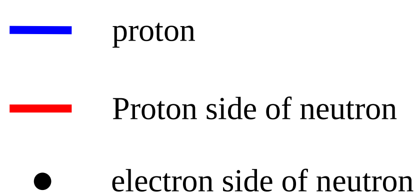

Here, the (z) axis nucleon bonding of (p), (d), and (f) orbital nucleons is shown. As for the octets, the (z) orbital proton and neutron positions as shown are considered not only to be influenced by bond alignments, but are also considered to be influenced by the protons and neutrons along the (z) axis, and influenced by the protons and neutrons in the octets in the (x-y) plane.

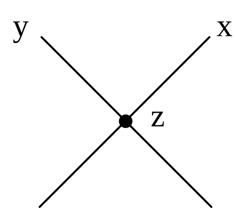

axes

FIG. 47

Figure (48) shows two (d) orbital nucleon configurations in the (x-y) plane which are considered to establish the $d_{x^2-y^2}$ and d_{xy} (d) orbitals.

($d_{x^2-y^2}$)   (d_{xy})

FIG. 48

It is considered that as atomic number increases so to does the repulsion and respective orbital eccentricity increase for newly bonded protons, and as the number of related nucleonic bonds increases for nucleons (i.e., as the number of sub-shell nucleons increases) so to increases the eccentricity of the resulting orbitals. While, the size of an orbital is considered to increase as the positional potential energy of an orbital increases according to its spin vector rotations (in the less massive direction) due to field repulsion and the number of related nucleonic bonds.

The (s) orbitals are considered to be bonded in nucleonic octets which are separate from the (p), (d), (f), etc. sub-shell protons bonded in nucleonic octets in the (x-y) plane which are considered to have bonds with nucleons which are also situated along the (z) axis (e.g., via the tilted alignment of the z-axis d-orbital protons of a d-sub-shell extending out to respective nucleons of other d-orbital sub-shell portions in octets in the x-y plane). Wherein, in the example given, the (d) orbital nucleons bond while aligned so as to pass over the relevant (s) orbital protons to some extent, i.e., (s) orbital protons are situated in field "pockets" so as to eliminate some repulsion. Thus, the (s) orbitals are considered to be less elliptical in shape, less asymmetric, and are considered to have less positional potential energy then, for example, (d) orbitals due to less field repulsion and a lesser number of related nuclear bonds, and, fill first since they are produced by inner positioned nucleons with such attributes.

Next, the unified field theory shows in figure (49A) how the Pauli exclusion principle is involved in fine and hyperfine structure in a hydrogen atom. Figure (49A) shows a side view of one electron at any given time in the horizontal plane on the top or bottom side of the (s) orbital formed by a single non-nuclearly bonded proton (hydrogen atom). It is considered, for example, as shown in figure (49A), that the right hand screw virtual particle paths (top side) of a first inverted low energy electron could couple with (and be accelerated by) the less bent bottom right hand screw side virtual particle paths of the (s) orbital proton, such that the right hand microscopic magnetic spins (B_m) of the electron are antiparallel with right hand microscopic magnetic spins of the proton, and such that the electron would oscillate with its magnetic moment (u) antiparallel with the magnetic field (B_o) which it generates while orbiting (fine structure), and antiparallel with the macroscopic magnetic field (B_M) of the proton (hyperfine structure). While, as shown in figure (49A) at another time, an effectively upright high energy electron in the same (s) orbital could oscillate with its left hand (bottom side) microscopic magnetic spins (B_m) antiparallel with left hand microscopic magnetic spins of the more bent top left hand screw side virtual particle paths of the proton, and oscillate with its magnetic moment (u) parallel with the magnetic field (B_o) which it generates while orbiting (fine structure), and parallel with the macroscopic magnetic field (B_M) of the proton (hyperfine structure). Wherein, the more bent top left hand screw side virtual particle paths of the proton are considered to comprise higher positional potential energy in this case.

Upright electron propagating into the page on a more bent orbital portion on the top left hand screw side of an (s) orbital (shown in a plane in a horizontally sectioned view). Note that the direction of the electron is aligned by factors including the bending of the virtual particle paths of the proton.

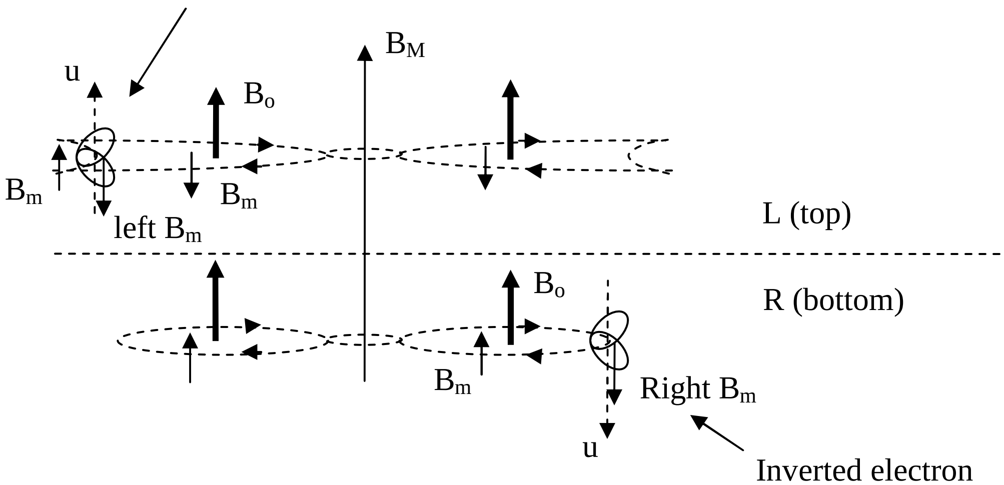

Inverted electron (lower energy) propagating out of the page on a less bent orbital portion on the bottom right hand screw side of an (s) orbital (shown in a plane in a horizontally sectioned view).

Electron at different times in more and less bent orbital portions in the (s) orbital of a hydrogen atom (shown in planes in a horizontally sectioned view).

B_o Orbital magnetic field

R L and L R Electrons with microscopic magnetic spins (solid arrows) and magnetic moments (u) (dashed arrows)

and Virtual particle path microscopic magnetic spins B_m

FIG. 49A

A similar example of the role of the Pauli exclusion principle in the fine and hyperfine structure in the unified field is shown in an (s) orbital of an atom formed by two nuclearly bonded protons in figure (49B).

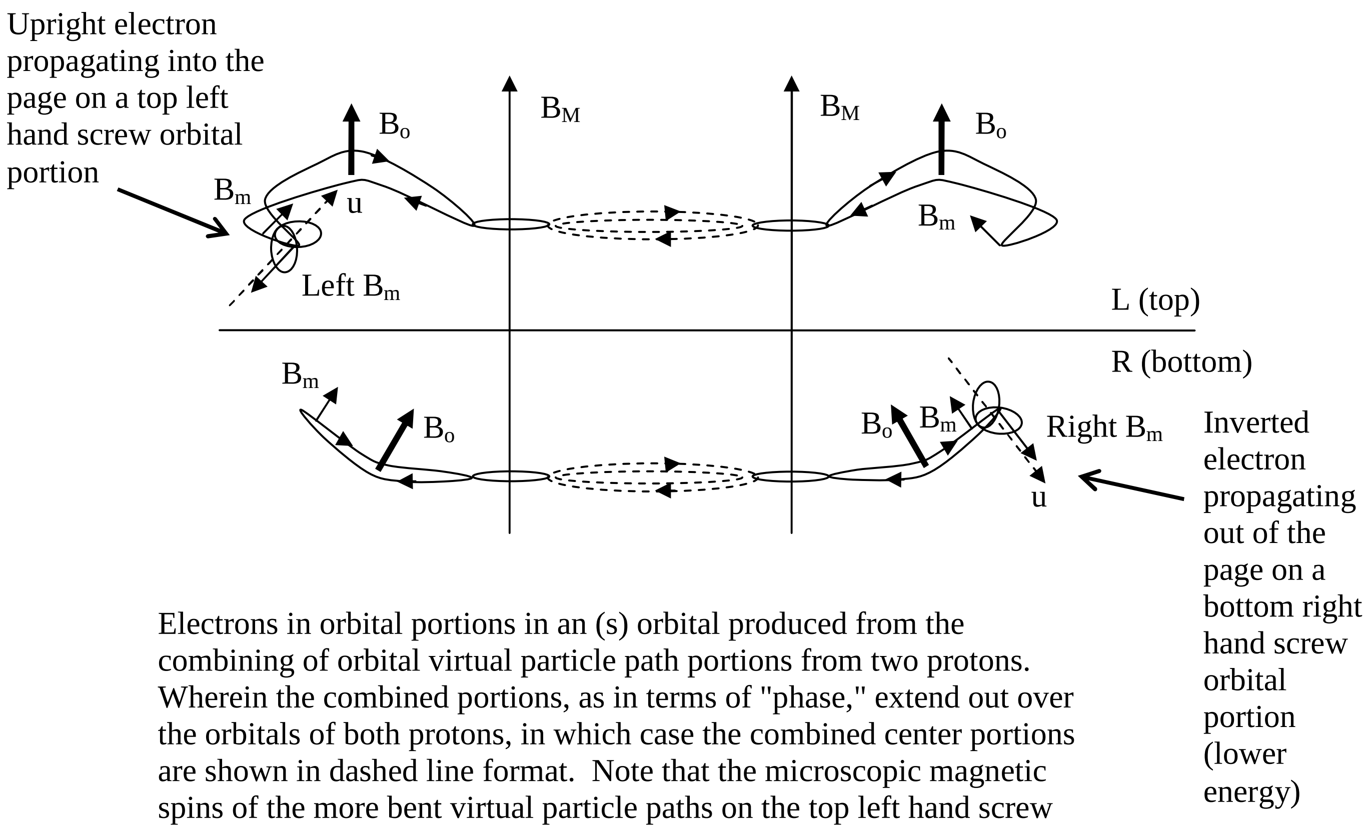

Electrons in orbital portions in an (s) orbital produced from the combining of orbital virtual particle path portions from two protons. Wherein the combined portions, as in terms of "phase," extend out over the orbitals of both protons, in which case the combined center portions are shown in dashed line format. Note that the microscopic magnetic spins of the more bent virtual particle paths on the top left hand screw orbital portion invert the electron so that it is effectively upright, while the alignments of microscopic magnetic spins of the less bent virtual particle paths on the bottom right hand screw orbital portion effectively produce an inverted electron.

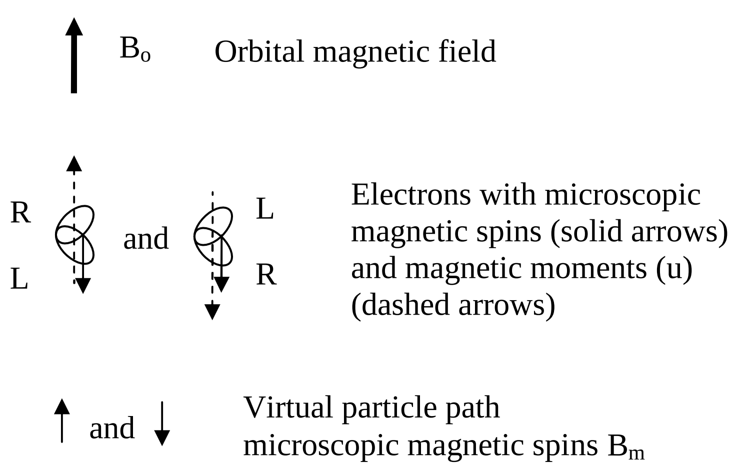

FIG. 49B

Still yet another example of the present unified field theory showing how electrons behave in atoms is illustrated in figure (50) which shows why electrons move outward from orbitals of lower to higher positional potential energy in atoms upon absorbing energy. Wherein, figure (50) shows an electron oscillating with its left hand (bottom side) microscopic magnetic spin (B_m) antiparallel with the left hand microscopic magnetic spin of a "somewhat more bent" virtual particle path of the top left hand screw side of a nuclearly bonded proton (lower portion of the drawing), and shows the respective spin vector alignments of a quantum during absorption. Wherein, the quantum produces spin vector rotations in the electron so that the spin vectors of the electron rotate towards the alignment of the spin vectors of the "even more bent" virtual particle path on an orbital higher in positional potential energy, such that the electron then propagates on the respective orbital higher in positional potential energy while aligning with the magnetic fields in its environment. (Note that a similar process would occur for elevating an electron in a hydrogen atom, i.e., a non-nuclearly bonded proton.)

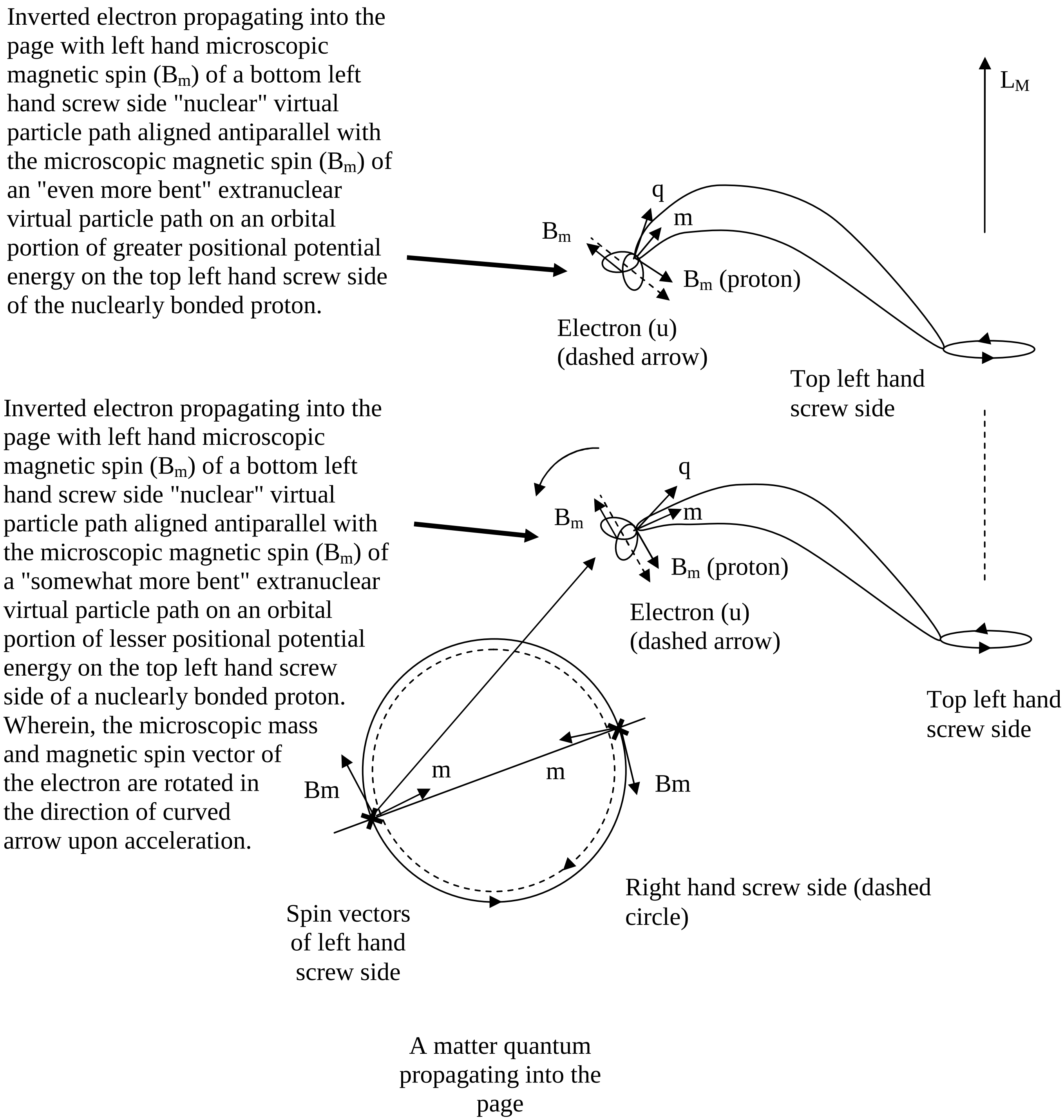

Here, a quantum is absorbed by an electron in the extranuclear region of an orbital. Wherein, the directions of rotation for increases in positional potential energy for the virtual particle paths of the proton are in the same direction as the direction of rotation for an increase in mass for the electron. Thus, the electron is accelerated by the quantum, and then couples with the virtual particle paths of an orbital at a different (greater) positional potential energy level, such that the electron then propagates on the respective orbital higher in positional potential energy while aligning with the magnetic fields in its environment (wherein only certain details of the absorption of the left hand screw side of the quantum are shown).

FIG. 50

Next, the combinability (phase) of the virtual particle paths of molecularly bonded protons is considered to occur according to their respective spin vector directions and effective interactions including electric repulsion by their respectively less and more bent virtual particle paths with respectively involved electrically charged particles. Figures (51A) (top view) and (51B) (side view) show sigma and pi molecular bonding orbital portions due to electrons on respectively resulting virtual particle paths (in agreement, in general, with convention).

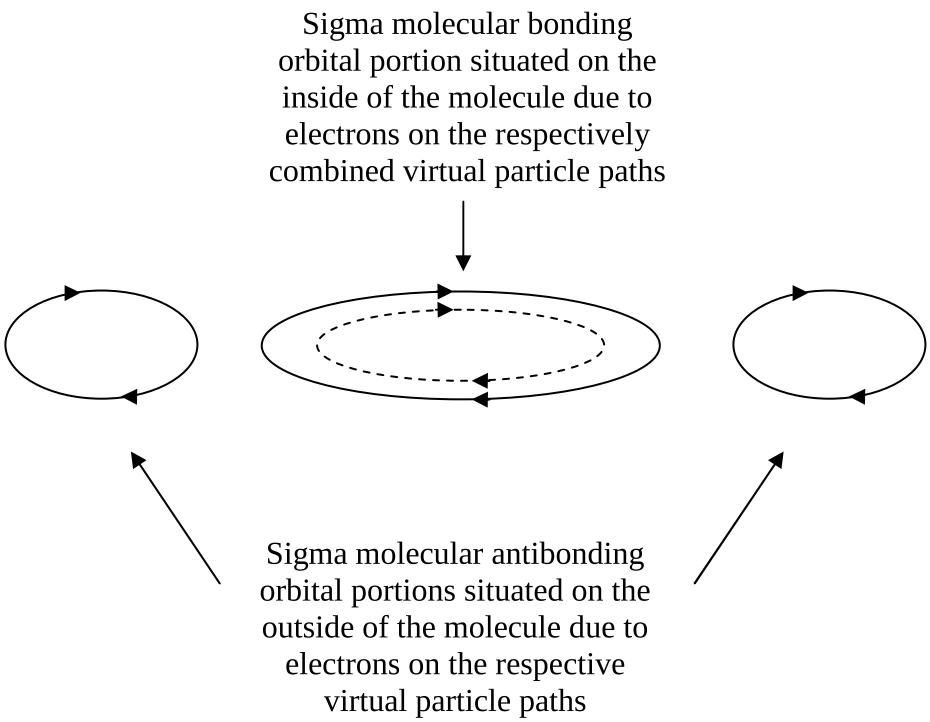

FIG. 51A

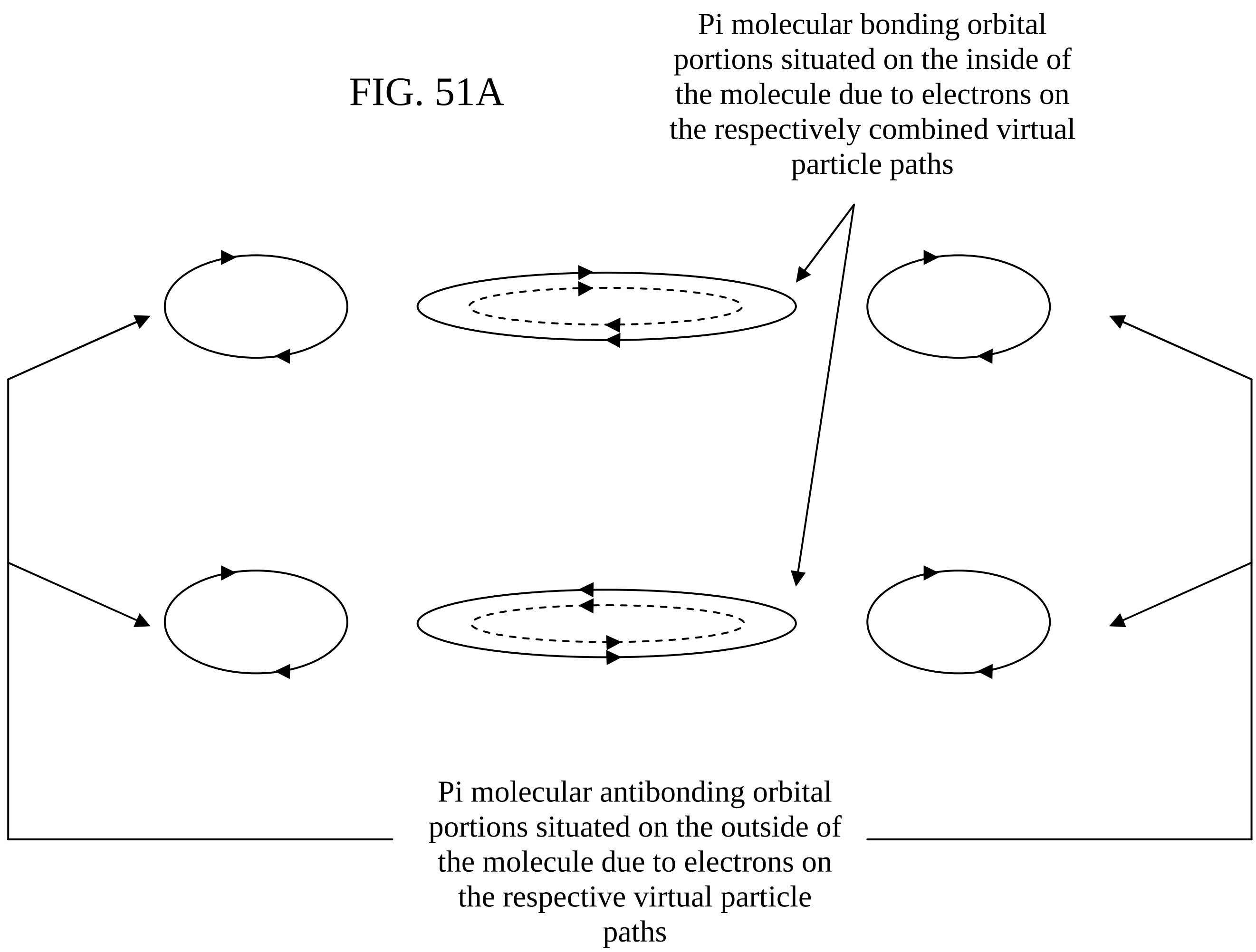

FIG. 51B

PARTICLE TRANSMUTATION AND GENERATION:

Now, it is considered the vast diversity of particles which are produced in particle physics have a cause which transcends conventional theory, and, if understood, would change the approach of conventional particle physics in its efforts to discover the underlying structure and function of mass-energy, and ultimately the universe. Respectively, the cause of such a vast diversity of particles is considered to simply relate to the manifestations which are produced by the accelerations and decelerations of the mass-energy of the unified field presented herein.

Accordingly, first, in certain types of accelerations, a particle can transmute from one type of particle into another type of particle. For example, in one such type of "transmutational acceleration," the top and bottom sides of an electrically charged particle would reflect almost totally together so as to change into an electrically neutral particle. The transmutation of an electron and a positron into matter and antimatter electromagnetic field quanta, respectively, upon annihilation is one example. In this case, the annihilating matter and antimatter are considered to interact in a symmetric manner so as to eliminate a significant extent of the eccentricities (including a significant extent of the bends) in their respective virtual particle path bands, such that the virtual particle paths of the top and bottom sides of each electrically charged particle (e.g., the electron and positron in the example) internally converge, narrow, and project forward. Wherein, the virtual particles on the top and bottom sides of the respectively produced quanta consequentially propagate away (while self interacting) with translational velocity (c).

It is considered that in another type of acceleration, that a neutral particle can produce two particles of opposite intrinsic spin and opposite electric charge while conserving electric charge, etc. as shown in figure (52). Wherein, for example, the top and bottom sides of an effectively electrically neutral gamma ray could, upon deceleration, open so as to produce an electron, in which case the top and bottom sides of the electron thus produced would split such that one portion would flip over so as to produce a positron of the opposite intrinsic spin and opposite electric charge, and the other portion would continue in the form of an electron as in the case of pair production. Note that it is considered that a matter quantum differs from an antimatter quantum according to their different top and bottom screw rotations, different top and bottom microscopic magnetic spin (B_m) directions, etc., similar to how a negatively and a positively electrically charged particle differ. However, it is considered that an antimatter quantum can act in a manner which is equivalent to that of a matter quantum by the top and bottom sides flipping over, for example, upon being absorbed by an electron. Here, nevertheless, the production of oppositely charged particles (including the production of matter and antimatter) from an electrically neutral particle can be more profoundly understood by such a process.

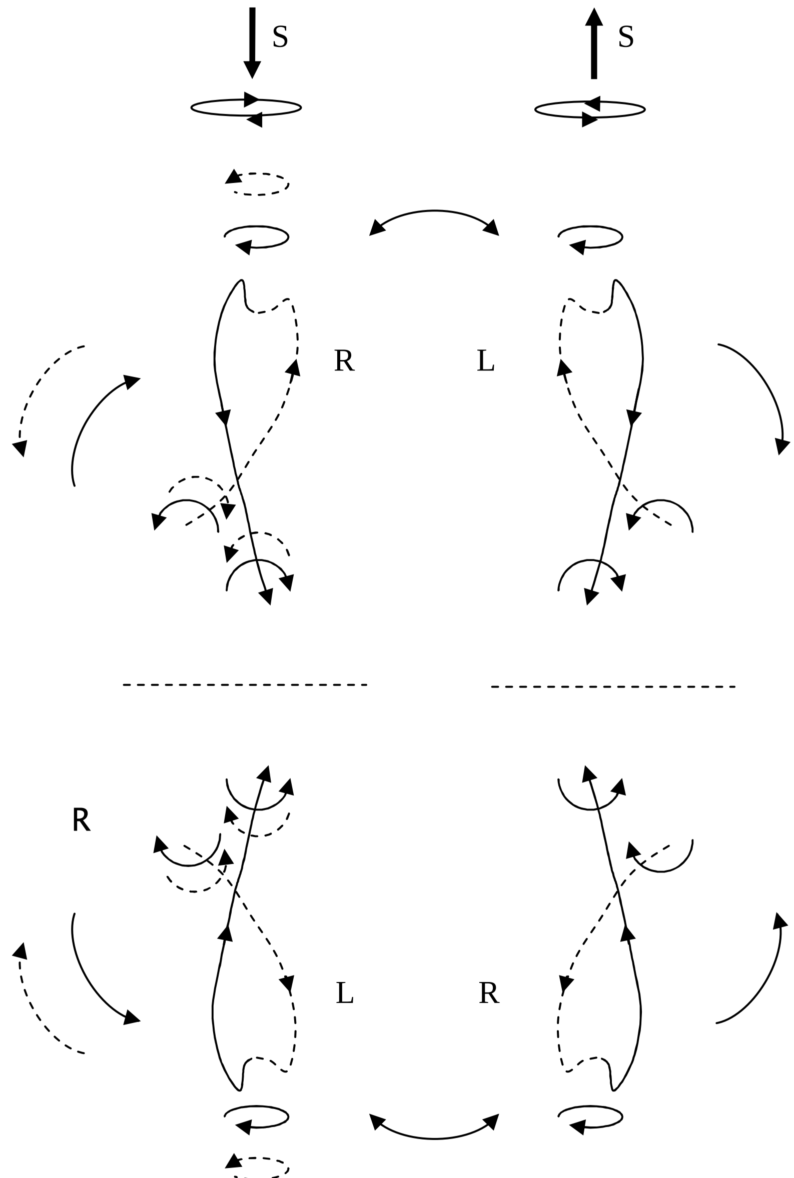

FIG. 52

In yet another type of acceleration, it is considered that a given electrically charged particle can emit another particle (e.g., during an oscillation). Wherein, in one such acceleration, the top and bottom sides of the electrically charged particle would emit a particle from the nuclear region which would have top and bottom sides which are almost totally reflected together (e.g., as with an electromagnetic field quantum). In which case, the top and bottom right and left hand screws of the emitted particle would be the same as the particle which emitted it, yet with bands of virtual particle paths with spin vectors of different alignment (and eccentricity) such that the emitted particle would have neither an effective nuclear region nor an effective bend in its extranuclear field, and thus have neither an effective mass nor electromagnetically attract or repel in a effective manner (but electromagnetically, electrically, and gravitationally interact as mentioned previously).

In still yet another type of acceleration, the dipole pattern of electromagnetic radiation can be emitted by the virtual particles on the virtual particle paths of an accelerated electrically charged particle (e.g., a non-relativistically accelerated electron). Wherein, the structure and function of a virtual particle are considered to be analogous to those of an accelerated electrically charged particle as stated above. While, in even still yet another type of acceleration, the forwardly directed pattern of electromagnetic radiation from a relativistically accelerated electron in a synchrotron is considered to be produced by the virtual particles on the virtual particle paths of the forwardly aligned and somewhat reflected top and bottom sides of the respectively accelerated electron as the electron follows a helical course while effectively propagating forward in the magnetic field of the synchrotron.

CONCLUSION:

In conclusion, one unifying general function for a unified field has been provided with the application of Planck units which not only unifies all of the conventional fields and respective forces, but also unifies mass-energy and electric charge with "spacetime," and includes quantum field theory and relativity as well. Accordingly, the unifying principles were applied in a description of the geometry (including internal structure) and functionality of certain aspects of the unified field including the geometry and functionality of electromagnetic, gravitational, and nuclear interaction, the geometry and functionality of Lorentz transformations, and the structure and function of elementary particles (including antiparticles), atoms, molecules, and bodies of astronomical dimensions. In broadening, the resulting unified field theory proposes to provide a basis for describing and solving problems in unified terms in other areas of physics which include subject matter which pertains to relevant "probabilistic" phenomena, chaos, big bang theory, and, in general, the universe as a whole (including the expansion of the universe, dark energy, and dark matter). While furthermore, it is proposed that the principles of the unified field theory presented are also applicable as a means of describing and solving problems in unified terms in other areas of the sciences.